Entrapment Efficiency and Release Kinetics of Antihypertensive and Anticancer Drugs using Biodegradable Polymer Particles

Thesis Submitted

By

Tanushree Basu

(Regn. No. 951309001)

In fulfilment of the requirement for the Degree of

Doctor of Philosophy

Under the Guidance

Dr. Satnam Singh
Professor

Dr. Bonamali Pal
Professor

THAPAR INSTITUTE
OF ENGINEERING & TECHNOLOGY
(Deemed to be University)

SCHOOL OF CHEMISTRY AND BIO-CHEMISTRY
Thapar Institute of Engineering & Technology,
PATIALA-147004
PUNJAB

May, 2019

Dedicated

To

My Parents

&

Teachers

Certificate

This is to certify that the thesis entitled ***"Entrapment Efficiency and Release Kinetics of Antihypertensive and Anticancer Drugs using Biodegradable Polymer Particles"*** being submitted by Miss. Tanushree Basu in fulfilment of the requirement for the award of the Degree of Doctor of Philosophy in the School of Chemistry and Biochemistry, Thapar Institute of Engineering and Technology, Patiala, is a record of candidate's own independent and original research work carried out by her under our supervision and guidance. The material embodied in this thesis has not been submitted in part or full to any other University or Institute for the award of any degree.

Dr. Satnam Singh
Professor
School of Chemistry and Biochemistry
Thapar Institute of Engineering
& Technology, Patiala- 147004
Punjab (India)

Dr. Bonamali Pal
Professor
School of Chemistry and Biochemistry
Thapar Institute of Engineering
& Technology, Patiala-147004
Punjab (India)

Scanned by CamScanner

Candidate's Declaration

I, hereby declare that the work presented in the thesis entitled "***Entrapment Efficiency and Release Kinetics of Antihypertensive and Anticancer Drugs using Biodegradable Polymer Particles***" in fulfilment of the requirement for the award of the Degree of Doctor of Philosophy, School of Chemistry and Biochemistry, Thapar Institute of Engineering and Technology, Patiala, is an authentic record of my own work carried out under the supervision of Dr. Satnam Singh, Professor and Dr. Bonamali Pal, Professor, School of Chemistry and Biochemistry, Thapar Institute of Engineering and Technology, Patiala, India. The matter embodied in this thesis has not been submitted in part or full to any other university or institute for the award of any degree in India or Abroad.

Place: Patiala

Date: 29-05-2016

Tanushree

Tanushree Basu

Scanned by CamScanner

Acknowledgements

I wholeheartedly thank the Almighty for giving me the strength to remain on the path to success.

Through this section of the thesis, I would like to convey my heartiest thanks to all those who supported and encouraged me in many ways for the accomplishment of this study and made it an unforgettable journey for me.

First and foremost, I would like to extend my sincere gratitude to my supervisors, Dr. Satnam Singh, Professor and Dr. Bonamali Pal, Professor, School of Chemistry and Biochemistry, Thapar Institute of Engineering and Technology, Patiala for giving me the valuable opportunity to work under their worthy guidance. Their immense knowledge, constructive ideas, and innovative way of teaching, efforts and time for giving me the useful suggestions on manuscript writing and research presentations were priceless. They have always supported, inspired, encouraged and challenged me in many ways for making me confident and enhancing my professional growth. They gave me the opportunities to present my research work in several conferences and other professional gatherings, through which my public speaking skills have improved immensely. I will always remain thankful to them for preparing me for my future career and without their inspiration; I would not be able to achieve so much today. I attribute the level of my doctoral degree to their motivation, encouragement and sustainable effort.

Scanned by CamScanner

I am also thankful to my doctoral committee members Dr. Kamaldeep Paul, Dr. Amjad Ali and Dr. Niranjan Das for their encouragement, constructive criticism and inspirations.
Many thanks to all the faculty members of School of Chemistry and Biochemistry, Thapar Institute of Engineering and Technology, Patiala for providing necessary guidance during my research work. I am also thankful to Mr. Chander Thakur, School of Chemistry and Biochemistry for the constant official help and cooperation.

I would also like to thank Dr. B. K. Chudasama and Ms. Poornima (School of Physics and Material Science, Thapar Institute of Engineering and Technology, Patiala) for Zeta potential and Conductance analysis and Mrs Raveena Thakur (GGDSD College, Chandigarh) for FTIR analysis. I also extend my thanks to Sophisticated Analytical Instruments (SAI) Laboratories, Thapar Institute of Engineering and Technology, Patiala, Sophisticated Analytical Instrumentation Facility (SAIF), Punjab University, Chandigarh, SAIF, IIT Bombay.

This word 'Thank you' seems insufficient for my friends who expressed their constant moral support, care and understanding towards me and providing a stimulating and fun filled environment. I am greatly thankful to my senior labmates Mrs. Rupinder Kaur, Mr. Rohit Singh, Mr. Inderpreet Singh, Mrs. Jaspreet Kaur, Mrs. Anila Gandhi, Mr. Bhupender Pal Thakur, and Mrs. Shweta Sareen who extended their support in a special way. I gained a lot from them, through their personal and scholarly interactions, their suggestions at various points in my research programme.

Scanned by CamScanner

I am also thankful to my dear friends Mr. Rayees Ahmed Rather, Mr. Roopchand Prajapati, Mrs. Samriti Dadhwal, Mrs. Sakshi Bhardwaj, Miss Manpreet Kaur Aulakh, Mr. Adil Batla, Mrs. Prerna Khanna, Mr. Balveer Painam, Mrs Kamalpreet Kaur, Mrs Sweety Gogoi, Mrs Pooja Chahal and Mr. Sahil Verma for their precious friendship and for making this journey easier. I will forever cherish the warmth shown by them, whose smiling faces always inspired me.

Words fail me to express my regards to my family for their encouragement and inspiration throughout my research work, which always kept me lifted up during the hard phases of my life. I would always remain indebted to my loving mother, Mrs. Anjali Basu and father, Mr. Tarun Kumar Basu, who always remained beside me as a source of motivation. I owe everything to them. My special thanks to my younger sister, Miss. Tanmayee Basu, for her unconditional love and support in every aspect.

Besides this, I am thankful to the persons who knowingly and unknowingly helped me during the successful completion of this work.

Tanushree

Tanushree Basu

Scanned by CamScanner

Table of Contents

List of Abbreviations

PNPs	Polymeric Nanoparticles
PLA	Poly Lactic Acid
PLGA	Poly-Lactide-Co-Glycolic Acid
Cs	Chitosan
NS	Nanosphere
pNIPAM	Poly (N-isopropyl acryl amide)
PEG	Poly Ethylene Glycol
SDS	Sodium Dodecyl Sulphate
DCM	Dichloro Methane
KP	Kolliphore
MTX	Methotrexate
TDC	Total Drug Content
EE	Entrapment Efficiency
UV	Ultra Violet
Vis	Visible
FTIR	Fourier Transform Infra Red
DLS	Dynamic Light Scattering
SEM	Scanning Electron Microscopy
TEM	Transmission Electron Microscopy
XRD	X-Ray Diffraction
JCPDS	Joint Committee on Powder Diffraction Standards
TGA	Thermo Gravimetric Analysis
AFM	Atomic Force Microscopy
BET	Brunauer, Emmett and Teller
HPLC	High Performance Liquid Chromatography
PBS	Phosphate Buffer Solution
ABS	Acetate Buffer Solution
a.u	Arbitrary Unit
t_R	Retention Time

h	Hour
min	Minute
nm	Nanometer
mg	Milli Gram
g	Gram
mL	Milli Liter
µL	Micro Liter
µm	Micrometer
mV	Milli Volt

List of Figures & Schemes

List of Tables

The work presented in this thesis enlightens the significance of biodegradable polymeric materials for their intended use as drug delivery carriers. Main emphasis has been given to the synthesis of polymeric nanoparticles (NPs) in the form of core@shell and hollow nanostructures by varying the nature of core, shell composition, their characterization and application in drug delivery. This whole thesis is divided into five chapters which are described below:

Chapter 1: Introduction and Literature: The first chapter provides brief introduction about the biodegradable polymeric nanoparticles, modified shapes, sizes and further their application in *in-vitro* release of antihypertensive and anticancer drugs from the polymer matrix. Literature review, research gap, objectives, experimental section and characterization techniques are also incorporated in this chapter.

Chapter 2: This chapter comprises of two sections.

Section A: Ramipril embedded nanospheres of biodegradable poly-D, L-lactide-co-glycolide: To study their release kinetics: This section demonstrates the development of biodegradable polymers for controlled drug delivery has gained immense importance as these can be broken down into biologically acceptable monomeric units that can be eliminated by natural metabolic pathways from the body. In order to improve the therapeutic efficacy of ramipril, an antihypertensive drug, a study has been carried out to ascertain the duration of its action. Ramipril loaded biodegradable nanoparticles of poly-D,L-lactide-co-glycolide (PLGA) were prepared by nanoprecipitation using tribloere stabilizer kolliphor P-188 (K P-188). Four different formulations F_1 to F_4 were prepared by altering the weight of K P-188: PLGA as 1:1.25, 1:2.50, 1:0.62 and 1:0.80. These were characterised by zeta potential, SEM and TEM studies. The F_3 formulation showed highest drug content and entrapment efficiency of 94% and 84%, respectively. *In-vitro* release study of these formulations at pH 7.3 in phosphate buffer indicated F_2 formulation to be efficient with an initial burst release followed by 74% sustained release of ramipril over 24 hours. The Korsemeyer–Peppas model for determining the kinetic drug release showed that ramipril release from PLGA matrix followed zero order rate kinetics and an anomalous (non-fickian) diffusion mechanism.

Section B: Core-Shell PLGA/PLA- pNIPAM nanocomposites loaded with Ramipril: This study demonstrates the core-shell morphology of poly- lactic /poly-lactic-co-glycolic acid- poly N-isopropylacrylamide nanocomposite the study of release kinetics of ramipril.

Poly- lactic acid and Poly-lactic-co-glycolic acid are two commonly used biopolymers in drug delivery. However, these polymers lack desirable attributes like resistance to aggregation in long term storage due to lyophilisation. To improve the efficacy of these polymers, these are encapsulated within a shell of poly (N-isopropylacrylamide) in order to endure lyophilisation. Single emulsion technique followed by aqueous free radical precipitation polymerization process is used to prepare core-shell, (Poly- lactic /Poly-lactic-co-glycolic acid- poly N-isopropylacrylamide) nanocomposite. The prepared nanocomposites were characterized by zeta potential, DLS and TEM studies and were further used as a delivery system for Ramipril, an antihypertensive drug. Drug loaded poly-lactic-co-glycolic acid core - poly (N-isopropylacrylamide) shell nanoparticle showed higher drug content (91%) and entrapment efficiency of 78%. *In-vitro* release study of the formulations at pH 5.3 in phosphate buffer indicated poly-lactic-co-glycolic acid to be more efficient than poly-lactic acid with a sustained release of 86% of ramipril from the polymer matrix within 24 hours. Further, to determine the kinetics of release, the data was fitted into Korsemeyer-Peppas and Higuchi model of drug release and it was observed that ramipril release from polymer matrix followed zero order rate kinetics and an anomalous (non-fickian) diffusion mechanism.

Chapter 3: Entrapment and Release Efficiency of Hollow Chitosan Nanospheres Incorporated Ramipril: Hollow biodegradable polymer nanoparticles as drug carrier possess effective low density and higher surface area. Chitosan hollow nanospheres were prepared using poly-D,L-lactide-co-glycolide as template by single emulsion method. The DLS studies showed increase in size from 125 nm to 186 nm for the formation of core@shell structure. The BET surface area increased from $62 m^2 g^{-1}$ for chitosan@poly-D,L-lactide-co-glycolide to $111 m^2 g^{-1}$ for hollow chitosan nanospheres. TEM analyses indicated core@shell, chitosan@poly-D,L-lactide-co-glycolide and the hollow morphology of the chitosan nanospheres. Ramipril in acetone (1.5mg/mL, 3mg/mL and 5mg/mL) was physically adsorbed onto hollow chitosan nanospheres and the amount of adsorbed ramipril was determined by HPLC. Higher entrapment efficiency (91%) with 96% of the drug content was observed for the sample with 5 mg/mL of the drug. The *in-vitro* release of ramipril of 86% and 73% was achieved in acetate (pH-3.3) and phosphate (pH-6.3) buffers respectively while only 48% of ramipril in Tris buffer (pH- 8.0) medium. Korsemeyer-Peppas model of drug release indicated the release of ramipril being swelling controlled.

Chapter 4: Cytotoxic Evaluation of Fe_3O_4 Modified PLGA-PEG for Improved Delivery of Methotrexate to Target Site in Cancer Therapy: Magnetic nanoparticles are recently gaining importance in drug delivery applications due to their capability to target molecules. Surface modification using magnetic nanoparticles enhances the ability of amphiphilic block polymers by increasing their surface properties. In this study, Fe_3O_4 modified PLGA-PEG nanocomposite is prepared by double emulsion method. Spinel cubic structure for Fe_3O_4 nanoparticles is obtained from XRD analysis. A shift in the 2ϴ values for the composite is attributed to interaction between Fe_3O_4 and PLGA-PEG. Also, a shift in the Fe-O band in the FTIR spectrum of Fe_3O_4-PLGA-PEG confirms the formation of nanocomposite. Reduction in agglomeration due to electrostatic repulsion between the polymer chains and magnetic particles confirming the formation of the nanocomposite was analyzed by TEM. The effectiveness of prepared magnetically modified nanoparticles was determined by encapsulating methotrexate (anticancer drug) into the nanocomposite. High entrapment efficiency of 95% was observed with polymer: drug 1:1 ratio. The *in-vitro* release profile showed that the pH of release medium played a significant role. At physiological pH of 7.3 there was only 15% methotrexate release while nearly 86% of methotrexate was observed at acidic pH of 4.0 over 72h. Release data fitted well into korsemeyer-peppas model of drug release (R^2=0.9868) indicating swelling controlled release of methotrexate. Further, the cytotoxic cell viability assay on SK-BR-3 (breast adinocarcinoma) cells showed that loaded methotrexate showed higher cell viability (17%) as compared to free methotrexate (29%) after 96h of incubation. The fluorescent cell imaging revealed that methotrexate released slowly from the nanoparticles and diffused into the nucleus without losing its cytotoxic effect on the cancer cells.

CHAPTER 1

1. Introduction and Literature

1.1 Background

1.1.1 Polymer Nanoparticles (PNPs)

The field of PNPs is rapidly escalating and playing an important role in a broad range of areas such as pharmaceutics, biotechnology etc [1-3]. Polymers are incredibly suitable materials for fabrication of diverse nanoparticle structures having many applications [4]. Both natural and synthetic polymers play a pivotal role in various life processes [5].

PNPs are the colloidal particles generally in the range 10-1000 nm [6-8]. These particles can be modified in response to temperature, pH etc. and can undergo reversible physical and chemical changes. This versatile nature of PNPs is responsible for their increased use as carriers for drug delivery systems [5].

1.1.2 Biodegradable Polymers

These are specific types of polymers which break down after their intended use to the natural by-products. Biodegradable PNPs are often applied for improving the impact of various types of hydrophobic/hydrophilic medicines and some bioactive agents as they break down after their intended use to the natural by-products [9]. Sodium alginate, chitosan, gelatin and albumin are used for preparation of biodegradable PNPs made of naturally occurring common polymers. Several co-polymers like Poly-lactides (PLA), Poly-glycolides (PGA) Poly-lactide-co-glycolides (PLGA), Poly-ϵ-Caprolactone (PCL), Poly(vinyl alcohol) (PVA), Poly(N-vinyl pyrrolidone) (PVP), Poly-cyanoacrylate (PCA) etc. are also used.

(a) Poly-d,l-lactide-co-glycolide (PLGA)

Due to the ability of PLGA to undergo breakdown in the body to naturally occurring metabolites viz., lactic acid and glycolic acid, it's considered as the most effective biodegradable PNP to develop nanomedicine systems [10].

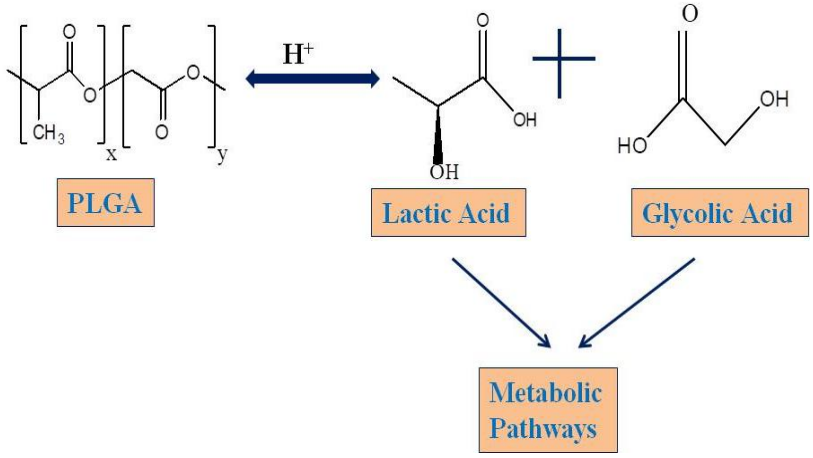

Scheme 1.1. Breakdown of PLGA

(b) Poly-lactic acid (PLA)

PLA degrades to its natural monomeric unit i.e., lactic acid that is further utilized in the metabolic pathway of carbohydrates. This property of PLA renders it biocompatibility and biodegradability [11].

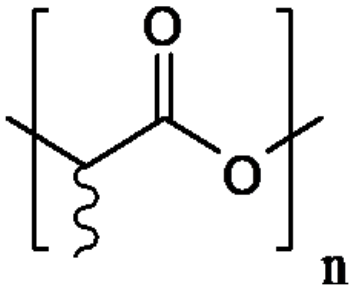

Scheme 1.2. Structure of PLA

(c) Chitosan

Chitosan is a natural polymer obtained by deacytylation of its biopolymer chitin. It's a mucoadhesive polycationic polymer at acidic pH which is not harmful and is biocompatible [12].

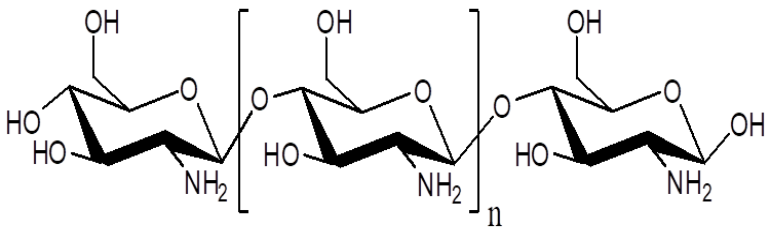

Scheme 1.3. Structure of Chitosan

1.1.2.1 Improved Drug Delivery

Controlled drug release and successive biodegradation are vital for developing successful formulations.

So to improve the degradation and loss of the drug and to improve its bioavailability, a variety of drug delivery systems are underway and the soluble biodegradable polymer formulations are one of the ways to improve the efficacy of the drugs.

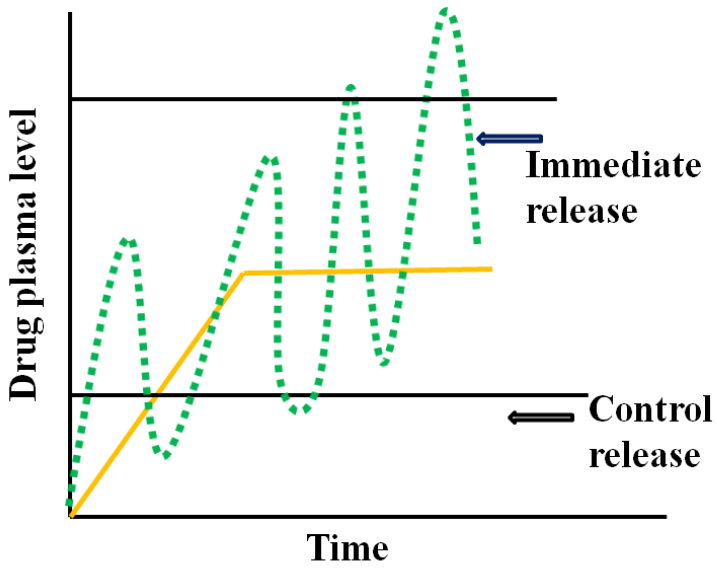

Scheme 1.4. Scheme showing advantage of controlled release over immediate release of drug

1.1.3 Why biodegradable polymer nanoparticles?

The drug loaded biodegradable PNPs improve the specificity, tolerability, efficiency and therapeutic value of the medicines [13-18] along with improvement in its premature loss and interaction of the drug with biological surroundings [19].

Also, nanodrug formulations are superior to traditional medicines w.r.t. its control release, target delivery and therapeutic efficiency. The target capability of these nanodrug formulations are affected by various parameters like surface modification, size of particle, charge on the surface and their hydrophobic nature. Among these, size of particles and distribution of size of NPs are the key factors in determining the interaction of the NPs with cell membrane and diffusion across the blood brain barriers [20, 21]. Surface charge is also an important parameter to determine if the NPs would agglomerate in blood stream or would stay as such, or interrelate with oppositely charged cells [22, 23].

Since last decade, studies have been carried out for the development of effective nanomedicines using biocompatible and biodegradable polymers [6]. Anitha et al. [24] have evaluated the ability of ortho-carboxymethyl chitosan to be used as transporter for water insoluble drugs in cancer drug delivery application. They used solvent evaporation technique followed by ionic gelation for the development of a NF based on ortho-carboxymethyl chitosan, to this curcumin the hydrophobic anticancer drug, was loaded. Quinones et al. [25] studied the sustained release profile of diosgenin monosuccinate attached to Cs. The study showed that upon introduction of appropriate changes in the steroidal moiety and linking it to

Cs, it would be an efficient pH reliant delivery system for sustained release of steroidal onco drugs.

The effect of surfactant/stabilizer on the particle size of Cs NPs was assessed w.r.t. encapsulation efficiency, swelling, and release profile of isonaizid in altered mediums. Swelling studies provided an important information about diffusion of drug, indicating Cs NPs were extremely susceptible to the change in pH of the environment [26]. Further, the release mechanism of the drug from polymer particles was tailored by varying the molecular weight of the polymer used [27-29]. In order to attain the desired properties of interest mode of preparation also played an important role [8]. The general method of synthesis and encapsulation of biodegradable nanomedicines is given in scheme 1.5. According to structural assembly, biodegradable PNPs can be nanospheres or nanocapsules. The drug molecules are either adsorbed on the surface or entrapped inside the polymer matrix [30, 31].

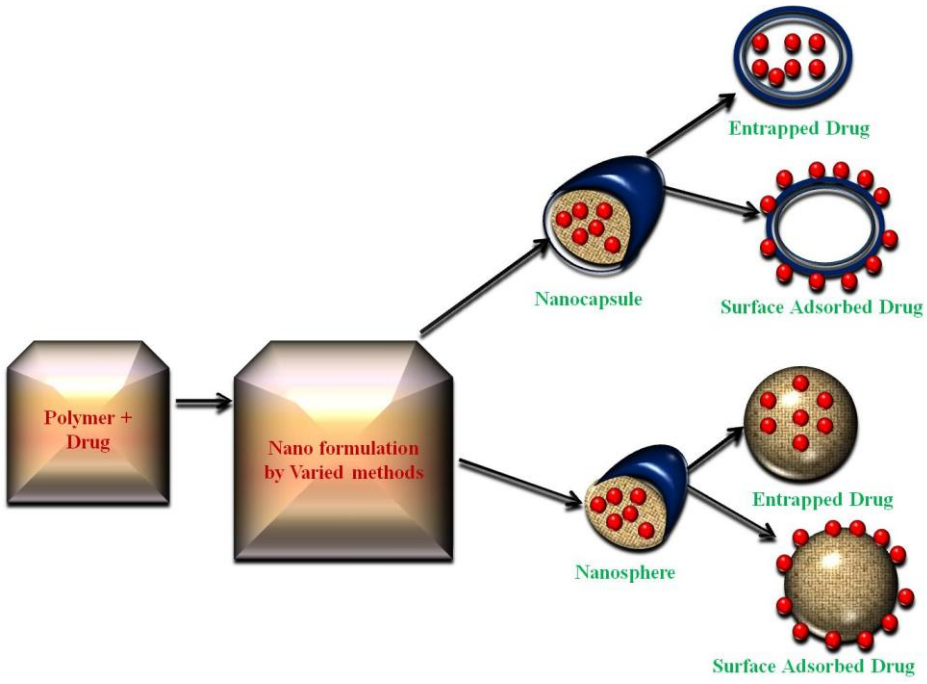

Scheme 1.5. Types of biodegradable nanoparticles

These biodegradable polymeric drug carriers (table 1.1) transfer the drug at the desired site through physio-chemical mechanism, i.e., either by diffusion, dissolution or degradation from the polymer matrix.

Table 1.1: Various polymeric nanoparticles and their release mechanism.

Polymer	Structure of Polymer	Surface modification	Release mechanism	References
PLGA	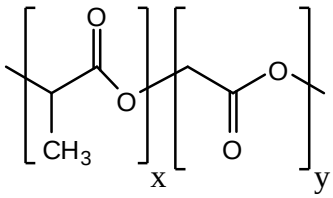	Poly(ethylene glycol)	Dissolution and diffusion	[32, 33]
PLA	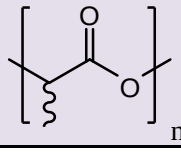	Poly(ethylene glycol)	Diffusion and degradation	[34, 35]
Chitosan	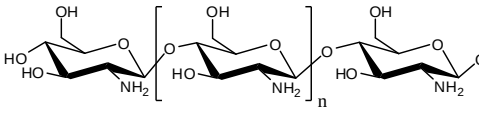	Poly(ethylene glycol)	Dissolution and diffusion	[36]
PCL	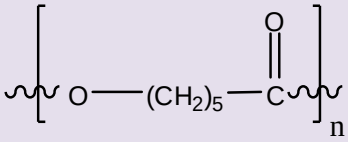	Pluronics , Methylpoly (ethylene glycol)	Diffusion	[9, 37]

Surface modification or functionalization of the PNPs is another factor to achieve the desired characteristics. For increasing the stability, retention time permeability, etc. the PNPs were coated/modified with different hydrophilic materials like poloxamer, PEG, dextran, etc [30]. Parveen et al. [38] reported the development of a surface coating by hydrophilic polymer PEG which was used to limit the phagocytic properties and to boost the endurance of the NPs. Hydrophilic PEG-82 was incorporated as a supplementary polymer coating to form PLGA–CS–PEG NPs and to further evaluate the effect of PEG modification for reducing the macrophage uptake for *in vitro* and *in vivo* experiments. Banik et al. reported the effect of particle size on the properties of chitosan-montmorillonite nanoparticles loaded with isonaizid.

The effect of surfactant coating on particle size of Cs NPs has been assessed with regard to swelling, encapsulation efficiency and release of isonaizid in different mediums. Swelling experiments provided an important information on drug diffusion properties signifying that the Cs NPs were highly sensitive to the pH of environment [26]. Z. Deng et al.

[39] investigated the use of silica coated hollow chitosan nanospheres for the release of model protein BSA from its matrix. They reported about 83% of BSA release Cs-SiO_2 hollow NPs from PBS at pH 4.0 compared to when released (17.4%) at pH 7.4. This variation in release behaviour of BSA is attributed to swelling behaviour of Cs-SiO_2 hollow NPs in acidic medium.

Although these nanocarreirs tend to protect the drug from degradation or enzymatic attack yet they tend to lack resistance to long term storage in many cases. This property can be modified using another thermo responsive polymer pNIPAM, which can endure the changes occurring due to change in the temperature. Thus, pNIPAM have a great potential in the field of biomedical applications [40]. Hence, the shape of PNPs also plays an important role in loading maximum drug onto the PNPs. For instance, hollow nanospheres have vast potential as drug carriers because of their high surface to volume ratios and low effective densities [41]. Melguizo et al. [42] explained the use of hollow poly(4-vinylpyridine) NPs for the loading of PTX to enhance the therapeutic efficacy of the drug for breast and lung cancer. They reported the uniform release of PTX after a fast release on first day in acidic medium. Also, Chao et al. reported the use of hollow Cs NPs for the loading of poorly water soluble/hydrophobic drugs [43]. The superior bioavailability and sustained release of PTX from Cs matrix was observed. Cs was found to be biodegradable and non-toxic upon degradation in *in-vitro* cytotoxicity experiments.

In the past several years, iron oxide (Fe_3O_4) NPs has gained attention to a greater extent. These NPs have the potential to be used as diagnostic agents. In association with other biodegradable PNPs, the Fe_3O_4 NPs can be used in targeted delivery [44]. El-Boubbou et al. [45] reported the preparation of chemotherapeutic agent formed of stabilized metal oxide NPs, which was found to be more efficient than free doxorubicin for the treatment of acute myeloid leukaemia (AML).

1.2 Research gaps

Literature survey revealed that drug loaded nanoparticles are mainly prepared from PLGA and chitosan polymers with drugs like lamivudine, isonaizid etc. by solvent evaporation method followed by ionic gelation. These PNPs are mainly having spherical shape the range of 100-400 nm. The drug binds to the polymer due to its affinity towards cationic charge over the polymer surface. About 60% of the drug is entrapped by means of adsorption. When the

drug loaded PNP is dispersed in biological pH medium like phosphate buffered solution, then about 50% of the drug was released from the polymer matrix due to diffusion of the drug through the surface of polymer or by direct degradation of the polymer matrix.

The interaction of polymer with the drug is an important parameter for drug loading. It mainly depends upon the nature of drug like the presence of functional group, its hydrophillicity or hydrophobicity, physical properties of the polymer like the shape, size and the charge over the surface of polymer due to presence of various kinds of functional groups.

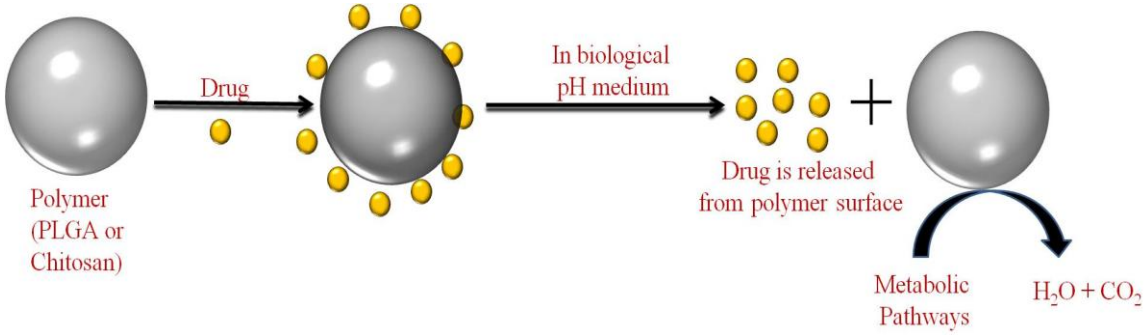

Scheme1.6. Entrapment of drug over surface of polymer

Shape and size of the prepared NP also influence the entrapment efficiency and release kinetics of the drug. As reported in the literature, the size range of the prepared nanoparticles is not a quantum size because larger the size, small amount of drug will be adsorbed on the surface of polymer and lesser will be the entrapment efficiency, in view of availability of only external surface for drug adsorption (Scheme1.6). Different anisotropic shapes like hollow nanospheres also affect the EE and release kinetic profile of the drug.

Smaller size of particles has an advantage over the larger ones because of higher surface area to volume ratio, which in turn influences the surface porosity and thickness, thereby helping greater adsorption of the drug over the polymer matrix. Size of prepared polymer nanoparticles also depends on the polymer to drug ratio. With higher ratio, particle aggregation can take place resulting in larger solid mass with lesser affinity towards the drug. The surface to the charge ratio is also an important factor for the entrapment of drug. Similar charge on the surface of polymer and the drug will repel each other and lesser drug would be entrapped. Addition of different surfactants like PEG, PVA, Pluronics etc., can stabilize this charge difference by providing the appropriate charge resulting in improvement in the entrapment efficiency. The affect in entrapment efficiency and release kinetics of the drug from nanoparticles with different anisotropic shapes as a function of surface thickness and porosity of the prepared PNPs is shown in Scheme 1.7.

For instance, the synthesis of hollow porous nanospheres with entrapped drug can have several advantages in slow release of the drug rather than being adsorbed over the surface of nanospheres. Less work has been reported regarding the synthesis of hollow nanospheres which could be advantageous for entrapping more of the drug and its slow release profile.

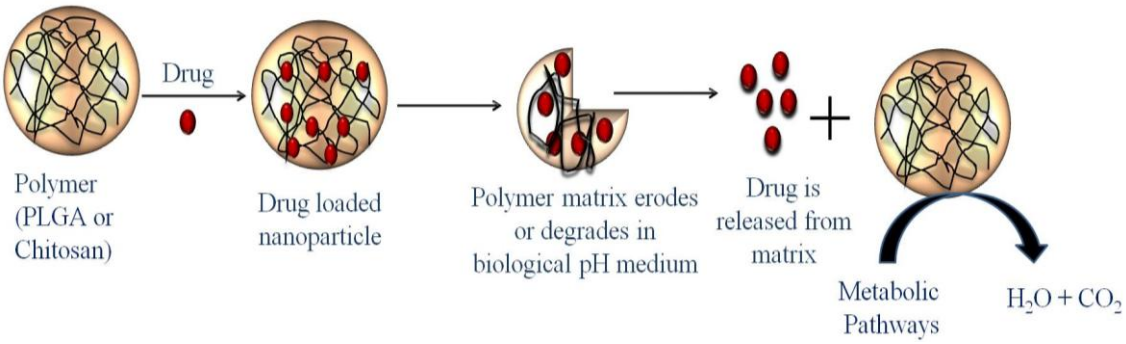

Scheme1.7. Release of drug from polymer matrix

Entrapment efficiency can be further improved with modification of the surface structure of nanoparticles by making them porous. The porous matrix of the hollow nanosphere will hold more of the drug within its pores, which will aid in its slow release. Moreover, the release of drug could be faster or slower depending upon the surface thickness of these PNPs with encapsulated drug. An optimum thickness could result in better release of the drug.

1.3 Objectives

Keeping in view the above points, the following objectives are designed:

- **(i)** Synthesis and characterization of biodegradable polymer (PLGA, PLA and Chitosan) for effective delivery of antihypertensive and anticancer drugs.
- **(ii)** Study of entrapment efficiency and drug content as a function of thickness and porosity of PLGA, PLA and Chitosan particles.
- **(iii)** *In-vitro* release kinetics to access the availability of drug from polymer particles.

1.4 Methodology

1.4.1 *Materials*

Poly-D,L-lactide-co-glycolide (50:50) $(C_3H_4O_2)_x(C_2H_2O_2)_y$, Poly-lactic acid $(C_3H_4O_2)_n$), Chitosan ($C_{56}H_{103}N_9O_{39}$) , Kolliphor P-188, N-isopropyl acryl amide (pNIPAM), Sodium dodecyl sulfate $CH_3(CH_2)_{11}OSO_3Na$, N,N'-methylene bisacrylamide (N,N'-MBA), Ammonium persulfate ($(NH_4)_2S_2O_8$), PEG 6000, Tween 80, Ferric chloride hexahydrate ($FeCl_3.6H_2O$), Ferrous chloride tetrahydrate ($FeCl_2.4H_2O$), Ramipril ($C_{23}H_{32}N_2O_5$),

Methotrexate ($C_{20}H_{22}N_8O_5$), Acetone (CH_3COCH_3), Glacial acetic acid (CH_3COOH), Ammonium hydroxide (NH_4OH) and De-ionized water (H_2O).

1.4.2 *Synthesis of polymer particles*

The biodegradable PNPs were prepared by single emulsion technique based on solvent evaporation [46, 47] and nanoprecipitation method [48, 49] shown in scheme 1.8. The performed polymers were dissolved in suitable solvent (acetone, DMSO, etc.) and stabilized with different surfactants (Pluronic F-68, Tween 80) etc. The organic phase was added to continuously stirred aqueous phase containing stabilizer (PVP, PVA, etc). After stirring the solution, synthesised NPs were collected by centrifugation and lyophilized for further characterisation. By varying the polymer to surfactant ratio and temperature conditions, different sizes and shapes (hollow nanospheres) of NPs were synthesized.

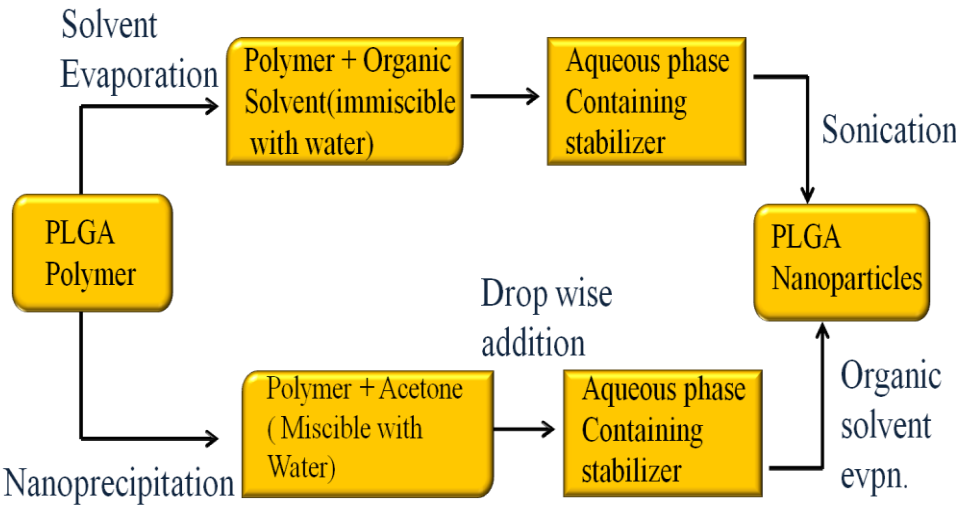

Scheme1.8. Flow chart for polymer particle synthesis

1.4.3 *Preparation of PLA / PLGA core*

The polymer core was prepared using single emulsion technique as reported elsewhere [50] shown in scheme 1.9. 0.25 g of PLA / PLGA was dissolved in 10 mL of DCM followed by addition of 20 mL of 1% KP-188 and homogenized with sonicator for 2 minutes. The emulsion was added to the continuously stirred aqueous phase (50 mL) and was kept overnight as such for complete evaporation of DCM. Core particles were washed four times with distilled water followed by centrifugation for 10 minutes at 10,000 rpm.

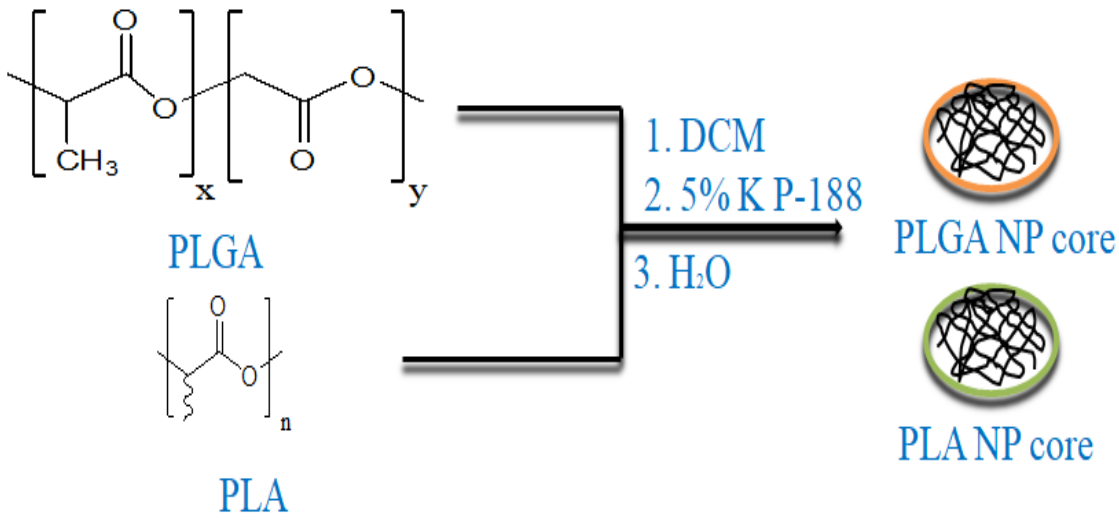

Scheme1.9. Schematic representation of PLA / PLGA core preparation

1.4.4 *Encapsulating pNIPAM shell over PLA/PLGA core*

The encapsulation was carried out using free radical polymerization technique under nitrogen atmosphere [51-53] as shown in scheme 1.10. pNIPAM (0.225 g), N,N'-MBA (0.017 g), SDS (0.01g), and APS (0.012g) were dissolved in distilled water and the contents were purged with nitrogen. 20 mL of the core solution was added to a three necked RB flask and solution was equilibrated for 20 minutes with constant stirring at 70^0C under nitrogen atmosphere. Further, 10 mL of the pNIPAM solution was mixed with the core solution and polymerization was allowed to continue. 5 mL of additional pNIPAM solution was added after 30, 50, 70 and 90 minutes respectively. After the final addition of pNIPAM solution, polymerization was allowed to continue further for 6 hours. Purification was carried by centrifugation using distilled water.

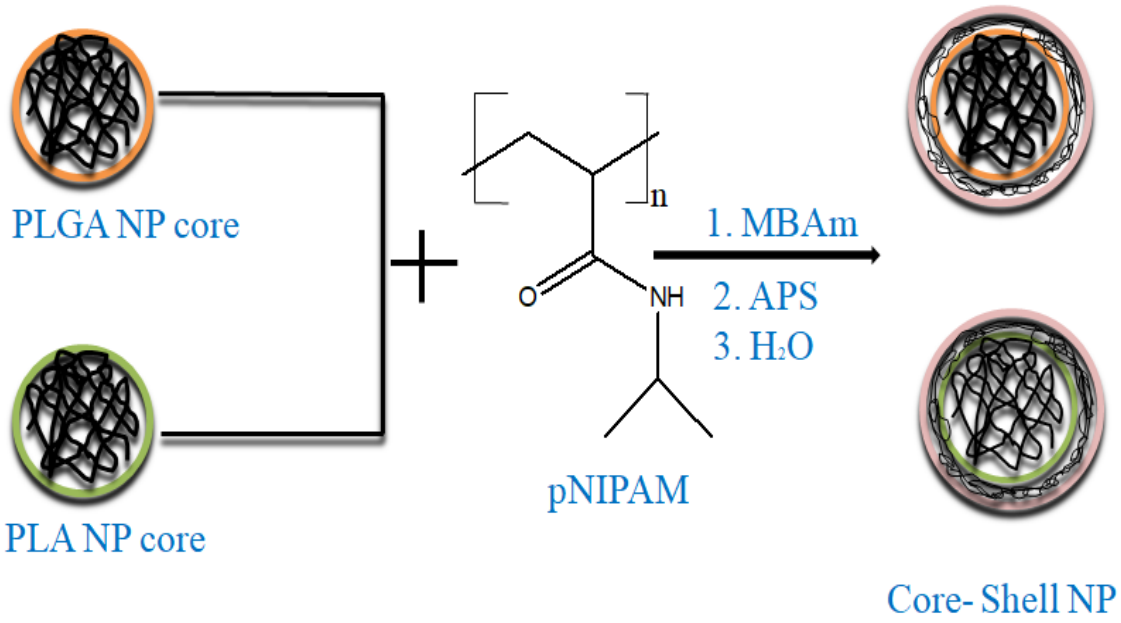

Scheme1.10. Schematic representation of encapsulation of pNIPAM shell over PLA/PLGA core

1.4.5 *Synthesis of ramipril loaded nanoparticles*

The ramipril loaded nanoparticles were synthesized using nanoprecipitation method [54]. The core plus shell nanoparticles were dissolved in acetone (25 mL) and ramipril (5mg) was solubilized in this solution. The contents were added drop wise to 50 ml of distilled water containing (200 mg) KP-188. The suspension was stirred for 6 hours. Acetone was evaporated using rota-evaporator and the volume of the suspension was made 10 ml with distilled water. The nanosuspension was centrifuged and drug loaded polymeric aggregates were collected.

1.4.6 *Preparation of PLGA nanoparticle template*

Single emulsion technique based on solvent evaporation was used to prepare the PLGA template as reported previously elsewhere with slight modifications [55, 56]. PLGA (0.2 mg) dissolved in 5 ml acetone and mixed with Tween 80 (600 µL) formed the stable organic layer. The contents were added drop wise into a continuously stirring 1% PEG aqueous solution (50 mL) followed by stirring for 2 h. Acetone was removed from the solution under reduced pressure using rota evaporator, the nanoparticles so obtained were centrifuged for 15 minutes at 10,000 rpm. Slurry was redispersed in 10 ml of 1% SDS and mildly stirred for 4

hours again. This suspension of nanoparticles was centrifuged again to remove any additional SDS, and then lyophilized overnight to obtain the PLGA template NP.

1.4.7 *Preparation of core@ shell Cs@PLGA nanosphere*

Firstly, 0.4 mg chitosan was dissolved in 10 ml acetic acid (0.1 M) and the volume was made up to 50 ml with distilled water. This aqueous solution of Cs was added to the 0.2 mg of PLGA template and was stirred for 14 hours. The resultant nanospheres were centrifuged to eliminate redundant chitosan. The chitosan adsorbed PLGA template was redispersed in 10 ml (2% w/v) d,l-glyceraldehyde aqueous solution as cross-linker [57] for 40 minutes under stirring for the solidification of chitosan layer over the PLGA template. The contents were washed with distilled water, centrifuged and lyophilized overnight to obtain Cs@PLGA Ns.

1.4.8 *Preparation of ramipril loaded hollow Cs NS*

The Cs@PLGA NS were again redispersed in 10 ml of acetone and gently stirred for 4 h for complete removal of the PLGA core. After the dissolution of the PLGA core, the solution was centrifuged, washed and redispersed in aqueous medium, and lyophilized.

The hollow NS were redispersed in 1 mL acetone solution containing ramipril and stirred gently for 2 h. The ramipril loaded hollow-Cs was recollected using centrifugation.

1.4.9 *Preparation of magnetic (Fe_3O_4) nanoparticles*

The magnetic (Fe_3O_4) nanoparticles were prepared by chemical co-precipitation method previously reported [58-60] with slight modification. $FeCl_3.6H_2O$ (1.58g, 0.008mol) and $FeCl_2.4H_2O$ (3.78g, 0.014mol) were dissolved in deionized water (320mL) having a molar ratio of Fe^{3+}: Fe^{2+} 2:1. The solution was stirred at 75°C for 1 h. Concentrated $NH_3.H_2O$ (40mL) was added and the pH of solution was adjusted to 10. The contents were stirred further for another 1h and allowed to cool. The precipitates so obtained were washed five times with distilled water using centrifugation at 6000 rpm for 5 minutes. The Fe_3O_4 particles were dried at 70°C and sintered at 200°C for 2h.

1.4.10 *Preparation of Methotrexate (MTX) loaded Fe_3O_4 –PLGA-PEG particles*

Double emulsion method was employed to prepare MTX loaded particles. MTX (2.5mg/mL) aqueous solution was emulsified for 1 minute in 10mL DCM containing 120mg PLGA-PEG and 1mg Fe_3O_4. This phase was added dropwise into 50 mL aqueous solution of PVA (1%)

and was emulsified for 1 minute, stirred at room temperature for another 5 h. The solvent was evaporated in rota-evaporator. The obtained NPs were centrifuged and washed three times with distilled water. In order to increase the MTX encapsulation in the nanoparticles, the aqueous phase used for washing was saturated with MTX. Bare Fe_3O_4–PLGA-PEG particles were also prepared by this method without the addition of MTX.

1.4.11 *Determination of total drug content and entrapment efficiency*

Total amount of drug/unit volume present in the formulation was measured by properly dispersing 0.1 ml of PNP volumetrically in 5 ml of appropriate solvent. The amount of drug present was determined either spetrophometrically or by HPLC. Each set of experiment was performed in triplicate. Likewise, bare PNPs by similar processing were taken as control. The TDC was determined by the equation [61] :

$$\text{TDC} = \frac{\text{Absorbance of sample}}{\text{Absorbance of standard}} \text{x}100$$

Entrapment Efficiency was determined by analysing the clear supernatant obtained by centrifuging the developed PNP dispersion for 2 h. The EE was calculated as:

$$EE = \frac{\text{TDC} - \text{Df}}{\text{TDC}} \text{ x } 100$$

Where, Df = amount of drug present in clear supernatant.

1.5 Characterizations

Various sophisticated instrumental techniques used to characterize the nanoparticles to get an idea of structural, morphological and physiochemical properties, etc. are listed below:

1.5.1 *Ultraviolet-Visible Spectrophotometer (UV-Vis spectrophotometer)*

The measurement of the reduction of a beam of light after it passes through a sample was carried out by UV-Vis absorption spectroscopy. Absorption spectra give the information about size distribution and the nanoparticles formation. The principle of this instrument is that when sample is exposed to light (having suitable energy for electronic transition within the molecule), required energy is absorbed and the transition of electron takes place from lower energy level to higher energy level. **Analytic Jena, SPECORD 205** instrument was used in order to examine the characteristic absorbance band of the synthesized NPs. Aqueous

suspension of all samples were analyzed in a 3.5 ml quartz cuvette in the detection range of 190-1100 nm.

1.5.2 *Fourier-Transform Infrared (FTIR) Spectroscopy*

FT-IR spectroscopy was used to obtain information about polymer-drug linkages. The working principle is based on the fact that bonds and group of bonds vibrate at characteristic frequencies. When a sample is exposed with infrared radiations, absorbed infrared energy excites molecules into higher vibrational states, which is characteristic to that particular molecule. All the FT-IR analysis of the samples was carried out on FT-IR, **Agilent Cary 630** spectrometer. The electromagnetic spectrum range was 400 nm to 4000 nm.

1.5.3 *Dynamic Light Scattering*

This technique is used to determine the hydrodynamic size of NPs which have been dissolved in suspension or solution. The particle size distribution was determined by using a **Brookhaven 90 plus Particle Size Analyzer** by taking ≈ 2.5-3 mL of dispersed NPs solution in a cuvette. The Brownian motion of small particles in suspension causes the laser light to be scattered in different intensities. By measuring the time scale of these light intensity fluctuations, DLS can yield information regarding the average size or size distribution of particles in solution.

1.5.4 *Zeta Potential Measurement*

When the NPs are suspended in an aqueous medium, the adsorption or ionization of ions takes place on the NPs surface, which leads to the formation of an electrical double layer resulting in the development of net charge, called zeta potential (ζ). Therefore, zeta potential is an important tool for understanding the state of NP surface and also predicts the long term stability of the NPs. The measurements were carried out on **Brookhaven Zeta Plus** at 25ºC using a cuvette comprising a palladium electrode mounted on a machine support immersed in ≈ 2-2.5 mL of NCs solution.

1.5.5 *Thermogravimetric Analysis (TGA)*

This technique was used to measure the thermal stability of the samples by using **Shimadzu TGA50** instrument. Thermal stability of a material as function of time and temperature in an

inert atmosphere was analyzed. When a material was heated weight loss, occurs due to phase changes, water loss, structural decomposition and gas evolution.

1.5.6 *BET Surface Area Analysis*

Surface area of the prepared samples was analyzed by Brunauer, Emmett and Teller (BET) surface area analyzer by physical adsorption/desorption of N_2 gas on the solid surface of powder samples. **Smartsorb 92/93** single point instrument was used for this purpose where 100 mg of samples were heated prior to analysis for about 2h.

1.5.7 *Scanning Electron Microscope (SEM)*

The external morphology (shape and size) of all the samples were analyzed by scanning electron microscopy. Morphology, topography, crystallographic and composition information about the sample surface can be investigated from SEM images. A beam of electrons is focused on a selected area of a sample at the time of SEM analysis and therefore an exchange of energy from the electron beam to the sample surface takes place. The electron gun produces electron at the top, referred to as primary electrons and these electrons are then analyzed, amplified and translated into images. **JSM-7600F** (0.1 to 30 kV) instrument was used for SEM images analysis, where samples were placed on a specimen stub with conducting tape and then coated with a thin layer of gold to reduce sample charging.

1.5.8 *Transmission Electron Microscopy (TEM)*

Transmission electron microscope is used to identify finest structural details of individual particles and their statistical size and shape distribution in the samples. In this technique, a beam of electrons is allowed to transmit through the sample and interact with it, due to this interaction an image is formed which is magnified and focused onto an imaging device. In this research, **TEM Hitachi-7500** of 20-200 kV voltage with 2.4 Å resolution was used to investigate the morphology of samples. Aqueous suspension of the sample was dropped on copper grid coated with carbon film and then analyzed. Analysis was done at sophisticated laboratory such as IIT-Bombay and Panjab University, Chandigarh, India.

1.5.9 *Powder X-Ray Diffraction (P-XRD)*

This technique is primarily used for identification of phase, composition and crystal system of the materials; it can also give information on unit cell dimensions. For the identification of crystal system, phase, composition and crystallinity of the materials this technique was used.

PANalytica X' pert PRO X-ray diffractometer with Cu Kα (λ = 1.54 Å) radiation was used for XRD pattern analysis. A smooth plain surface paper was used to press the powder samples into a sample holder. The XRD study was done from Sophisticated Analysis Instrumentation Laboratory (SAI Lab), Thapar University, Patiala, India.

1.6 *In- vitro* release studies of synthesized NPs

Preweighed NPs were suspended in phosphate buffer solution (PBS) at pH 7.3 and acetate buffer solution (ABS) at pH 4.3 and subjected to dissolution. 5 mL aliquots were withdrawn at regular time intervals of 2h upto 24h and were replaced with an equal quantity of fresh buffer medium each time. Concentration of drug released was monitored spectrophotometrically and by HPLC.

1.7 References

[1] X. Wang, C.J. Summers, Z.L. Wang, Nano Letters, 4 (2004) 423-426.

[2] J. Jang, J.H. Oh, Chemical Communications, (2002) 2200-2201.

[3] S. Geetha, C.R. Rao, M. Vijayan, D. Trivedi, Analytica Chimica Acta, 568 (2006) 119-125.

[4] Z. Fan, M. Shelton, A.K. Singh, D. Senapati, S.A. Khan, P.C. Ray, ACS nano, 6 (2012) 1065-1073.

[5] C. Vauthier, G. Ponchel, Polymer Nanoparticles for Nanomedicines: A Guide for their Design, Preparation and Development, Springer, 2017.

[6] J. Kreuter, Colloidal drug delivery systems, CRC Press, 1994.

[7] P. Couvreur, Critical reviews in therapeutic drug carrier systems, 5 (1987) 1-20.

[8] J.P. Rao, K.E. Geckeler, Progress in Polymer Science, 36 (2011) 887-913.

[9] D.B. Shenoy, M.M. Amiji, International journal of pharmaceutics, 293 (2005) 261-270.

[10] R.H. Ansary, M.B. Awang, M.M. Rahman, Tropical Journal of Pharmaceutical Research, 13 (2014) 1179-1190.

[11] A.J. Lasprilla, G.A. Martinez, B.H. Lunelli, A.L. Jardini, R. Maciel Filho, Biotechnology advances, 30 (2012) 321-328.

[12] M. Prabaharan, Journal of biomaterials applications, 23 (2008) 5-36.

[13] U. Schroeder, H. Schroeder, B. Sabel, Life sciences, 66 (2000) 495-502.

[14] T. Safra, F. Muggia, S. Jeffers, D. Tsao-Wei, S. Groshen, O. Lyass, R. Henderson, G. Berry, A. Gabizon, Annals of Oncology, 11 (2000) 1029-1033.

[15] J. Kreuter, V. Petrov, D. Kharkevich, R. Alyautdin, Journal of controlled release, 49 (1997) 81-87.

[16] R.S. Raghuvanshi, Y.K. Katare, K. Lalwani, M.M. Ali, O. Singh, A.K. Panda, International journal of pharmaceutics, 245 (2002) 109-121.

[17] J.-C. Leroux, E. Allémann, F. De Jaeghere, E. Doelker, R. Gurny, Journal of controlled release, 39 (1996) 339-350.

[18] C.-M.J. Hu, R.H. Fang, B.T. Luk, L. Zhang, Nanoscale, 6 (2014) 65-75.

[19] F. Alexis, E. Pridgen, L.K. Molnar, O.C. Farokhzad, Molecular pharmaceutics, 5 (2008) 505-515.

[20] M. Rawat, D. Singh, S. Saraf, S. Saraf, Biological and Pharmaceutical Bulletin, 29 (2006) 1790-1798.

[21] Y. Tarahovsky, Biochemistry (Moscow), 75 (2010) 811-824.

[22] M.S. Muthu, S.-S. Feng, Nanomedicine, 5 (2010) 1017-1019.

[23] S.-S. Feng, Expert review of medical devices, 1 (2004) 115-125.

[24] A. Anitha, S. Maya, N. Deepa, K. Chennazhi, S. Nair, H. Tamura, R. Jayakumar, Carbohydrate Polymers, 83 (2011) 452-461.

[25] J.P. Quiñones, R. Szopko, C. Schmidt, C.P. Covas, Carbohydrate Polymers, 84 (2011) 858-864.

[26] N. Banik, A. Hussain, A. Ramteke, H.K. Sharma, T.K. Maji, RSC Advances, 2 (2012) 10519-10528.

[27] K. Derakhshandeh, M. Erfan, S. Dadashzadeh, European journal of pharmaceutics and biopharmaceutics, 66 (2007) 34-41.

[28] K. Derakhshandeh, G. Hochhaus, S. Dadashzadeh, Iranian journal of pharmaceutical research: IJPR, 10 (2011) 425.

[29] M. Afshari, K. Derakhshandeh, L. Hosseinzadeh, Journal of microencapsulation, 31 (2014) 239-245.

[30] A. Kumari, S.K. Yadav, S.C. Yadav, Colloids and Surfaces B: Biointerfaces, 75 (2010) 1-18.

[31] F. Danhier, E. Ansorena, J.M. Silva, R. Coco, A. Le Breton, V. Préat, Journal of controlled release, 161 (2012) 505-522.

[32] L. Brannon-Peppas, J.O. Blanchette, Advanced drug delivery reviews, 64 (2012) 206-212.

[33] F. Danhier, N. Lecouturier, B. Vroman, C. Jérôme, J. Marchand-Brynaert, O. Feron, V. Préat, Journal of controlled release, 133 (2009) 11-17.

[34] Z. Amoozgar, Y. Yeo, Wiley Interdisciplinary Reviews: Nanomedicine and Nanobiotechnology, 4 (2012) 219-233.
[35] K. Sonaje, J. Italia, G. Sharma, V. Bhardwaj, K. Tikoo, M.R. Kumar, Pharmaceutical research, 24 (2007) 899-908.
[36] E. Assaad, Y.J. Wang, X.X. Zhu, M.A. Mateescu, Carbohydrate Polymers, 84 (2011) 1399-1407.
[37] H. Xu, Z. Hou, H. Zhang, H. Kong, X. Li, H. Wang, W. Xie, International journal of nanomedicine, 9 (2014) 231.
[38] M. Rajan, V. Raj, International Review of Chemical Engineering, 5 (2013) 145-155.
[39] Z. Deng, Z. Zhen, X. Hu, S. Wu, Z. Xu, P.K. Chu, Biomaterials, 32 (2011) 4976-4986.
[40] N. Ormategui, S. Zhang, I. Loinaz, R. Brydson, A. Nelson, A. Vakurov, Bioelectrochemistry, 87 (2012) 211-219.
[41] X. Wang, J. Feng, Y. Bai, Q. Zhang, Y. Yin, Chemical reviews, 116 (2016) 10983-11060.
[42] R. Contreras-Cáceres, M.C. Leiva, R. Ortiz, A. Díaz, G. Perazzoli, M.A. Casado-Rodríguez, C. Melguizo, J.M. Baeyens, J.M. López-Romero, J. Prados, Nano Research, 10 (2017) 856-875.
[43] J. Jiang, Y. Liu, C. Wu, Y. Qiu, X. Xu, H. Lv, A. Bai, X. Liu, Drug Development and Industrial Pharmacy, (2017) 1-10.
[44] E. Woźniak, M. Špírková, M. Šlouf, V.M. Garamus, M. Šafaříková, I. Šafařík, M. Štěpánek, Colloids and Surfaces A: Physicochemical and Engineering Aspects, 514 (2017) 32-37.
[45] K. El-Boubbou, D. Azar, A. Bekdash, R.J. Abi-Habib, Journal of Biomedical Nanotechnology, 13 (2017) 500-512.
[46] S. Zhou, X. Deng, Reactive and Functional Polymers, 51 (2002) 93-100.
[47] A. Zaichenko, N. Mitina, O. Shevchuk, K. Rayevska, V. Lobaz, T. Skorokhoda, R. Stoika, Pure and Applied Chemistry, 80 (2008) 2309-2326.
[48] Z. Zili, S. Sfar, H. Fessi, International journal of pharmaceutics, 294 (2005) 261-267.
[49] I.L. Blouza, C. Charcosset, S. Sfar, H. Fessi, International journal of pharmaceutics, 325 (2006) 124-131.
[50] P. Xu, E. Gullotti, L. Tong, C.B. Highley, D.R. Errabelli, T. Hasan, J.-X. Cheng, D.S. Kohane, Y. Yeo, Molecular pharmaceutics, 6 (2008) 190-201.
[51] I. Berndt, W. Richtering, Macromolecules, 36 (2003) 8780-8785.
[52] C.D. Jones, L.A. Lyon, Langmuir, 19 (2003) 4544-4547.

[53] C.D. Jones, L.A. Lyon, Macromolecules, 33 (2000) 8301-8306.

[54] Z. Zili, S. Sfar, H. Fessi, Int J Pharmaceut, 294 (2005) 261-267.

[55] Y. Yang, W. Jia, X. Qi, C. Yang, L. Liu, Z. Zhang, J. Ma, S. Zhou, X. Li, Macromolecular bioscience, 4 (2004) 1113-1117.

[56] X. Deng, S. Zhou, X. Li, J. Zhao, M. Yuan, Journal of Controlled Release, 71 (2001) 165-173.

[57] B. Oliveira, M. Santana, M.I. Ré, Brazilian Journal of Chemical Engineering, 22 (2005) 353-360.

[58] A. Kumar, G. Sharma, M. Naushad, S. Thakur, Chemical Engineering Journal, 280 (2015) 175-187.

[59] P. Enzel, N. Adelman, K.J. Beckman, D.J. Campbell, A.B. Ellis, G.C. Lisensky, J. Chem. Educ, 76 (1999) 943-948.

[60] D. Schütt, Institute Angewandte Polymerforschung: thesis Selim MS, Cunningham LP, Srivastava R, Olson JM (1997). Preparation of nano-size magnetic gamma ferric oxide (γ-Fe_2O_3) and magnetite (Fe_3O_4) particles for toner and color imaging applications. Recent Progress in Toner Technologies, (2004) 108-111.

[61] S. Jagdale, Y. Dangat B. Kuchekar, International Journal of Pharmacy and Pharmaceutical Sciences, 4 (2012) 309-318.

CHAPTER 2

Section A: Ramipril embedded nanospheres of biodegradable poly-D, L-lactide-co-glycolide: To study their release kinetics

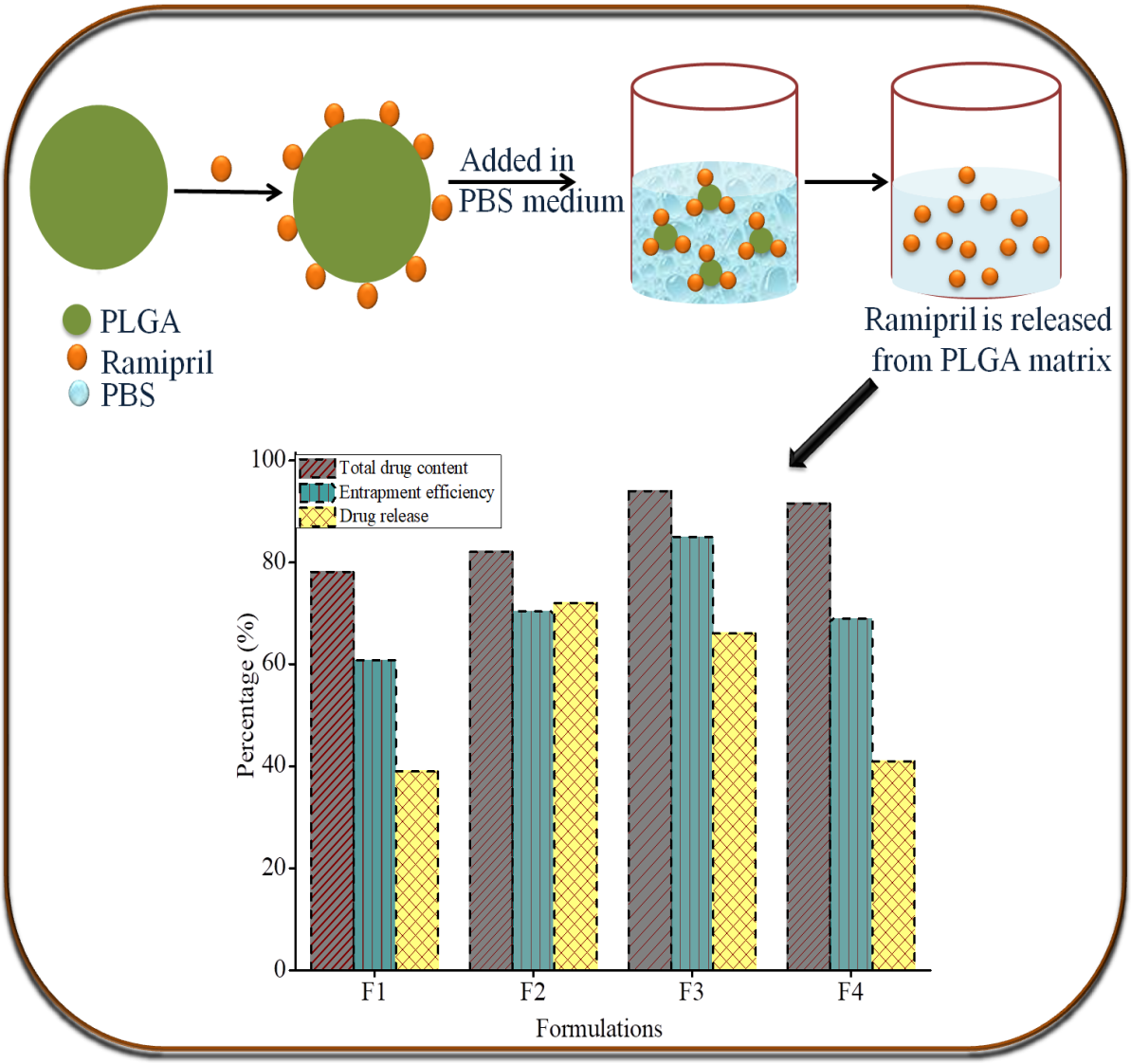

2.1 Introduction

It is estimated that about 40% of new chemical entities or many existing drugs, although efficient yet are poorly water soluble or lipophilic in nature leading to poor oral bioavailability and have high intra and inter-subject variability and lack of dose proportionality [1-3]. A new and novel field of biodegradable polymer nanoparticles (PNPs) is emerging. Over the past few decades, there has been considerable interest in developing biodegradable nanoparticles (NPs) varying from 10-1000 nm [4-6] as effective drug delivery devices.

Liposomes have been used as potential drug carriers instead of conventional dosage forms because of their unique advantages like their ability to protect drugs from degradation, target the drug to the site of action and to reduce its toxicity or side effects [7-9]. However, developmental work on liposome has been limited due to inherent problems such as low encapsulation efficiency, rapid leakage of water-soluble drug in the presence of blood components and poor storage stability. However, polymeric NPs offer some specific advantages over liposomes. For instance, NPs help to increase the stability of drugs/proteins and possess useful controlled release properties. Polymers are very convenient materials for the manufacture of numerous and varied molecular designs that can be integrated into unique nanoparticle structures with many potential medical applications [10, 11]. Among those, polymeric nanoparticulate systems from biodegradable and biocompatible polymers are interesting alternative for controlled drug delivery and drug targeting [12-17]. PLGA has gained attention for the preparation of wide variety of delivery systems containing several drugs [18-21] due to its biodegradability, biocompatibility [22-27] and low toxicity [28-30] and has been approved for human use by FDA [22, 31-33].

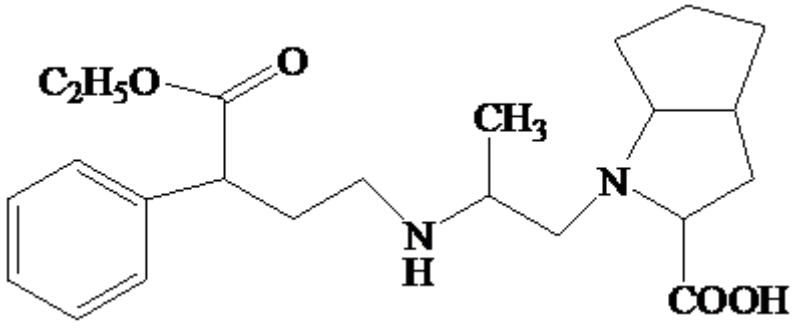

Figure 2.1: Structure of Ramipril

The copolymers of PLGA degrade in body via hydrolytic cleavage of ester linkage to lactic and glycolic acid. These two monomers are then metabolized in body through Krebs cycle and are finally eliminated in the form of CO_2 and H_2O [31, 34-37]. Ramipril [(2S,3aS,6aS)-1[(S)-N-[(S)-1-carboxy-3-phenylpropyl]alanyl]octahydrocyclopenta[b]pyrrol-2-carboxylic acid-1-

ethyl ester] (figure 2.1) is a potent and long acting angiotensin converting enzyme (ACE) inhibitor. Ramipril inhibits ACE and reduces the angiotensin II levels resulting in the reduction of aldosterone secretion leading to lowering of blood pressure [38-41]. In hypertensive patients, ramipril is used to treat high blood pressure (hypertension), congestive heart failure and chronic renal failure [42-46]. Peak plasma concentrations of active metabolite of ramipril i.e., ramiprilat are reached within 2 to 4h and the absolute bioavailability of ramipril and ramiprilat are 28% and 44% respectively. Moreover, ramipril show poor solubility in aqueous medium. As PLGA is easily metabolized in body by enzymatic actions so it will not hinder with the action of drug during its release and will provide a suitable medium for this lipophilic drug.

Hence, ramipril loaded PLGA nanoparticles using tribloere polymeric stabilizer (Kolliphor P-188) were prepared and studied for its release profile from polymer with an aim to improve its dissolution rate for increase in its activities.

2.2 Experimental section

2.2.1 Materials

Poly-D,L-lactide-co-glycolide (50:50) and Kolliphor P-188 were purchased from Sigma-Aldrich. Ramipril was received as a gift sample from Mefro Pharmaceuticals (Mohali, Punjab, India). All other reagents were obtained from Loba Chemie, India and used as received without further purification. De-ionized water was obtained using an ultra filtration system (Milli-Q, Millipore).

2.2.2 Synthesis of drug loaded nanoparticles

Synthesis of drug loaded NPs was done using nanoprecipitation method [47]. The details are given in **Chapter 1, section 1.4.2 and 1.4.5.**

PLGA (125/250 mg) was dissolved in 25 ml of acetone and ramipril (5mg) was solubilized in this solution. The contents were added drop wise to 50 ml of deionised water containing (100/200 mg) Kolliphor P-188. Composition of nanosuspensions of K P-188: PLGA by weight was F_1 (1:1.25), F_2 (1:2.50), F_3 (1:0.62), F_4 (1:0.80) and is given in table 2.1.

Table 2.1. Composition and polydispersity of various formulations.

Formulation code	Amount of PLGA (mg)	Amount of Acetone (ml)	Amount of Ramipril(mg)	Amount of Kolliphor P-188 (mg)	Amount of water (ml)	Polydispersity Index
F_1	125	25	5	100	50	0.179
F_2	250	25	5	100	50	0.032
F_3	125	25	5	200	50	0.119
F_4	250	25	5	200	50	0.125

2.2.3 Drug content and Entrapment Efficiency of ramipril

The determination of total drug content and entrapment efficiency was determined spectrophotometrically, the details are provided in **Chapter 1, section 1.4.11.**

2.2.4 Characterization

Synthesized NPs were characterized by various techniques like UV-Vis, FTIR, DLS, SEM and TEM, the details of these techniques are given in **Chapter 1**, **section 1.5**.

2.2.5 In-vitro drug release of ramipril and kinetic studies

The amount of drug released was determined at 207 nm with UV-vis spectrophotometer **(Chapter 1**, **section 1.4.12)**. The data obtained from the *in-vitro* release study of the different formulations (F_1-F_4) was fitted into various models of drug release kinetics and resulting regression coefficient values were calculated. The data was also fitted into korsemeyer-peppas model to determine the release exponent 'n' value for describing the mechanism of drug release.

2.3 Results and Discussion

2.3.1 Structural and morphological characterization

The UV-vis absorption of ramipril showed absorption bands at 237 nm and 257nm, whereas formulations (F_1-F_4) showed only one absorption band at 207 nm (figure 2.2). The absence of bands of ramipril indicates entrapment of ramipril in PLGA.

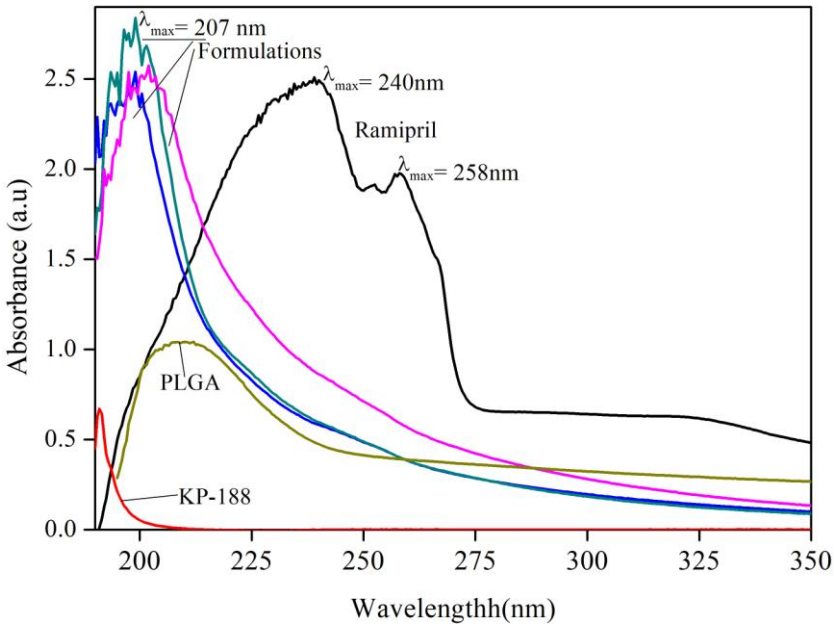

Figure 2.2: UV-Vis absorption spectra of Ramipril, PLGA, K P-188 and Formulations

The FT-IR spectra of ramipril, PLGA and formulation are shown in figure 2.3. Ramipril showed absorption band at 3277 cm^{-1} due to –NH and –OH stretching's of acid group [48, 49], bands at 2930 cm^{-1} and 2860 cm^{-1} appear due to C-H aromatic stretching and C-H aliphatic stretching's, respectively. The band at 1748 cm^{-1} and 1644 cm^{-1} are due to C=O of acid and ester groups. C-H aliphatic vibrations are observed in the fingerprint region. The

spectra of PLGA showed C=O absorption at1748 cm^{-1} and C-H deformation of O-CH_2 group at 1414cm^{-1} [50]. In the formulation, absorption bands at 1748 cm^{-1} and 1644 cm^{-1} are due to carbonyl and ester groups of acid. Moreover, band at 2860 cm^{-1} have appeared due to C-H aliphatic stretching. An intense absorption band at 1088 cm^{-1} was observed in the formulation as PLGA show a band at 1081 cm^{-1}. The presence of bands at 2860 cm^{-1}, 1748 cm^{-1} and 1088 cm^{-1} indicated that chemical interaction that could alter the chemical structure of ramipril in formulation did not occur.

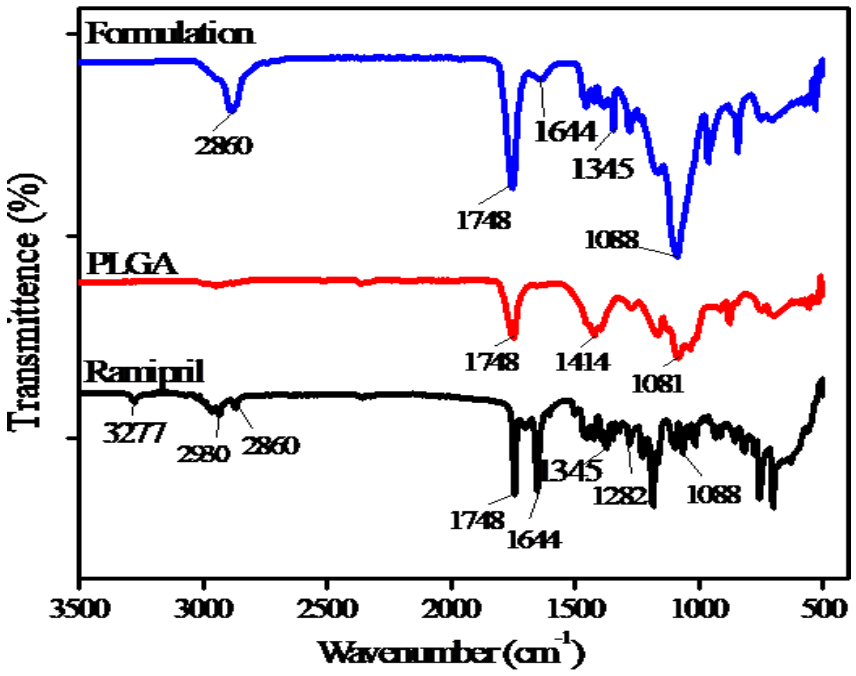

Figure 2.3: FTIR spectrum of Ramipril, PLGA and Formulation

DLS studies showed the average particle size of 121-156 nm for these formulations (figure 2.4). The variation in particle size of these formulations is due to different weights of K P-188 to PLGA in these formulations. The low polydispersity index (0.032-0.179) indicated that the particles were nearly uniform in size. The increase in PLGA amount resulted in increase in size of

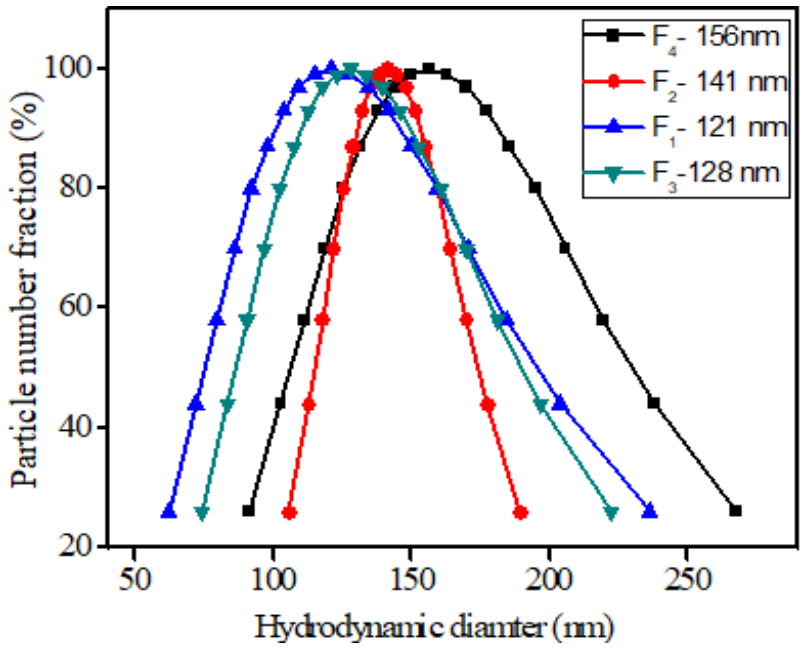

Figure 2.4: Average particle size distribution of various formulations

ramipril loaded particles which in turn facilitated aggregation. Addition of K P-188 stabilizer resulted in reduction of aggregation.

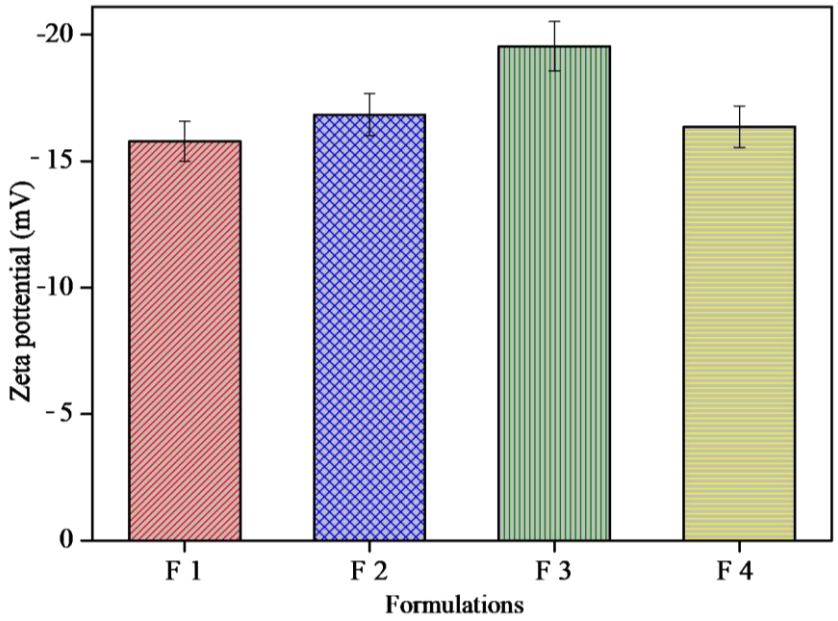

Figure 2.5: Zeta potential of various formulations

Zeta potential of the prepared formulations ranged from -15.78 to -19.54 mV (figure 2.5) indicating moderate stability of the nanosuspensions and its negative value indicates the presence of hydroxyl groups of PLGA. The SEM images of the nanoformulations are shown in (figure 2.6). The images indicate the entrapment of ramipril as discrete spherical nano patches within PLGA matrix. TEM studies (figure 2.7) showed that the size of nanoparticles (121-156 nm) in these formulations is in correlation with particle size distribution measured by dynamic light scattering (DLS) i.e., about 121-156 nm for these formulations.

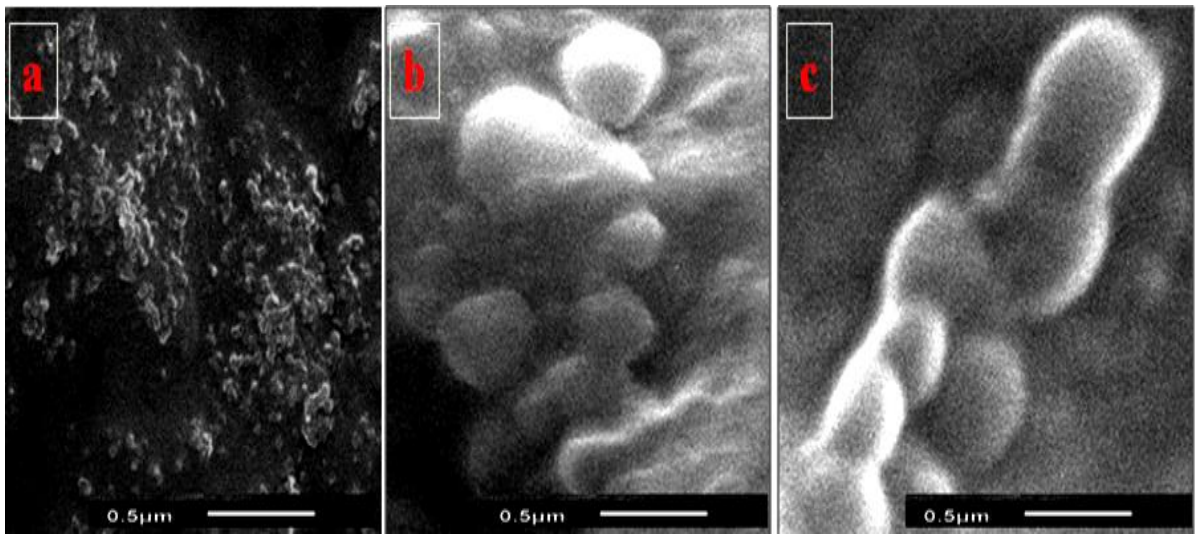

Figure 2.6: SEM images of ramipril loaded polymer particles

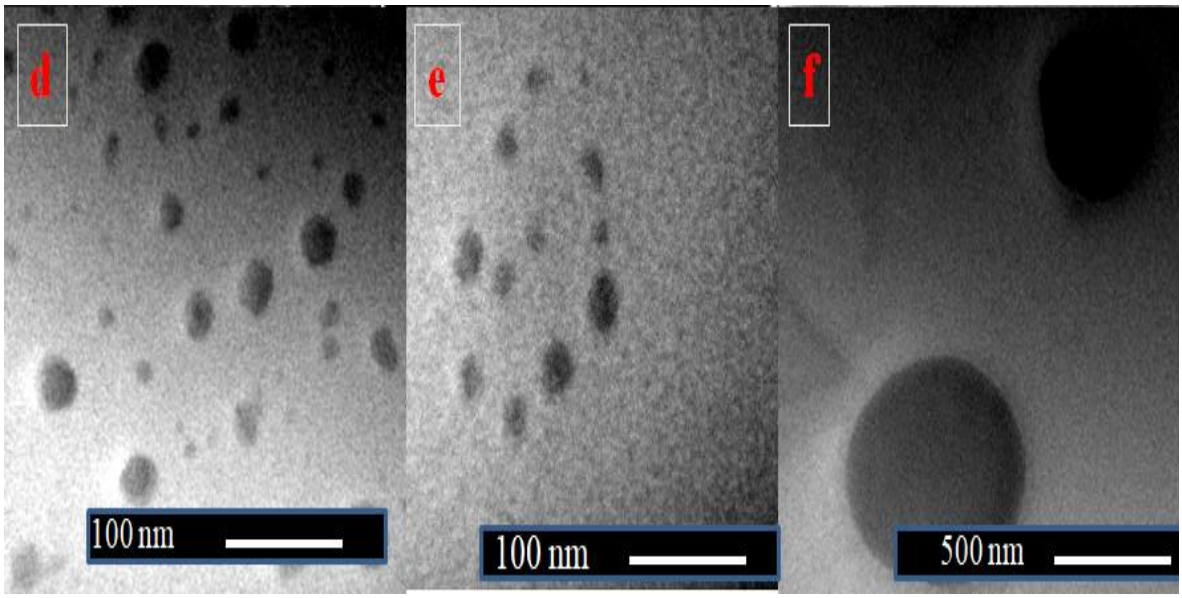

Figure 2.7: TEM images of the formulations

2.3.2 Drug content and Entrapment efficiency of ramipril

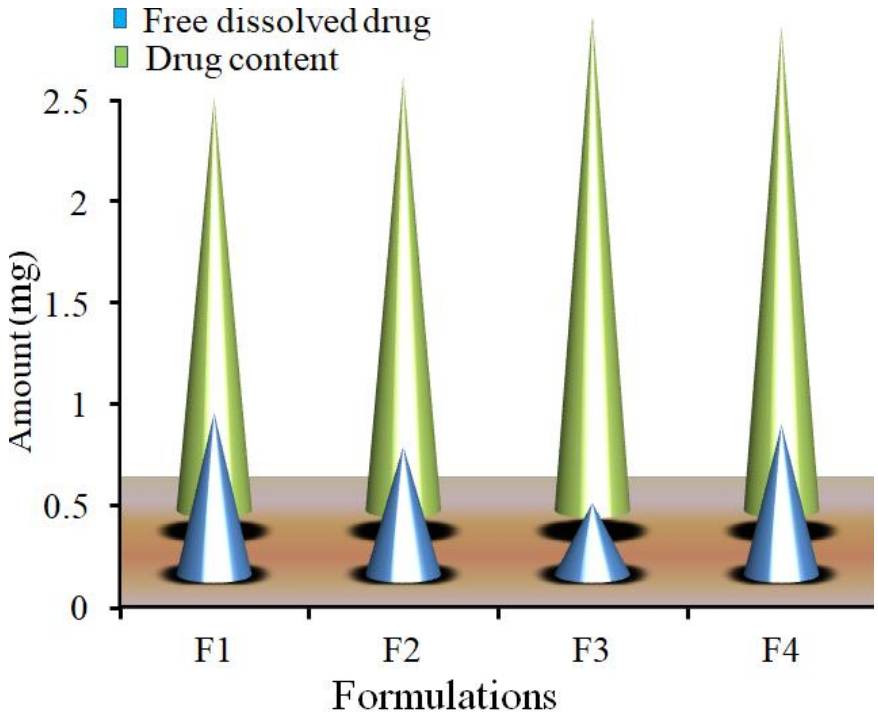

Figure 2.8: Drug content and free dissolved drug in various formulations

Total drug content was measured by UV-Vis spectroscopy at 207 nm. The nanosuspension was centrifuged and the free drug content was determined in clear supernatant and results are shown in figure 2.7 ranging from 0.355 mg – 0.799 mg due to limited solubility of ramipril in aqueous phase. The TDC in the nanosuspension varied from 2.04-2.39 (F_1-F_4).

It has been observed that drug content in the formulations increased with increasing amount of PLGA. Formulation F_3 showed maximum percentage (94%) of drug content (figure 2.9). It can be seen that entrapment efficiency also increased with increase in amount of PLGA.

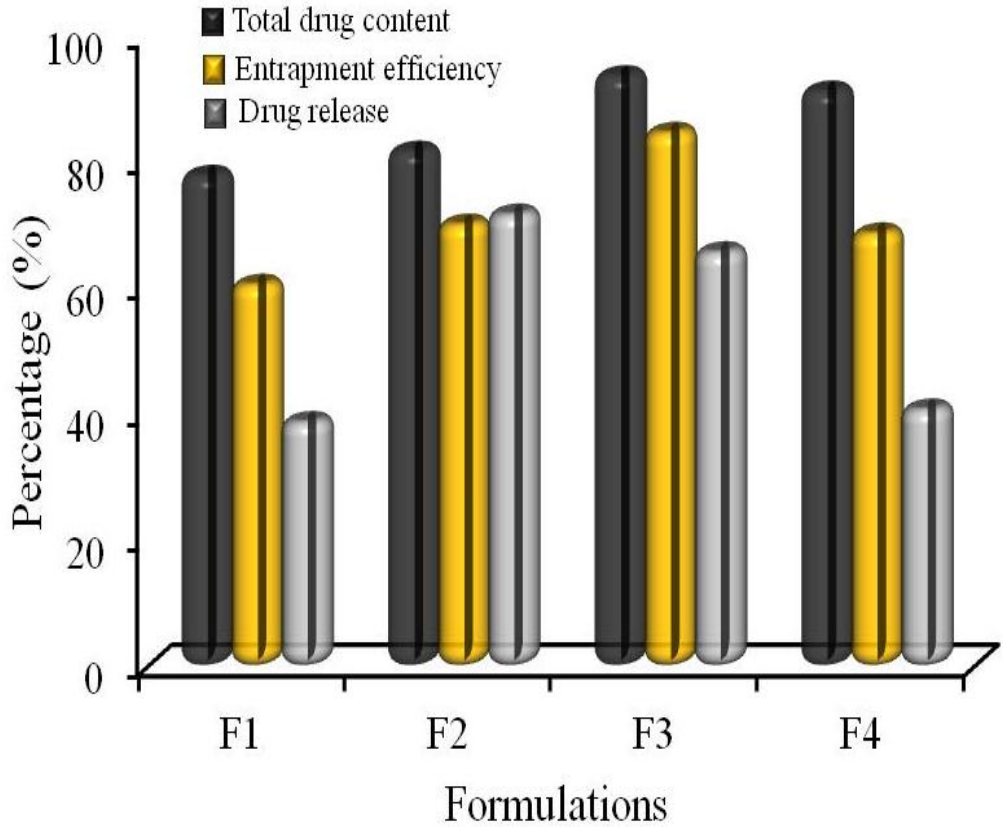

Figure 2.9: Percentage of total drug content, entrapment efficiency and drug release in the formulations

2.3.3 In-vitro release of ramipril

The release of ramipril from PLGA matrix in phosphate buffer solution (PBS) of pH 7.3 (figure 2.10) showed initial burst release followed by sustained release in F_2 and F_4 formulations. After 24 h of incubation in PBS, the percentage release of drug was 74% and 59% respectively in these formulations. The observed initial burst release of ramipril was due to free dissolved drug in the nanoformulations having high concentration of K P-188. On the other hand the nanoformulations (F_1 and F_3) having smaller size prepared using lower amount of PLGA showed higher release of drug in 24 h. This higher release of drug was seen because of greater adsorption of ramipril over the PLGA surface.

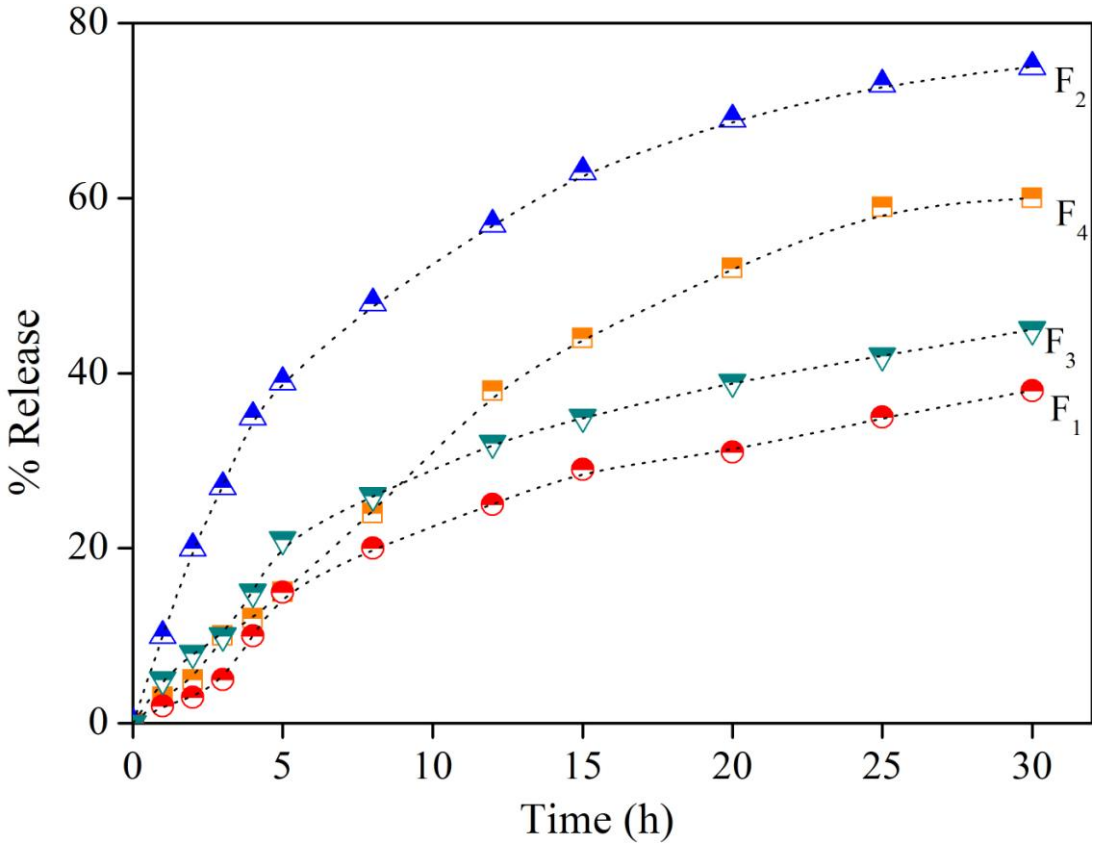

Figure 2.10: In-vitro release profile of drug in phosphate buffer solution

2.3.4 In-vitro release kinetics study

The release exponent (n) values for the different formulations obtained from fitting the drug release profile into the korsemeyer- peppas model are shown in figure 2.11. The 'n' value of 0.85- 1.0 obtained for (F_1-F_4) indicated that the drug release follows a zero order (figure 2.12) release mechanism and anomalous (non-fickian) diffusion mechanism [51-54] signifying that the release of ramipril from the matrix of PLGA is both diffusion as well as swelling controlled. Correlation coefficients of kinetic plots for formulations (F_1- F_4) are shown in table 2.2.

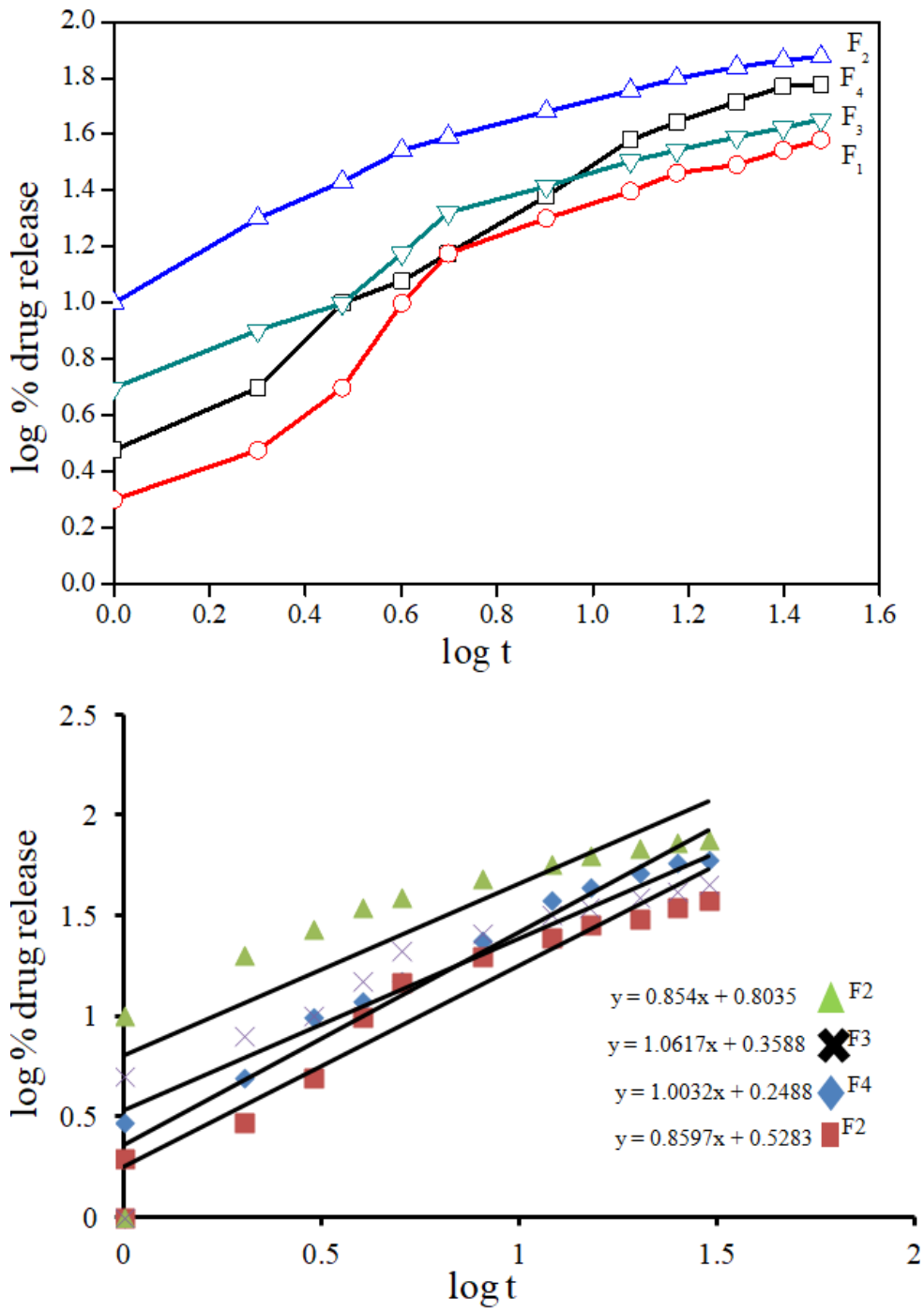

Figure 2.11: Korsemeyer-Peppas plot for various formulations

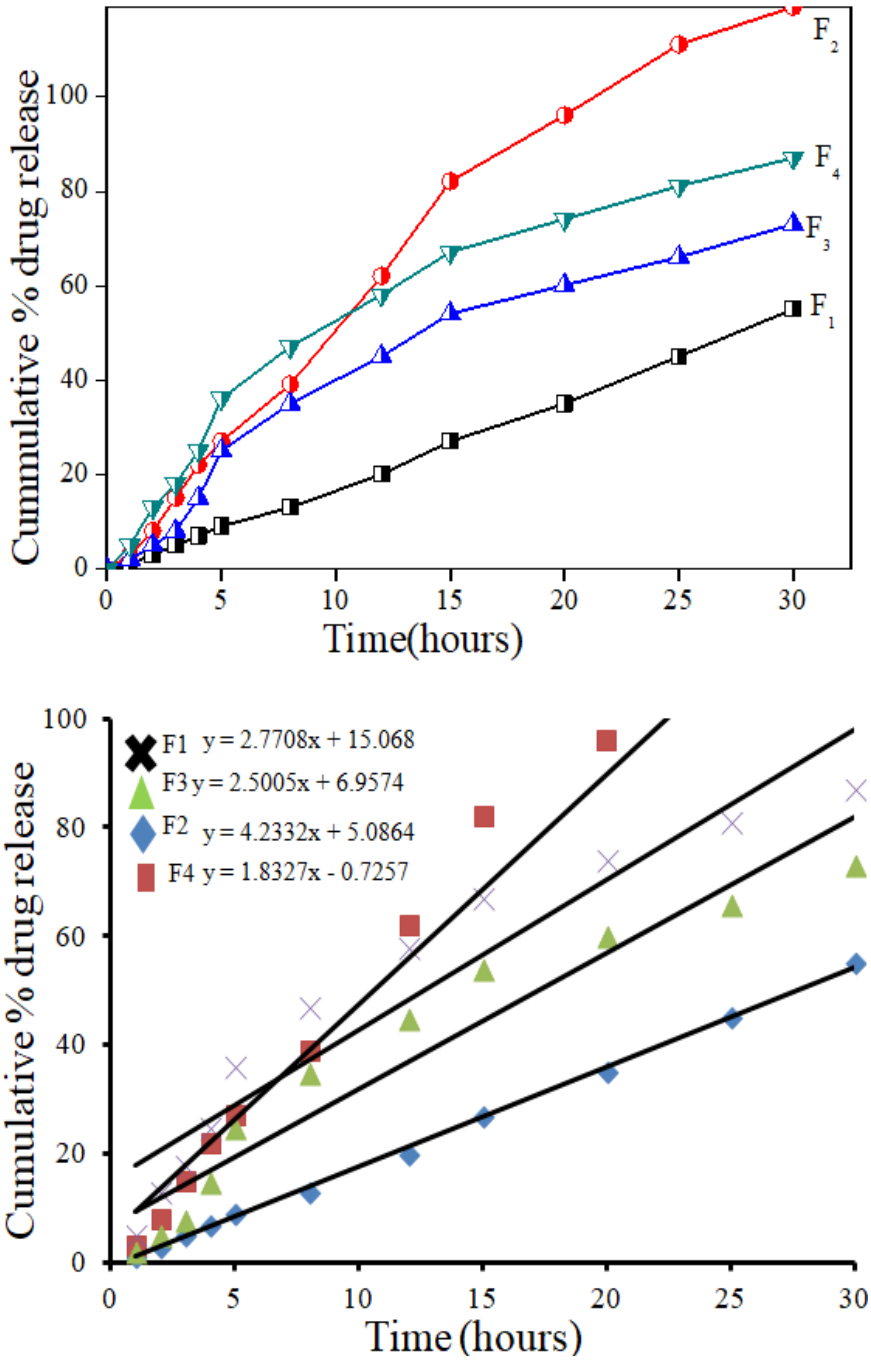

Figure 2.12: Zero order plots for various formulations

Table 2.2. Correlation coefficients of kinetic plots of formulations.

Formulation code	Korsemeyer-Peppas (n value)	Zero order
F_1	0.859	4.28
F_2	0.854	2.59
F_3	1.06	2.91
F_4	1.00	1.82

2.4 Conclusions

The study showed that formulation approach can improve the therapeutic efficacy of ramipril. The nanoprecipitation method is suitable for preparation of ramipril loaded PLGA nanoparticles with fairly high encapsulation efficiency. Variations in PLGA and K P-188 concentrations lead to changes in entrapment efficiency and release profile of the drug. The synthesized nanoparticles were in a size range of 121-156 nm having uniform size. Highest percentage of entrapment efficiency was obtained in F_3 formulation. However, in F_2 formulation almost same amount of ramipril was released as entrapped. Formulation F_2 showed an initial burst release followed by sustained release up to 74% over 24 hours in PBS. This release pattern of ramipril from PLGA matrix was attributed to its non- fickian diffusion mechanism which indicates that the release is both diffusion and swelling controlled. The sustained release of ramipril from polymer matrix indicated that the use of similar formulations can be useful in reducing the frequency of administration of ramipril in the treatment of hypertension.

2.5 References

[1] T. Kommuru, B. Gurley, M. Khan, I. Reddy, International Journal of Pharmaceutics, 212 (2001) 233-246.

[2] T. Gershanik, S. Benita, European Journal of Pharmaceutics and Biopharmaceutics, 50 (2000) 179-188.

[3] B.K. Kang, J.S. Lee, S.K. Chon, S.Y. Jeong, S.H. Yuk, G. Khang, H.B. Lee, S.H. Cho, International Journal of Pharmaceutics, 274 (2004) 65-73.

[4] K.S. Soppimath, T.M. Aminabhavi, A.R. Kulkarni, W.E. Rudzinski, Journal of Controlled Release, 70 (2001) 1-20.

[5] J. Panyam, V. Labhasetwar, Advanced Drug Delivery Reviews, 55 (2003) 329-347.

[6] A. Kumari, S.K. Yadav, S.C. Yadav, Colloids and Surfaces B: Biointerfaces, 75 (2010) 1-18.

[7] R. Fernández-Urrusuno, P. Calvo, C. Remuñán-López, J.L. Vila-Jato, M.J. Alonso, Pharmaceutical Research, 16 (1999) 1576-1581.

[8] Y. Pan, Y.-j. Li, H.-y. Zhao, J.-m. Zheng, H. Xu, G. Wei, J.-s. Hao, International Journal of Pharmaceutics, 249 (2002) 139-147.

[9] K. Janes, P. Calvo, M. Alonso, Advanced Drug Delivery Reviews, 47 (2001) 83-97.

[10] D. Peer, J.M. Karp, S. Hong, O.C. Farokhzad, R. Margalit, R. Langer, Nature Nanotechnology, 2 (2007) 751-760.
[11] M.E. Davis, D.M. Shin, Nature reviews Drug Discovery, 7 (2008) 771-782.
[12] R. Gref, Y. Minamitake, M.T. Peracchia, V. Trebetskoy, V. Torchilin, R. Langer, Science, 263 (1994) 1600-1604.
[13] S.M. Moghimi, A.C. Hunter, J.C. Murray, Pharmacological Reviews, 53 (2001) 283-318.
[14] V. Labhasetwar, C. Song, R.J. Levy, Advanced Drug Delivery Reviews, 24 (1997) 63-85.
[15] V. Labhasetwar, C. Song, W. Humphrey, R. Shebuski, R.J. Levy, Journal of Pharmaceutical Sciences, 87 (1998) 1229-1234.
[16] V. Sinha, K. Bansal, R. Kaushik, R. Kumria, A. Trehan, International Journal of Pharmaceutics, 278 (2004) 1-23.
[17] T.K. Dash, V.B. Konkimalla, Journal of Controlled Release, 158 (2012) 15-33.
[18] E. Allemann, R. Gurny, E. Doelker, European Journal of Pharmaceutics and Biopharmaceutics, 39 (1993) 173-191.
[19] P. Couvreur, C. Dubernet, F. Puisieux, European Journal of Pharmaceutics and Biopharmaceutics, 41 (1995) 2-13.
[20] D. Quintanar-Guerrero, E. Allémann, H. Fessi, E. Doelker, Drug Development and Industrial Pharmacy, 24 (1998) 1113-1128.
[21] J. Mauduit, M. Vert, STP Pharma Sciences, 3 (1993) 197-197.
[22] H.K. Makadia, S.J. Siegel, Polymers, 3 (2011) 1377-1397.
[23] C. Ezeala, in, 2016.
[24] F. Danhier, E. Ansorena, J.M. Silva, R. Coco, A. Le Breton, V. Préat, Journal of Controlled Release, 161 (2012) 505-522.
[25] D.N. Kapoor, A. Bhatia, R. Kaur, R. Sharma, G. Kaur, S. Dhawan, Therapeutic Delivery, 6 (2015) 41-58.
[26] S.J. Holland, B.J. Tighe, P.L. Gould, Journal of Controlled Release, 4 (1986) 155-180.
[27] S.Li and M. Vert, Degradable Polymers: Principles and Applications, 2 (2013) 71-131.
[28] M. Leroueil-Le Verger, L. Fluckiger, Y.-I. Kim, M. Hoffman, P. Maincent, European Journal of Pharmaceutics and Biopharmaceutics, 46 (1998) 137-143.
[29] Y. Ogawa, European Journal of Hospital Pharmacy, 2 (1992) 120-127.
[30] D. Fleisher, C. Li, Y. Zhou, L.-H. Pao, A. Karim, Clinical Pharmacokinetics, 36 (1999) 233-254.

[31] R.A. Jain, Biomaterials, 21 (2000) 2475-2490.
[32] J.M. Anderson, M.S. Shive, Advanced Drug Delivery Reviews, 64 (2012) 72-82.
[33] R. Jain, C. Rhodes, A. Railkar, A. Malick, N. Shah, Journal of Microencapsulation, 17 (2000) 343-362.
[34] J. Panyam, W.-Z. Zhou, S. Prabha, S.K. Sahoo, V. Labhasetwar, The FASEB Journal, 16 (2002) 1217-1226.
[35] J. Panyam, V. Labhasetwar, Pharmaceutical Research, 20 (2003) 212-220.
[36] S. Prabha, V. Labhasetwar, Pharmaceutical Research, 21 (2004) 354-364.
[37] J. Panyam, V. Labhasetwar, Molecular Pharmaceutics, 1 (2004) 77-84.
[38] S.A. Atlas, Journal of Managed Care Pharmacy, 13 (2007) 9-20.
[39] A. Giestas, I. Palma, M.H. Ramos, Acta Medica Portuguesa, 23 (2010) 677-688.
[40] D. Ljutić, I. Jeličić, Medicus, 19 (2010) 139-146.
[41] J.M. Flack, S.A. Atlas, J.L. Pool, W.B. White, Journal of Managed Care Pharmacy, 13 (2007) 1-39.
[42] P. Ekambaram, A.A.H. Sathali, Journal of Young Pharmacists, 3 (2011) 216-220.
[43] S.M. Havanoor, K. Manjunath, S.T. Bhagawati, V.P. Veerapur, International Journal of Biopharmaceutics, 5 (2014) 218-224.
[44] B.K. Ramu, K. Raghubabu, International Journal of Chemistry Research, 2 (2011) 16-19.
[45] T. Basu, B. Pal, S. Singh, Advanced Science, Engineering and Medicine, 8 (2016) 444-449.
[46] R. Chandra, M. Pant, H. Singh, D. Kumar, A. Sanghi, International Journal of Drug Delivery Technology, 6 (2016) 64-67.
[47] Z. Zili, S. Sfar, H. Fessi, International Journal of Pharmaceutics, 294 (2005) 261-267.
[48] S. Jagdale, Y. Dangat, B. Kuchekar, International Journal of Pharmacy and Pharmaceutical Sciences, 4 (2012) 309-318.
[49] V. Budhwaar, A. Nanda, International Journal of Applied Pharmaceutics, 5 (2013) 19-25.
[50] N. Pirooznia, S. Hasannia, A.S. Lotfi, M. Ghanei, Journal of Nanobiotechnology, 10 (2012) 1186-1477.
[51] G. Singhvi, M. Singh, International Journal of Pharmaceutical Studies and Research, 2 (2011) 77-84.
[52] S. Ummadi, B. Shravani, N.R. Rao, M.S. Reddy, B. Nayak, Iternational Journal of Pharma Sciences, 3 (2013) 258-269.

[53] S. Dash, P.N. Murthy, L. Nath, P. Chowdhury, Acta Poloniae Pharmaceutica, 67 (2010) 217-223.
[54] H. Lokhandwala, A. Deshpande, S. Deshpande, International Journal of Pharma and Biosciences, 4 (2013) 728-773.

Section B: Core-Shell PLGA/PLA- pNIPAM nanocomposites loaded with Ramipril

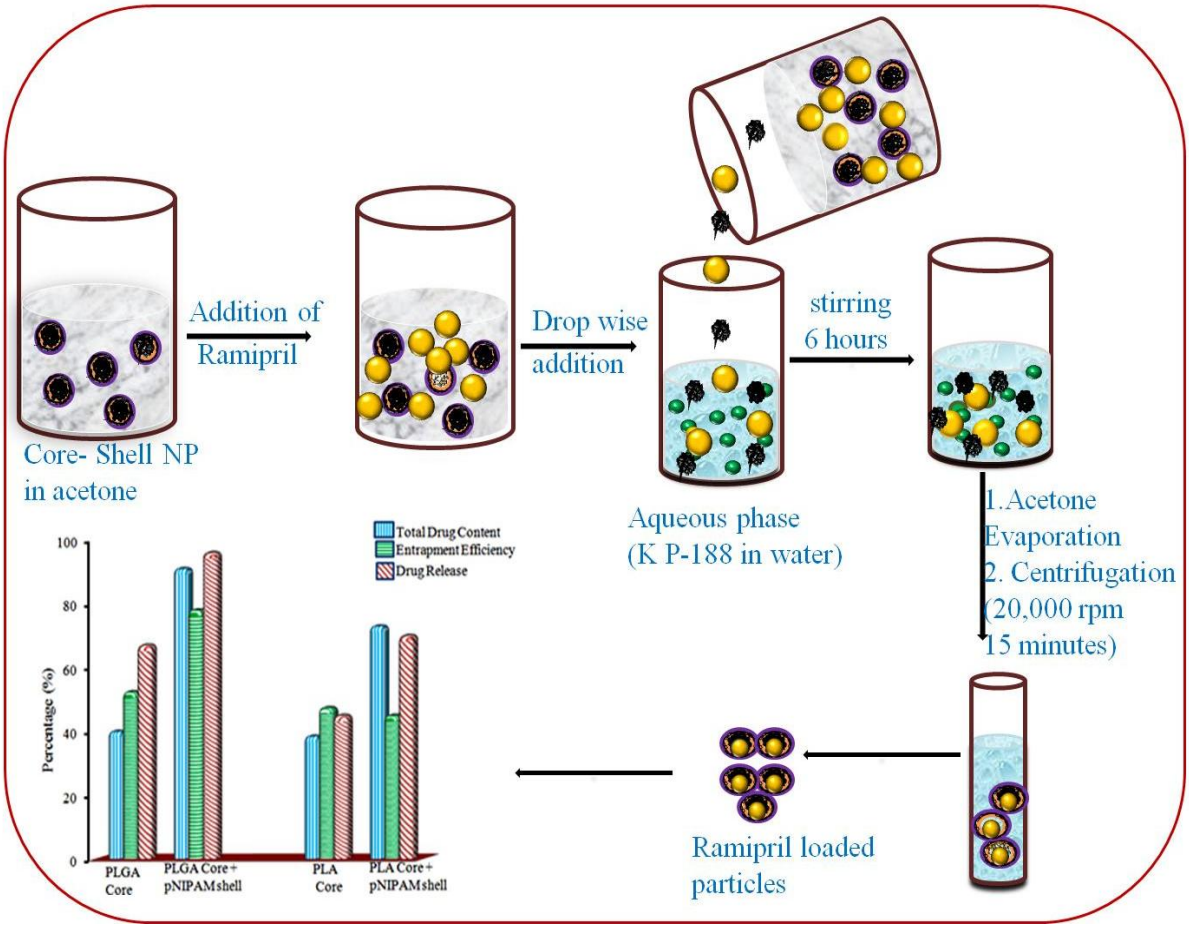

2.6 Introduction

Biodegradable colloidal particles have received a significant interest as a possible means of delivering drugs by several routes of administration [1]. Special interest has been focused on the use of particles prepared from polyesters like PLGA and PLA, due to their biocompatibility and biodegradability through natural pathways in the body [2, 3]. Although PLGA and PLA NPs have been used commercially by many investigators for their advantageous properties but still there are some limitations for them to be used as drug delivery agents [4-7]. The long-term storage of aqueous suspensions of PLGA and PLA nanoparticle is difficult, due to hydrolytic degradation of the polymer and subsequent release of the encapsulated therapeutic. To overcome this issue, researchers have used lyophilisation to prepare therapeutics containing PLGA and PLA NPs for long-term storage. However, this simple solution introduces an additional difficulty i.e., lyophilisation that causes NPs to aggregate into clumps and upon rehydration, fall's out of solution readily [8, 9]. In an attempt to overcome the limitations linked to PLGA and PLA NPs, and to increase their functionality, the NPs are encapsulated within a shell of poly (N-isopropylacrylamide) (pNIPAM), because of its versatility with some inherently unique properties. The pNIPAM shell has been synthesized as a homopolymer or a copolymer with incorporation of a variety of chemical moieties with defined concentrations that can be further modified with active targeting functional groups. Also, it is one of the most stimuli-responsive polymers [10]. pNIPAM has a great potential for applications in biomedical fields [11-13] and immobilization of enzymes [14]. Moreover, pNIPAM has the ability to tolerate lyophilisation [15], so it was hypothesized that a pNIPAM shell would protect the encapsulated PLGA and PLA NPs from aggregation during lyophilisation. Therefore, by encapsulating them in pNIPAM shell, the NPs will have the ability to respond to environmental stimuli, such as temperature. This response could then further be used for loading and/or controlling the release of therapeutics from the pNIPAM layer [16]. The PLGA core will then act as drug reservoir while its release depends on the shell thickness of the pNIPAM layer [17].

These poorly water soluble antihypertensive drugs when administered in polymeric vehicles like PLGA or PLA show better effects as compared to when administered conventionally, as these polymeric carriers prevent them from degradation in gastrointestinal tract (GIT) and boost their transmucosal transportation in the body [18]. Also the enhanced transport and prolong release of drug may improve the plasma half life of the drug. Hsu et al. [19] reported the effect of particle size on the efficiency and absorption of drug in the

mucosal membrane. The particles of size less than 500 nm can pass the M cells and the GIT easily, thereby transporting the drug to systemic circulation [3].

The aim of the study is to assess the release of ramipril, an antihypertensive drug from biodegradable polymers PLA and PLGA modified with pNIPAM and to determine the release kinetics of ramipril. Enhanced efficiency and release of ramipril has been observed upon modification of the surface of PLA and PLGA with pNIPAM. The shell of pNIPAM prevents the PLA and PLGA core from clustering and has given enhanced release efficiency as compared to bare counterparts. Nanoprecipitation resulted in physical adsorption of ramipril on the surface of core-shell matrix. This adsorption is mainly due to hydrophobic interaction of drug with the polymer.

2.7 Experimental section

2.7.1 Materials

Poly-D,L-lactide-co-glycolide (50:50) (PLGA), Poly-lactic acid (PLA), Kolliphore P-188 (KP-188), N-isopropyl acryl amide (pNIPAM) and Sodium dodecyl sulphate (SDS) were purchased from Sigma-Aldrich. N, N'-methylene bisacrylamide (N, N'-MBA) and Ammonium persulfate (APS) were purchased from Spectrochem India. Ramipril was received as a gift sample from Mefro Pharmaceuticals (Mohali, Punjab, India). All other reagents were obtained from Loba Chemie, India and used as received without further purification. De-ionized water was obtained using an ultra filtration system (Milli-Q, Millipore).

2.7.2 Encapsulation of pNIPAM shells over PLA and PLGA core

Synthesis of core-shell structure was carried out in two steps:

2.7.2.1 Preparation of PLA / PLGA core

Single emulsion technique was used to prepare the core, the details of which are given in **Chapter 1, section 1.4.3.**

2.7.2.2 Encapsulating pNIPAM shell over PLA/PLGA core

Free radical precipitation polymerization technique was used for the process of encapsulation, the details of which are given in **Chapter 1, section 1.4.4.**

2.7.3 Synthesis of ramipril loaded nanoparticles

The details of drug loading method are given in **Chapter 1, section 1.4.5.**

2.7.4 Characterization

As synthesized core-shell NPs were characterized by various techniques, the details of the techniques are given in **Chapter 1**, **section 1.5**.

2.7.5 Drug content and Entrapment Efficiency of ramipril

The determination of total drug content and entrapment efficiency was determined spectrophotometrically, the details of which are given in **Chapter 1, section 1.4.11.**

2.7.6 In-vitro drug release of ramipril and kinetic studies

The amount of drug released was determined at 29°C and 210 nm by HPLC using Phosphate buffer: ACN (30:70 v/v) as mobile phase. 20 µL of sample was injected with a flow rate of 2.0 mL/min, the details of which are given in **Chapter 1**, **section 1.4.12.**

The data obtained from the *in-vitro* release study was fitted into various drug release kinetic models and the resulting regression coefficient values were calculated. The data was also fitted into korsemeyer- peppas and higuchi model to determine the release exponent 'n' value for describing the mechanism of drug release.

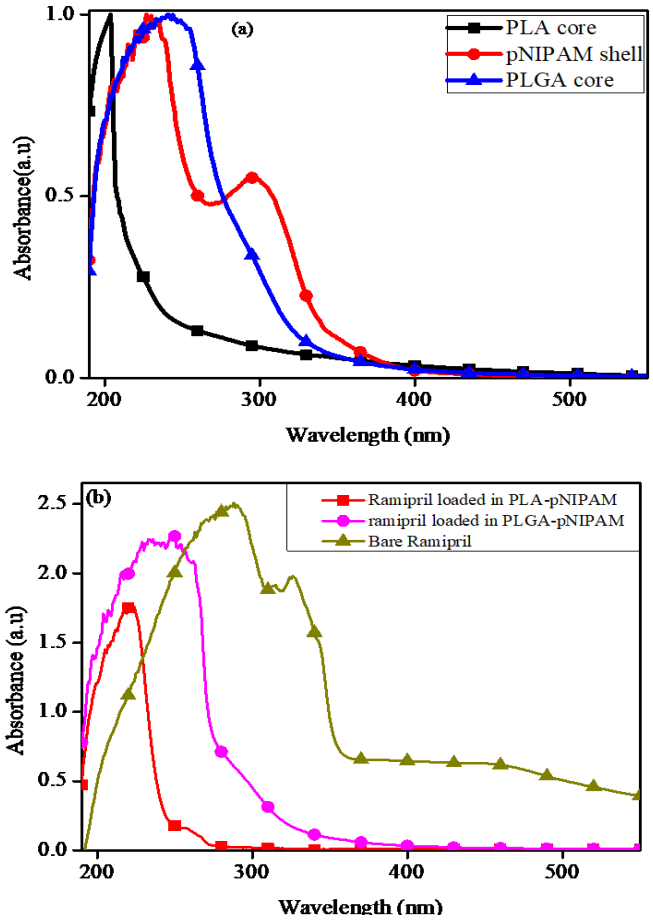

Figure 2.13: UV-Visible absorption spectra of (a) PLA core, PLGA core and pNIPAM shell (b) Bare ramipril and ramipril loaded in core-shell nanoparticles

2.8 Results and Discussion

2.8.1. Structural and morphological characterization

The UV-Vis absorption of PLA/PLGA showed absorption bands at 202nm/240nm, but pNIPAM shell showed two absorption bands at 229nm and 296nm figure 2.13(a). Figure 2.13 (b) and figure 2.14, shows the absorption bands for pure ramipril

at 237 nm and 257 nm however after entrapment of drug in core-shell and bare polymer matrix, the absorption bands were observed at 249nm/220nm for PLGA/PLA.

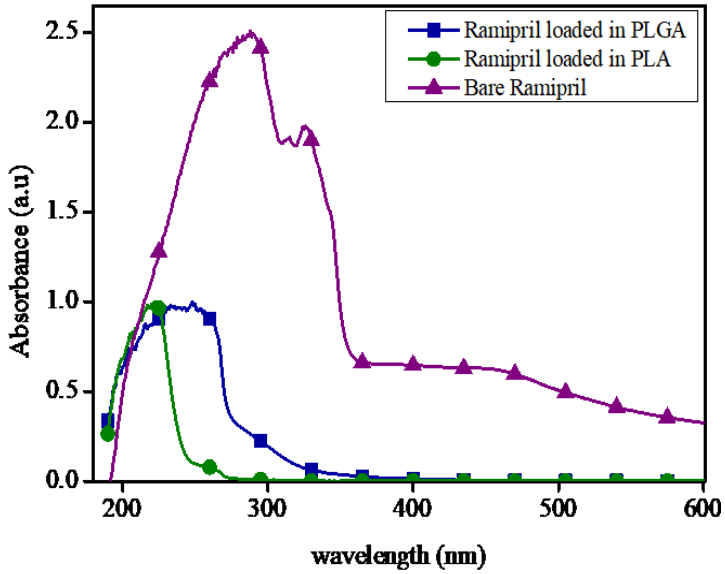

Figure 2.14: UV-Vis absorption spectra of bare ramipril, ramipril loaded in PLGA and ramipril loaded in PLA

The FT-IR spectra of ramipril, PLGA, PLA and formulations are shown in figure 2.15. Ramipril showed absorption band at 3277 cm^{-1} due to –NH and –OH stretching's of acid group, bands at 2930 cm^{-1} and 2860 cm^{-1} appear due to C-H aromatic stretching and C-H aliphatic stretching's, respectively. The band at 1748 cm^{-1} and 1644 cm^{1} are due to C=O of acid and ester groups. C-H aliphatic vibrations are observed in the fingerprint region. The spectra of PLGA showed C=O absorption at1748 cm^{-1} and C-H deformation of O-CH_2 group at 1414 cm^{-1}, while PLA showed bands at 1748cm^{-1} due to stretching of C=O group and at 1445 cm^{-1} due to asymmetric and symmetric C-C(=O)-O vibrations. pNIPAM showed absorption bands at 3277 cm^{-1} due to N-H stretching, at 2960 cm^{-1} due to asymmetric stretching vibrations of –CH_3 group

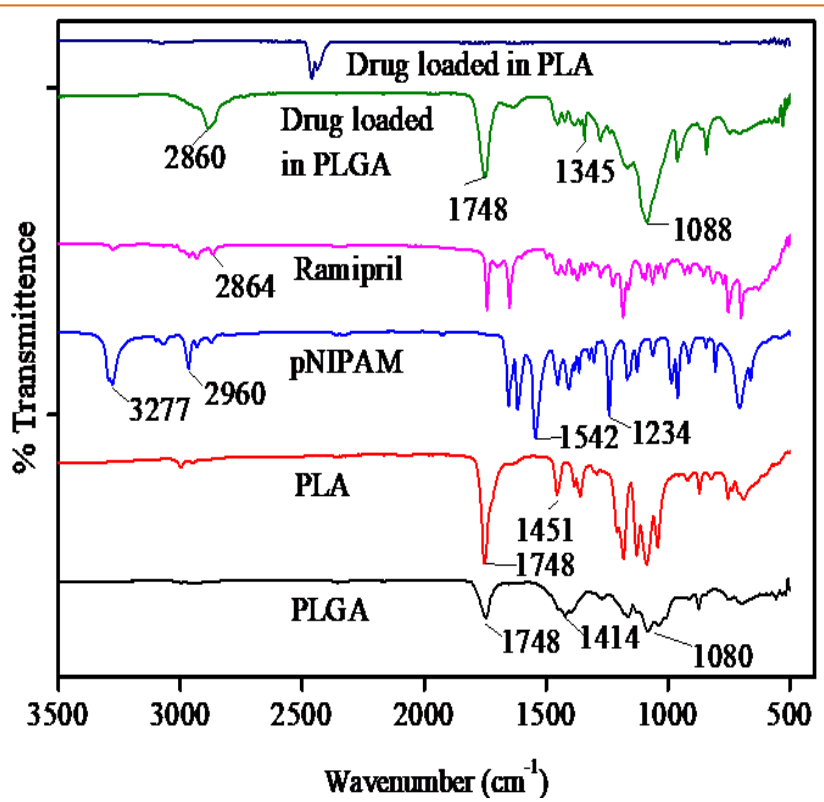

Figure 2.15: FT-IR spectra of ramipril, PLGA, PLA, pNIPAM, Ramipril loaded in PLGA-pNIPAM and ramipril loaded in PLA-pNIPAM

and at 1542 cm^{-1} due to amide linkage. In the formulations, absorption bands at 1748 cm^{-1} and 1644 cm^{-1} are due to carbonyl and ester groups of acid. Moreover, band at 2860 cm^{-1} have appeared due to C-H aliphatic stretching. An intense absorption band at 1088 cm^{-1} was observed in the formulation possibly as PLGA showed a band at 1081 cm^{-1}. The presence of bands at 2860 cm^{-1}, 1748 cm^{-1} and 1088 cm^{-1} indicated that the drug has been encapsulated within the polymer matrix and that any kind of interaction which could change the properties of ramipril, did not took place.

An increase in size of the nanocomposite was observed by DLS studies shown in figure 2.16 along with its corresponding comparative histogram in figure 2.17. It was observed from figure 2.17 that the particle size increased from 70-170 nm in case of PLA while for PLGA it increased from 68-155 nm after successive addition of pNIPAM shell and drug loading. The low polydispersity index (0.141-0.389) indicated that the particles were nearly of the uniform size.

Zeta potential of the prepared formulations ranged from -28.40 to -32.7 mV (table 2.3) indicating reasonable stability of the nanosuspensions. Shell thickness calculated for PLGA/PLA was 18.5 nm/43.5 nm.

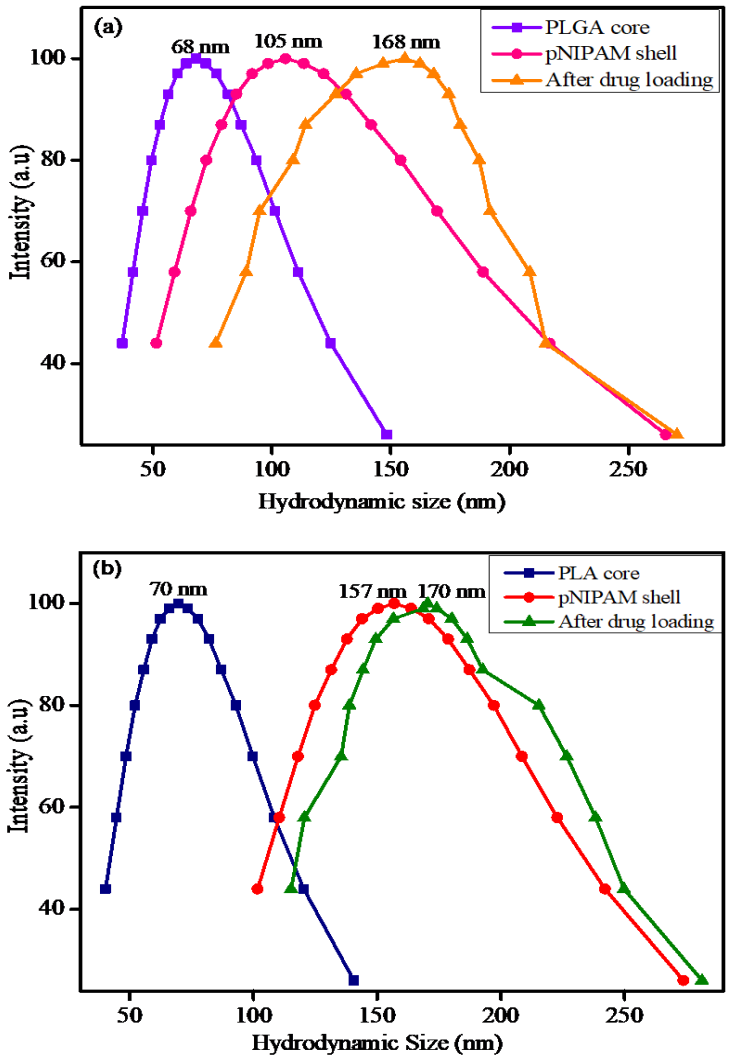

Figure 2.16: Average hydrodynamic size of (a) PLGA core and (b) PLA core after successive addition of pNIPAM and ramipril loading

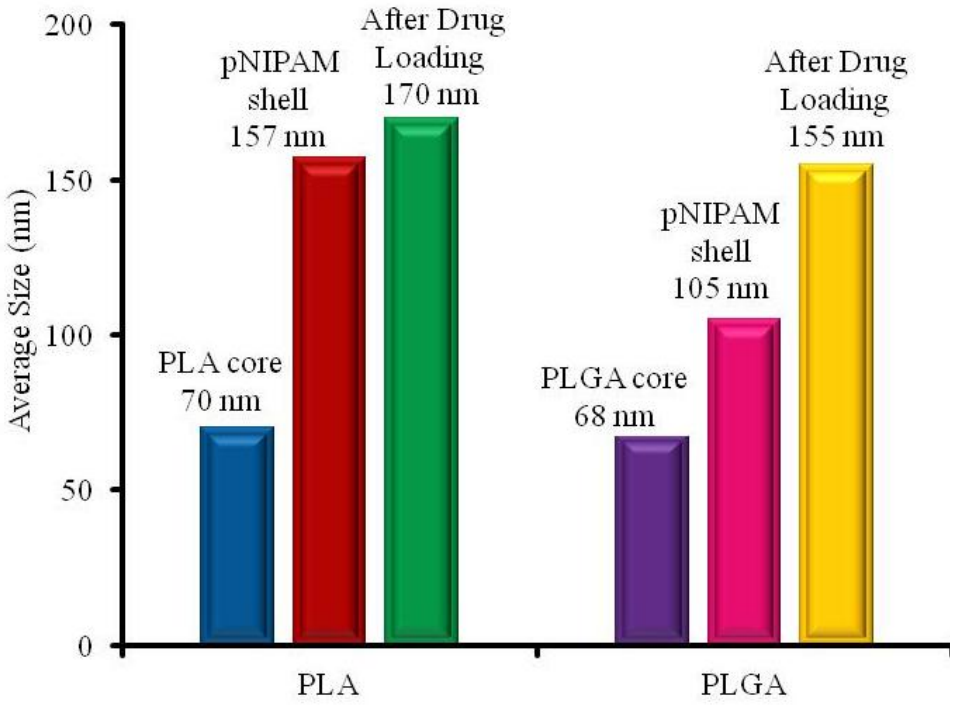

Figure 2.17: Comparative histogram showing average particle size distribution of bare (PLGA/PLA), pNIPAM shell and ramipril loaded PLGA / PLA- pNIPAM

Lyophilisation is useful in long term storage of therapeutics loaded onto PLGA and PLA NPs. However, it can cause aggregation of the NPs preventing resolubilization of the clustered NPs. The TEM images (figure 2.18), clearly indicate the aggregation of core NPs after lyophilisation. On the other hand, encapsulation of core NPs within pNIPAM shell prevented aggregation, confirming that pNIPAM shell fully encapsulated the core NPs. It was also observed that lyophilisation of core + shell NP system doesn't affected the size or zeta potential of the NPs (table 2.3).

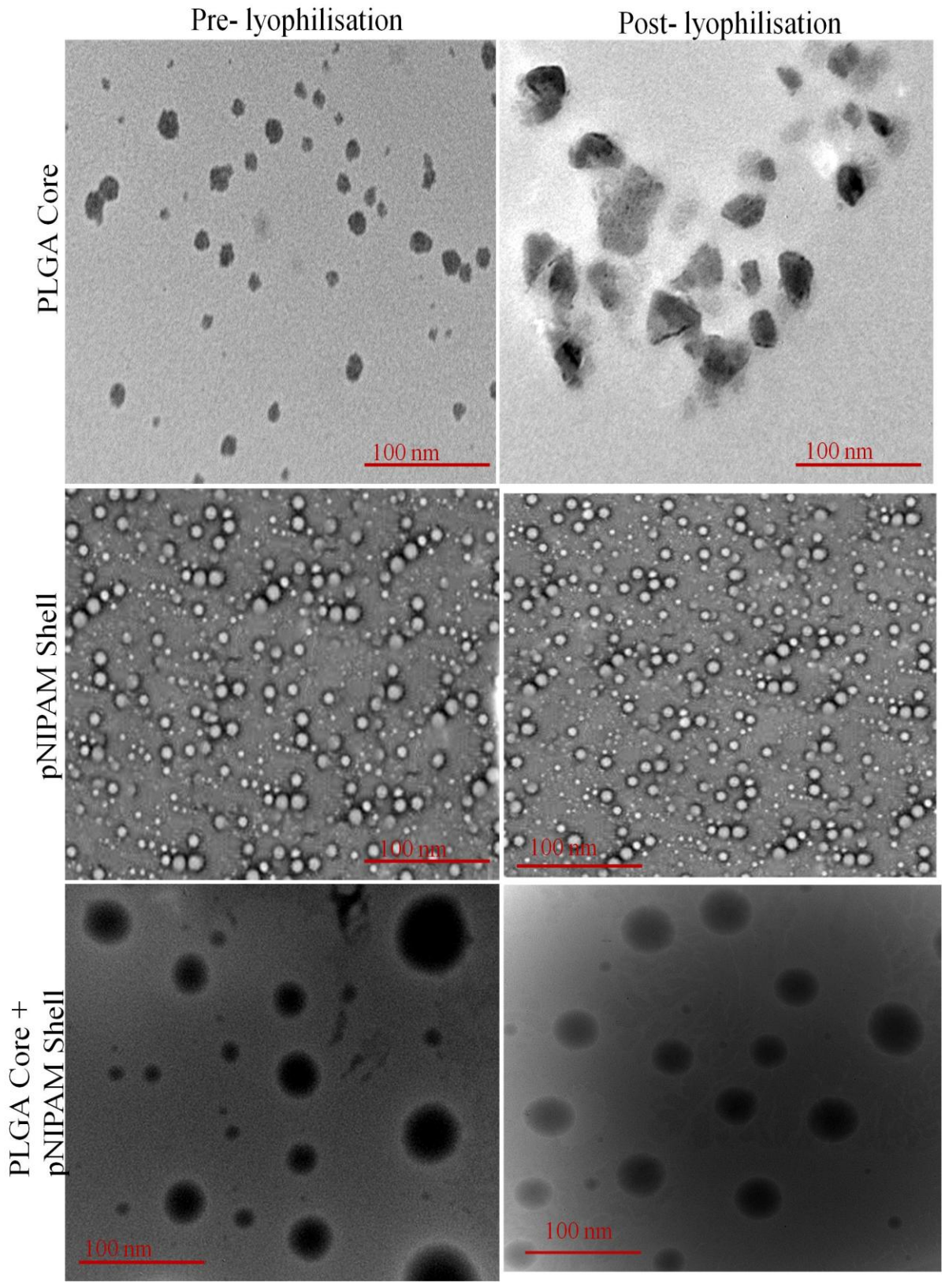

Figure 2.18: TEM images of nanoparticles both pre- and post lyophilized

Table 2.3: Zeta Potential and polydispersity of formulations.

S.No	Sample Name	Polydispersity Index (PDI)	Zeta Potential (mV) Pre-lyophilisation	Zeta Potential (mV) Post-lyophilisation	*Shell Thickness (nm)
1.	PLGA core	0.389	-28.4± 0.5	-28.4± 0.8	-
2.	PLGA core – pNIPAM shell	0.272	-32.7± 0.7	-32.7± 0.6	18.5
3.	PLA core	0.141	-22.7± 0.9	-22.7± 1.0	-
4.	PLA core – pNIPAM shell	0.220	-30.3± 1.2	-30.3± 1.3	43.5

*Shell thickness was determined by subtracting corresponding core from core + shell sample and dividing by 2.

2.8.2 Drug content and Entrapment efficiency of ramipril

Total drug content was measured by UV-Vis spectroscopy. The nanosuspension was centrifuged and the free drug content was determined in clear supernatant (figure 2.19 & table 2.4). Very low TDC and entrapment efficiency was obtained for drug loaded in PLGA/PLA only. This may be attributed to the initial burst of the polymer after resolubilization due to lyophilisation.

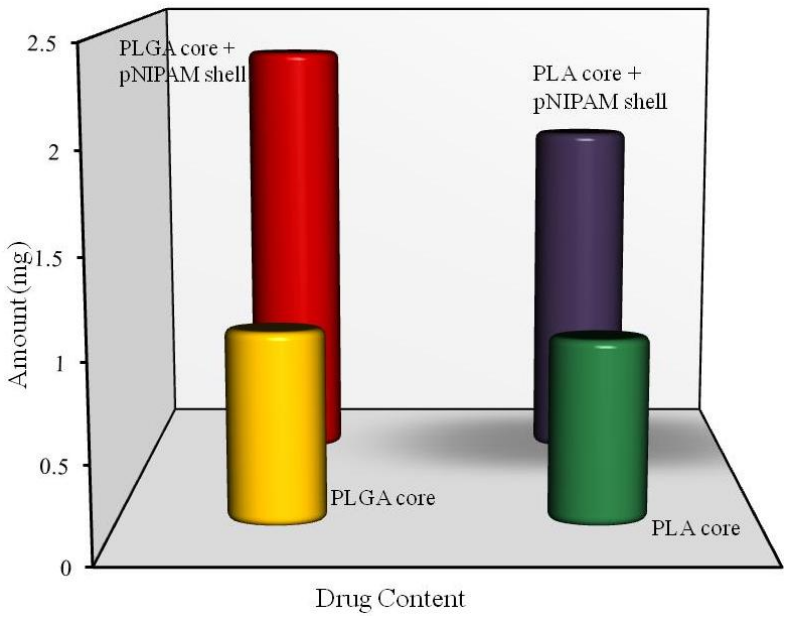

Figure 2.19: Drug content in formulations

Table 2.4: Amount of free dissolved drug and drug content in various formulations.

S.No	Sample Name	Free dissolved drug (mg)	Drug Content (mg)	Total Drug Content (%)	Entrapment efficiency (%)
1.	PLGA core	0.48	1.01	40	52.4
2.	PLGA core – pNIPAM shell	0.35	2.3	91	78
3.	PLA core	0.51	0.97	38.49	47.42
4.	PLA core – pNIPAM shell	0.72	1.84	73	60

However the TDC increased for the core-shell system to 73 - 91% for PLA/PLGA as shown in figure 2.20. Also the entrapment efficiency was increased for the core-shell nanoparticle system. Higher drug content and entrapment efficiency (78%) was obtained for drug loaded in PLGA coated with pNIPAM.

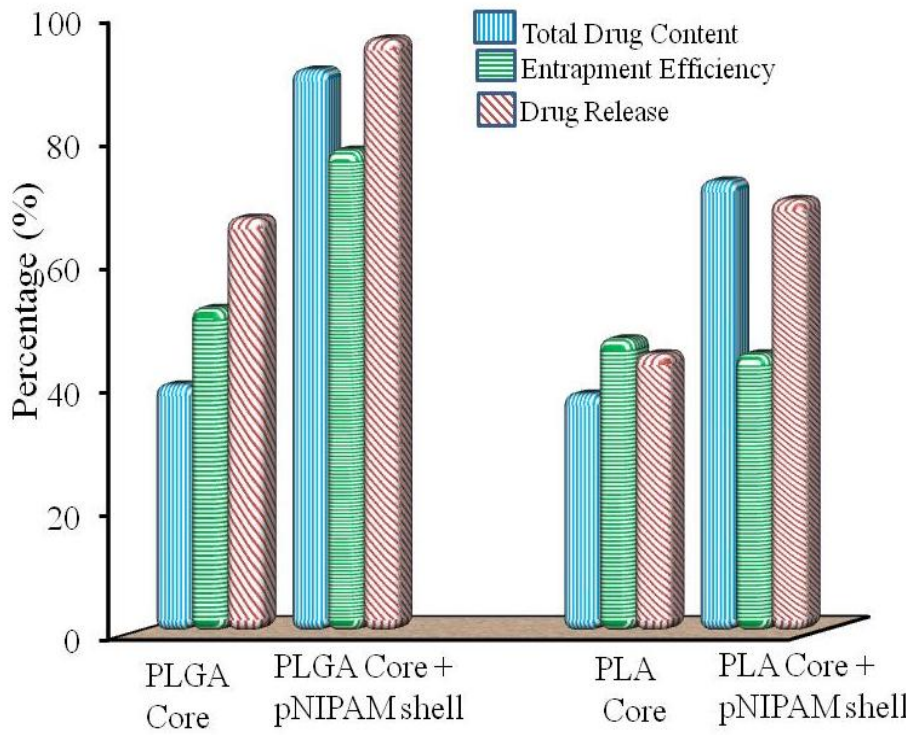

Figure 2.20: Percentage of total drug content, entrapment efficiency and ramipril release in the formulations

2.8.3 In-vitro release of ramipril

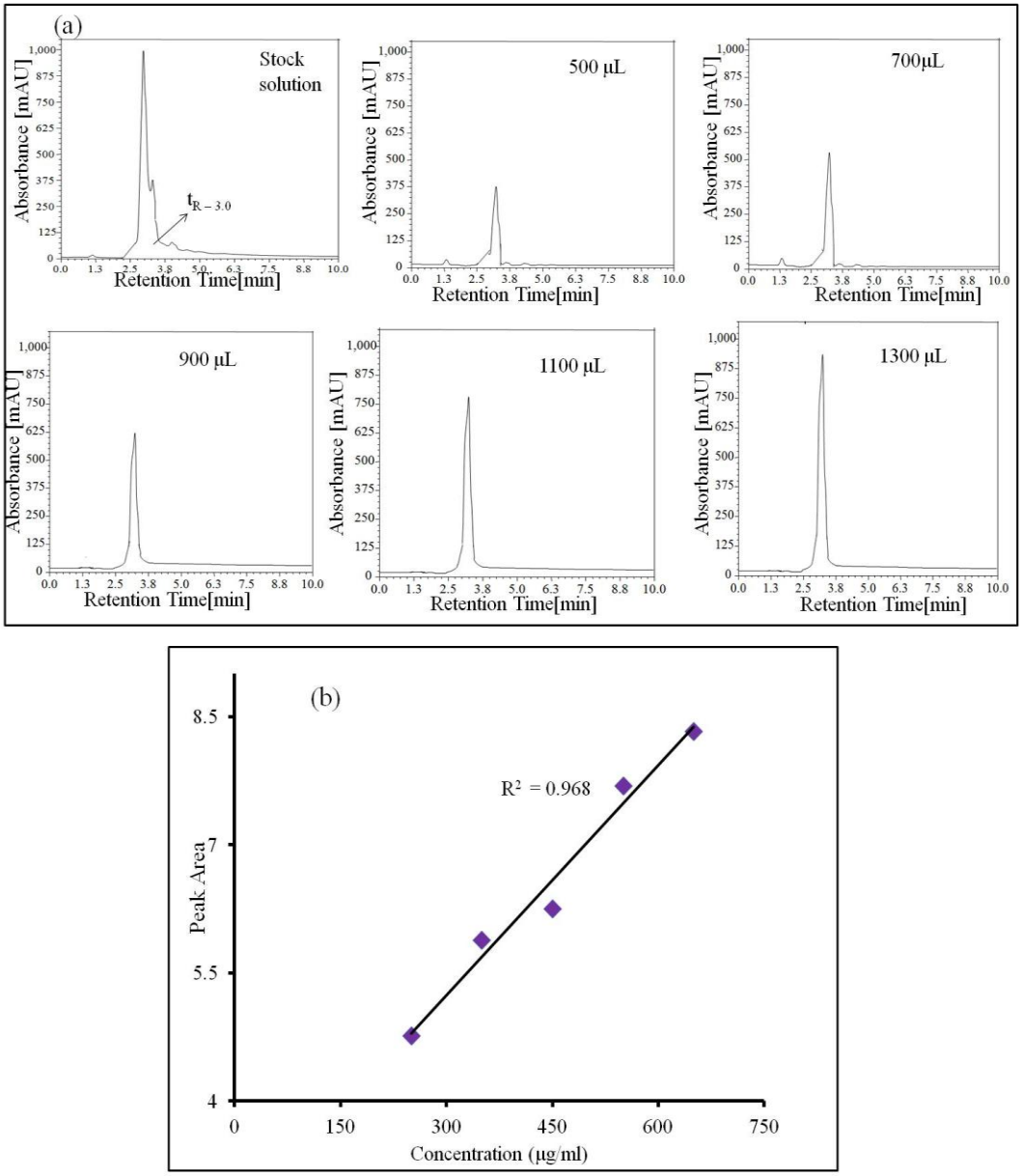

Figure 2.21: (a) HPLC chromatogram for standard stock solution of ramipril and (b) calibration curve for standard stock solution

The release profile of ramipril was determined using HPLC. Firstly, appropriate aliquots of ramipril stock solution were taken in different 10 ml volumetric flasks and diluted with the mobile phase to obtain the final concentration. A calibration curve for standard solution of drug was plotted between average peak area versus concentration shown in figure 2.21. It was

observed that the release of ramipril from PLGA/PLA matrix in PBS of pH 5.3 (figure 2.22 and the corresponding chromatographs in figure 2.23) shows initial burst release followed by sustained release. After 24 hrs of incubation in PBS, the percentage release of drug was 67% and 45% for PLGA and PLA respectively.

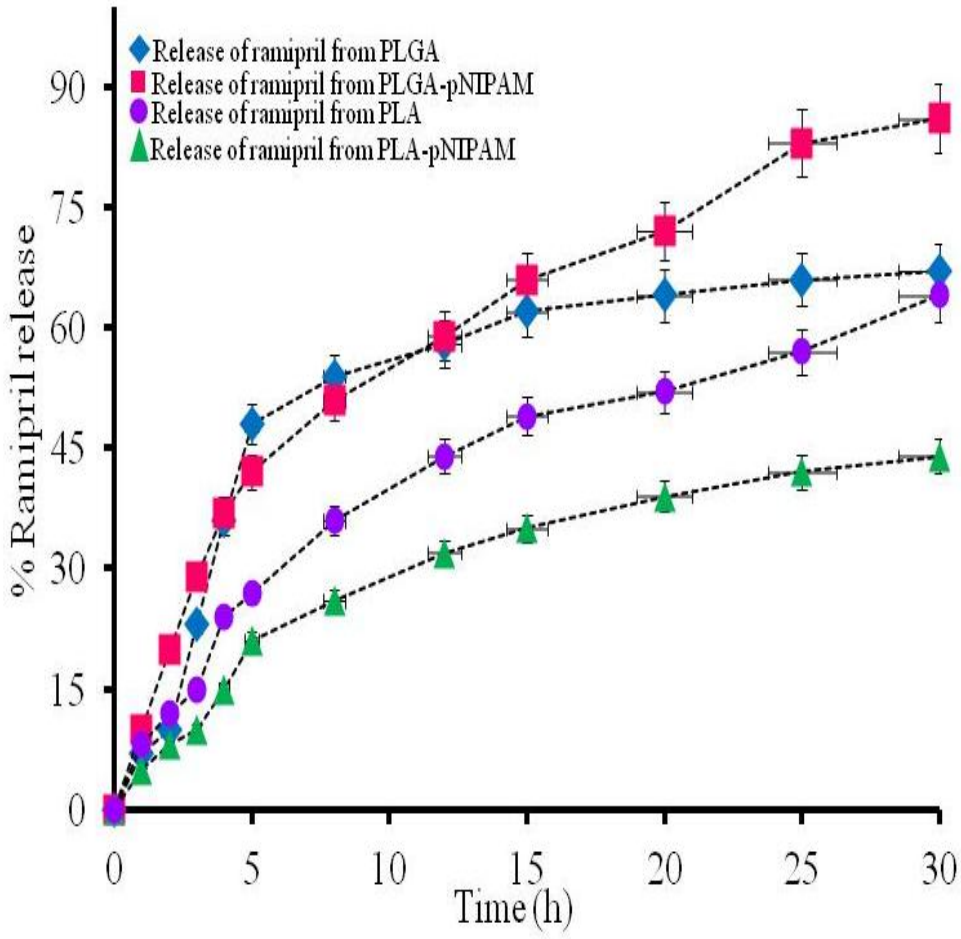

Figure 2.22: *In-vitro* release profile of ramipril in phosphate buffer solution

The initial burst release was due to presence of free dissolved drug. However an increase in percentage release of drug was observed from the core-shell system. PLGA+ pNIPAM showed highest release of drug (96%) while PLA+ pNIPAM showed 70% of drug release.

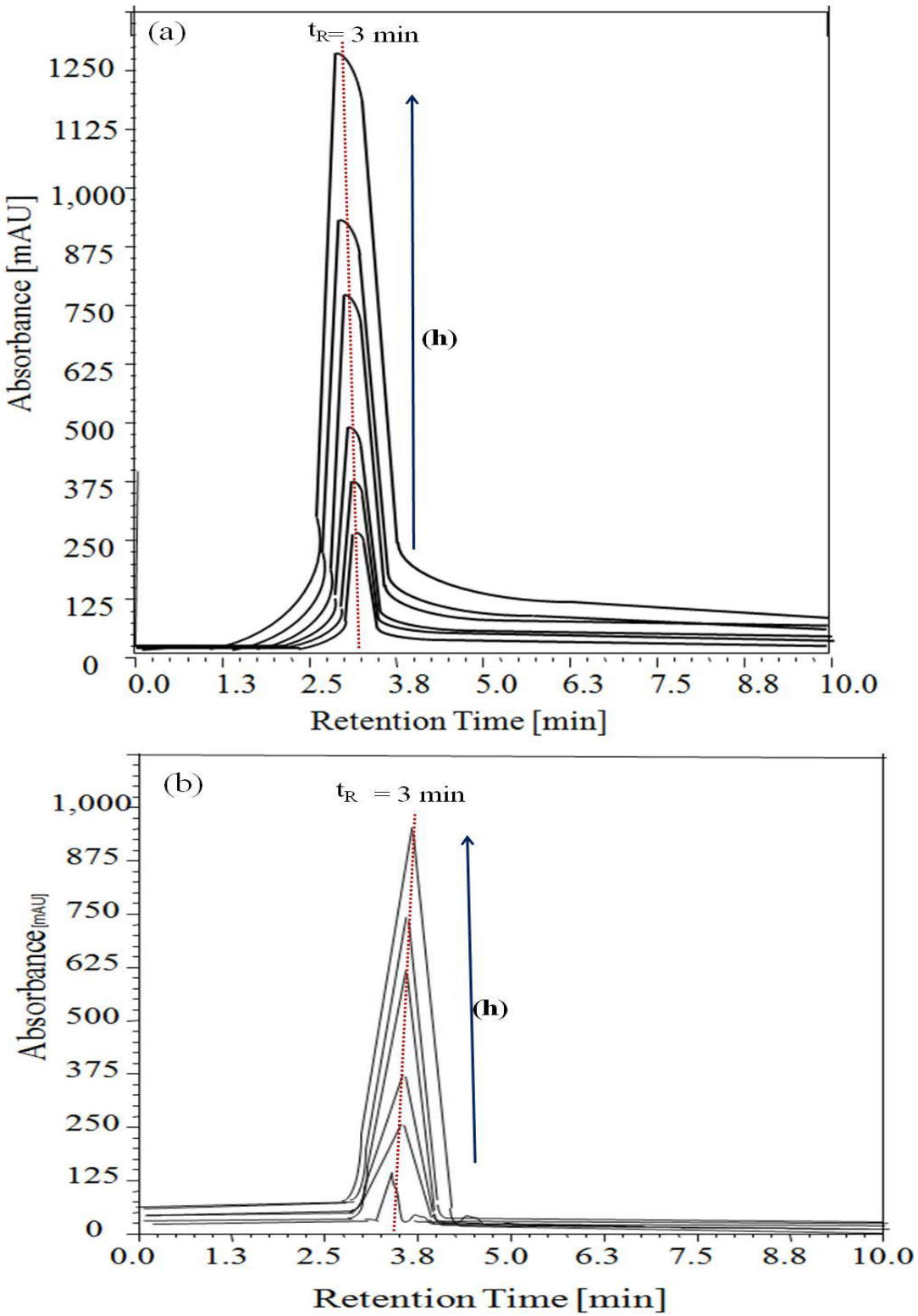

Figure 2.23: Corresponding chromatograms showing release of ramipril from (a) PLGA-pNIPAM and (b) PLA-pNIPAM matrix in phosphate buffer

Proposed mechanism of release of ramipril from core-shell matrix

The ramipril encapsulated NP when placed in buffer solution of appropriate pH environment, allows initially the penetration of water from the surface to the inside of the core-shell NP. This in turn activates the hydrolytic cleavage within the polymer and diffusion of encapsulated ramipril starts from the NP. As the degradation of the core-shell NP continues thereby increasing the rate of ramipril diffusing from the matrix. The schematic representation of the release mechanism is shown in figure 2.24. This controlled release of ramipril from core-shell matrix tends to increase the bioavailability of ramipril. Also decrease in the dosage of the drug by providing greater effects in single dose can be achieved.

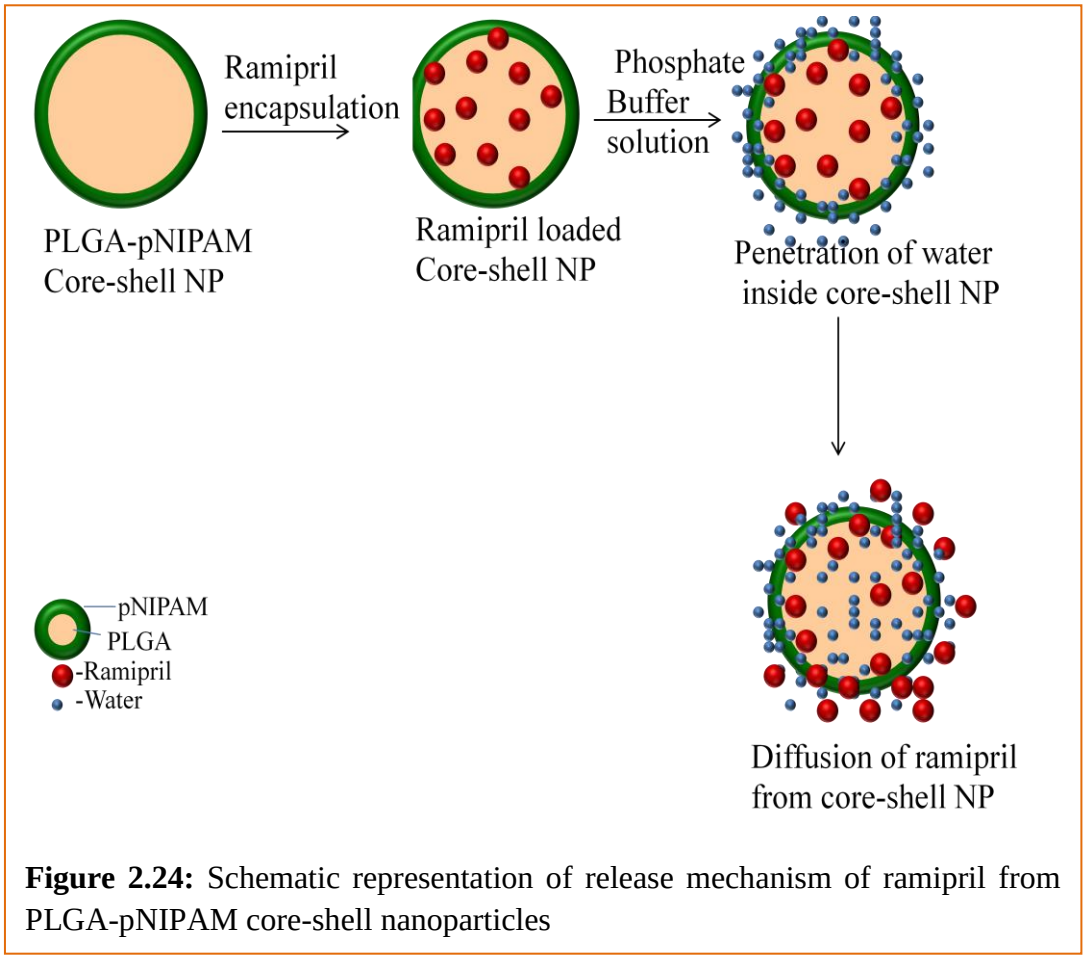

Figure 2.24: Schematic representation of release mechanism of ramipril from PLGA-pNIPAM core-shell nanoparticles

2. 8.4 In-vitro release kinetics study

Figure 2.25 shows the release exponent (n) values for PLGA and PLA obtained by fitting the drug release profile into Korsemeyer-Peppas and higuchi model of drug release. The 'n'

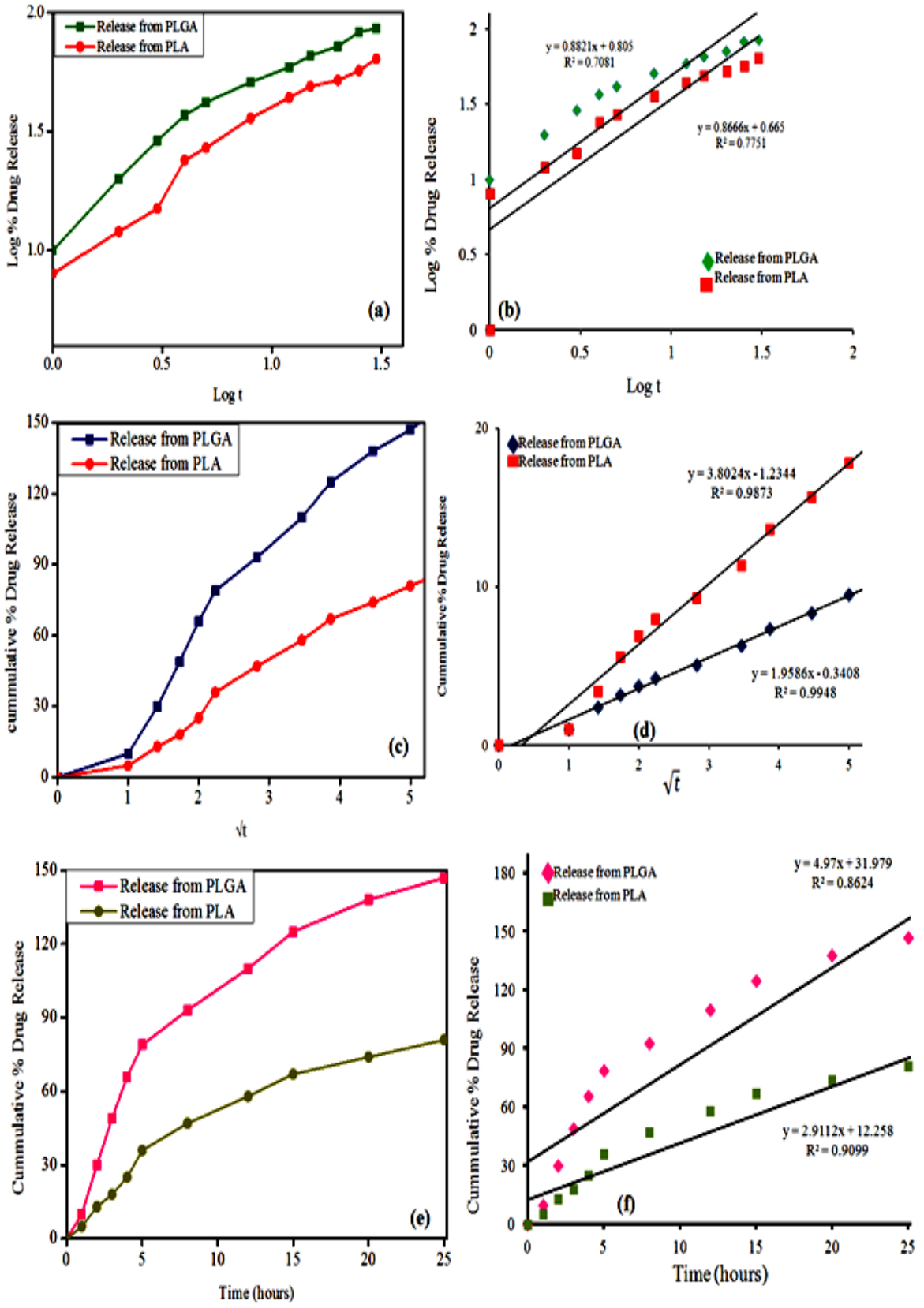

Figure 2.25: Kinetic models of ramipril release (a-b) Korsemeyer-Peppas plots, (c-d) Higuchi plots and (e-f) Zero order plots

value of 0.882 and 0.866 for PLGA and PLA showed that the drug release followed zero order (figure 2.25 (e-f)) rate and an overall anomalous (non-fickian) diffusion mechanism, which indicates that the release of ramipril from the matrix of PLGA and PLA was diffusion controlled. The corresponding correlation coefficients of these kinetic plots are shown in table 2.5.

Table 2.5: Correlation coefficients of kinetic plots of formulations.

Formulation code	Korsemeyer-Peppas (n value)	Zero order
Release from PLGA	0.882	4.97
Release from PLA	0. 866	2.91

2.9 Conclusion

In summary, to improve the functionality of poly-lactic-co-glycolic acid and poly-lactic acid as therapeutic agents, these were encapsulated within poly (N-isopropylacrylamide) shell. Poly (N-isopropylacrylamide) was chosen due to its ability to protect the core nanoparticles from aggregation and external stimuli. Also these (poly- lactic /poly-lactic-co-glycolic acid- poly N-isopropylacrylamide) core- shell nanoparticles are non-toxic in nature suggesting biocompatibility. These core-shell (poly- lactic /poly-lactic-co-glycolic acid- poly N-isopropylacrylamide) nanoparticles were used to study the release profile of ramipril an antihypertensive drug. The synthesized nanocomposites were in a size range of 68 – 170nm. Higher percentage of entrapment efficiency (78%) was obtained for ramipril loaded in poly-lactic-co-glycolic acid- poly N-isopropylacrylamide nanoparticles. Also, a sustained release upto 96% over 24 hours in PBS medium was obtained for poly-lactic-co-glycolic acid- poly N-isopropylacrylamide nanoparticles core-shell as a matrix. This release pattern is attributed to its non-fickian nature which suggested that release of ramipril is diffusion controlled. Overall, PLGA showed better characteristics than PLA as a drug carrier in case of ramipril adsorption over its matrix. These abilities of the core – shell nanoparticle system will prove to be important in future *in-vivo* studies focused on probing the capability of these nanoparticles to deliver the therapeutics.

2.10 References

[1] D. Lemoine, C. Francois, F. Kedzierewicz, W. Preat, M. Hoffman, P. Maincent, Biomaterials, 17 (1996) 2191-2197.

[2] J. Panyam, W.-Z. Zhou, S. Prabha, S.K. Sahoo, V. Labhasetwar, The FASEB Journal, 16 (2002) 1217-1226.

[3] R.A. Jain, Biomaterials, 21 (2000) 2475-2490.

[4] C. Wischke, S.P. Schwendeman, International Journal of Pharmaceutics, 364 (2008) 298-327.

[5] M.L. Hans, A.M. Lowman, Current Opinion in Solid State Material Science, 6 (2002) 319-327.

[6] J. Panyam, V. Labhasetwar, Advance Drug Delivery Reviews, 55 (2003) 329-347.

[7] J.M. Anderson, M.S. Shive, Advance Drug Delivery Reviews, 28 (1997) 5-24.

[8] M. Chacon, J. Molpeceres, L. Berges, M. Guzman, M.R. Aberturas, European Journal of Pharmaceutical Sciences, 8 (1999) 99-107.

[9] M. Holzer, V. Vogel, W. Mantele, D. Schwartz, W. Haase, K. Langer, European Journal of Pharmaceutics and Biopharmaceutics, 72 (2009) 428-437.

[10] X.Z. Zhang, R.X. Zhuo, European Polymer Journal, 36 (2000) 2301-2303.

[11] K. Suzuki, T. Yumura, Y. Tanaka, M. Akashi, Journal of Controlled Release, 75 (2001) 183-189.

[12] C.J. De Groot, M.J.A. Van Luyn, W.N.E. Van Dijk-Wolthuis, J.A. Cadée, J.A. Plantinga, W.D. Otter, W.E. Hennink, Biomaterials, 22 (2001) 1197-1203.

[13] D. Duracher, A. Elaissari, F. Mallet, C. Pichot, Langmuir, 16 (2000) 9002-9008.

[14] J.-T. Zhang, S.-W. Huang, S.-X. Cheng, R.-X. Zhuo, Journal of Polymer Science Part A: Polymer Chemistry, 42 (2004) 1249-1254.

[15] C.-J. Cheng, L.-Y. Chu, J. Zhang, H.-D. Wang, G. Wei, Colloid and Polymer Science, 286 (2008) 571-577.

[16] A. Afrassiabi, A.S. Hoffman, L.A. Cadwell, Journal of Membrane Science, 33 (1987) 191-200.

[17] L. Zeng, L. An, X. Wu, Modeling Drug-Carrier Interaction in the Drug Release from Nanocarriers, Journal of Drug Delivery 2011 (2011)1-15.

[18] M. Cetin, M.S. Aktas, I. Vural, M. Ozturk, Journal of Microencapsulation, 29 (2012) 156-166.

[19] C.-H. Hsu, Z. Cui, R.J. Mumper, M. Jay, AAPS PharmSciTech, 4 (2003) 24-35.

CHAPTER 3

Entrapment and Release Efficiency of Hollow Chitosan Nanospheres Incorporated Ramipril

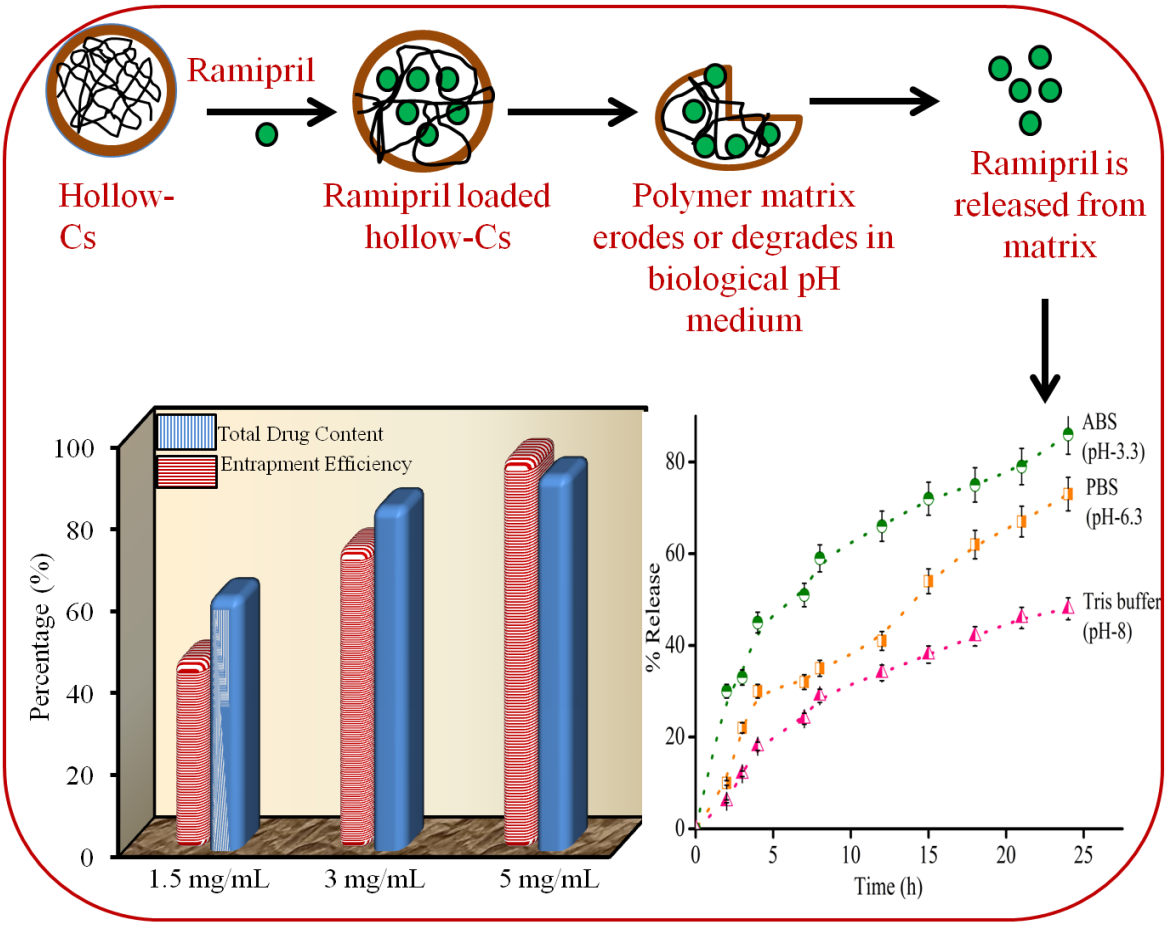

3.1 Introduction

Biodegradable polymers have gained immense importance in the field of controlled drug delivery due to their size and simplistic fabrication. The main advantage of biodegradable drug loaded polymers is their enhanced therapeutic effect of drug and subsequent lower dose requirement and reduction in toxic side effects [1]. PLGA and chitosan (Cs) are two widely used biodegradable polymers. PLGA is biocompatible, non-toxic biopolymer that degrades into lactic and glycolic acid in the body.

Similarly, Cs, a biopolymer of chitin monomeric units is an excellent flocculent, adhering to negatively charged surfaces is non-toxic, biocompatible, biodegradable and also have fungicidal activities [2-6], apart from having a unique chemical structure as a linear polyelectrolyte with a high charge density and reactive hydroxyl and amino groups [7]. Chitosan and its derivatives are widely used as drug delivery vehicles [8] like, chitosan modified with PLGA nanoparticles for improved drug delivery was reported by Wang et al. [9]. Also, Campos et al. [10] reported the use of chitosan as solid lipid nanoparticle (SLN) for effective delivery of paclitaxel. Cs microspheres have been used in gastric drug delivery [11]. For increasing insulin's intestinal absorption and to enhance its pharmacological bioavailability insulin loaded chitosan nanospheres have been used [12].

Chitosan also exhibits various fascinating biological activities like induced disease resistance in plants, antimicrobial activity etc. [13, 14]. All these properties of chitosan makes it useful in different fields like food and chemical engineering, pharmaceuticals, nutrition etc. [15]. In recent years, hollow nanospheres have attracted great potential as drug delivery carriers due to high surface area and low effective density [16]. Several methods for preparation of hollow nanospheres are available [17] like emulsion polymerization [18, 19], self-assembly of block copolymers [20-22] and template polymerization [23, 24], etc.

The template method is the most frequently employed to synthesize hollow nanospheres, as it can control the core size and the hollow structure can easily be obtained after removal of template by evaporation or thermolysis. Drug loading in polymer nanoparticles takes place by two ways, firstly- addition of drug during the preparation of particles itself and secondly-after the formation of the particles. In case of hollow nanospheres, the second method is applicable i.e., the drug is loaded afterwards and hence, the aqueous/organic interface produced by water-in-oil micro emulsion. The acute shearing strength is brought by the high-speed homogenizer causes drug (like bio macromolecules)

denaturation and the aggregation could be avoided, which is advantageous compared to non-hollow nanoparticles [25].

In this study, template method was employed to prepare hollow Cs nanospheres. Presence of positive charge over the surface of Cs allows it to bind readily to the negatively charged surfaces. For superior binding of the chitosan shell to the PLGA template core, the negative charge on the surface of PLGA template was enhanced by treating it with sodium dodecyl sulfate (SDS). The adsorption of chitosan over PLGA template occurred mainly due to the electrostatic interactions between sulphuric acid groups of SDS present on the PLGA template and amino groups of chitosan. The adsorbed Cs layer was further crosslinked to the PLGA template with a non-toxic crosslinker d,l-glyceraldehyde to further solidify the chitosan layer over the PLGA template. The hollow chitosan nanospheres (CsNs) were obtained by subsequent removal of PLGA template in acetone as shown in scheme 3.1.

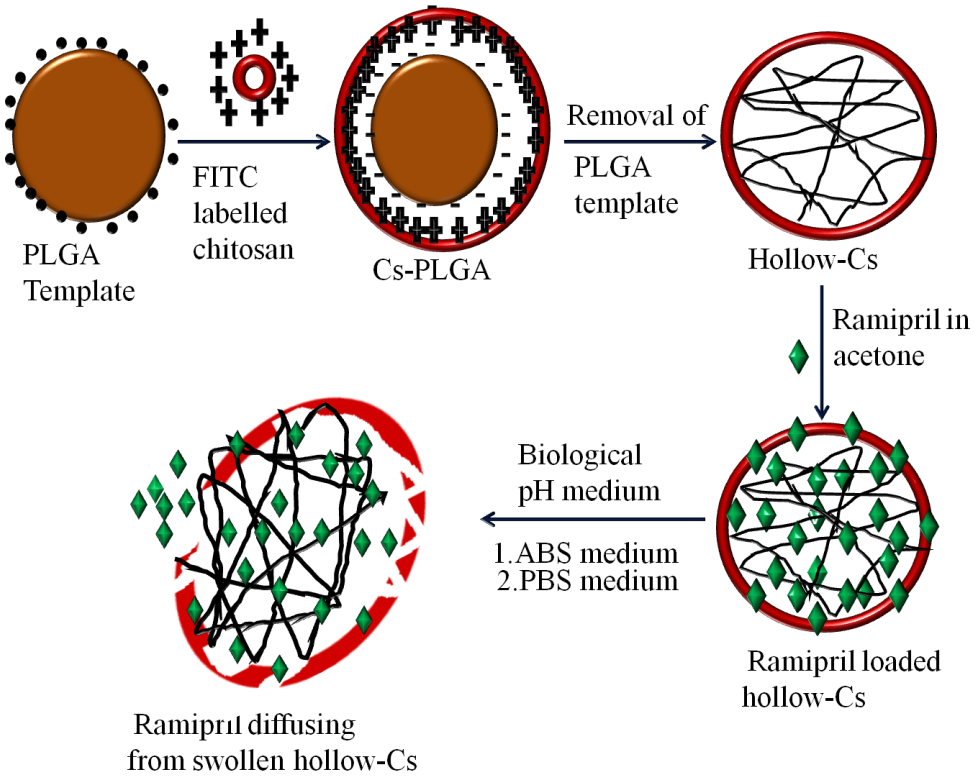

ABS- Acetate buffer solution
PBS- Phosphate buffer solution

PLGA- poly-D,L-lactide-co-glycolide
Cs- Chitosan

Scheme 3.1: Schematic representation showing preparation of hollow chitosan nanospheres and diffusion of ramipril through hollow chitosan matrix in different biological pH mediums

3.2 Experimental section

3.2.1 Materials

Poly-D, L-lactide-co-glycolide (50:50), Chitosan, PEG 6000, and Tween 80 were purchased from Sigma-Aldrich. Ramipril was received as a gift sample from Mefro Pharmaceuticals (Mohali, Punjab, India). All other reagents were obtained from Loba Chemie, India and used as received without further purification. De-ionized water was obtained using an ultra filtration system (Milli-Q, Millipore).

3.2.2 Preparation of PLGA nanoparticle template

The details of PLGA template preparation are given in **Chapter 1, section 1.4.6.**

3.2.3 Preparation of core@ shell Cs@PLGA nanospheres

The details of Cs@PLGA nanospheres preparation are given in **Chapter 1, section 1.4.7.**

3.2.4 Preparation of ramipril loaded hollow Cs NS

The details of loading of ramipril in hollow Cs NS is given in **Chapter 1, section 1.4.8.**

3.2.5 Characterization

As synthesized core@shell NPs were characterized by various techniques, the details of the techniques are given in **Chapter 1**, **section 1.5**.

3.2.6 In-vitro drug release of ramipril and kinetic studies

Preweighed nanospheres (0.1g) were suspended in 50 mL of Tris buffer pH 8.0, phosphate buffer solution (PBS) pH 6.3 and acetate buffer solution (ABS) pH 3.3. At pre determined intervals, 5 ml of sample was withdrawn and replaced with fresh Tris buffer, PBS and ABS. The withdrawn sample was centrifuged at 10,000 rpm for 15 minutes and the amount of drug released was determined by HPLC using Tris buffer: ACN (30:70 v/v), Phosphate buffer: ACN (30:70 v/v) and Acetate buffer: ACN (30:70 v/v) as mobile phase. 20 µL of sample was injected with a flow rate of 1.0 ml/min at 210nm wavelength.

The data obtained from the *in-vitro* release study was fitted into korsemeyer- peppas drug release kinetic model to determine the release exponent ‘n’ value for describing the mechanism of drug release and the resulting regression coefficient values were calculated.

3.3 Results and Discussion

3.3.1. Structural and morphological characterization

The DLS studies showed build up of Cs shell over PLGA template with an increase in average particle size of Cs@PLGA Ns (186 nm) in comparison to 125 nm of PLGA template (figure 3.1(a)). The observed polydispersity along with DLS for PLGA template was 0.651 while for CS@PLGA Ns it was 0.428 which indicated that the particles were evenly distributed in the solution.

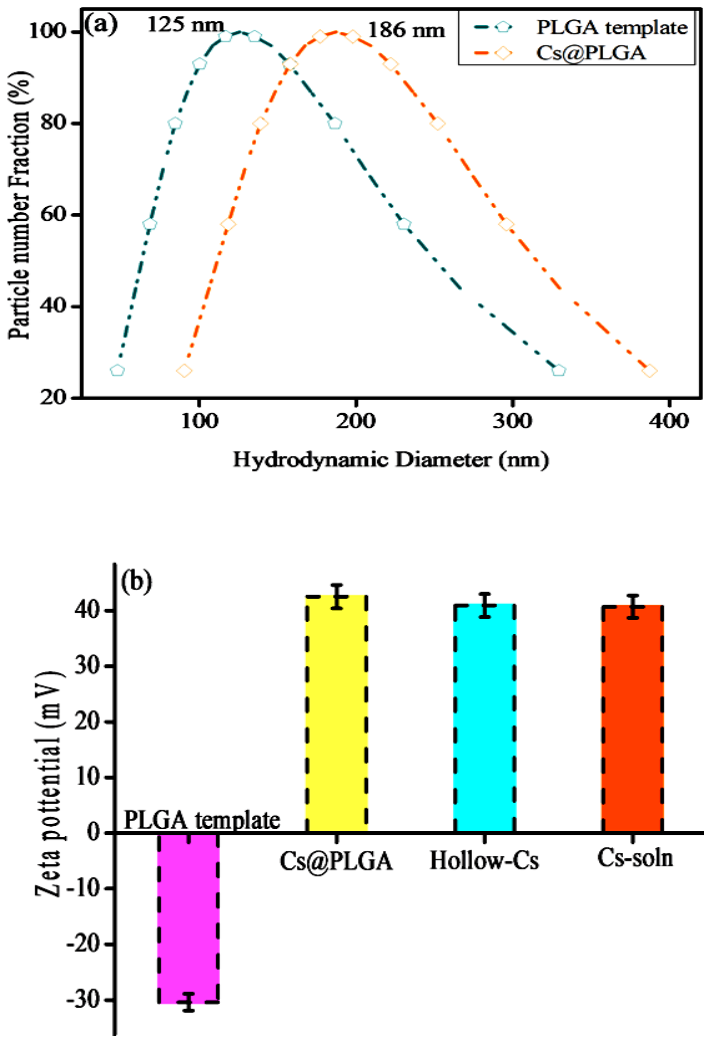

Figure 3.1: (a) Average particle size and (b) Zeta potential of PLGA template and chitosan coated PLGA nanospheres

A shift in the zeta potential value from PLGA template to Cs@PLGA was observed (figure 3.1(b)). PLGA template showed a zeta potential of -30.4 ± 0.3 mV due to the presence of hydroxyl groups on its surface, whereas Cs@PLGA showed a zeta potential of + 42.5± 0.2 mV. This shift in surface charge can be attributed to adsorption of Cs layer over PLGA surface due to the presence of positively charged amino groups on the surface of Cs. In addition the zeta potential of hollow-Cs and bare Cs-solution was also observed. Nearly similar values were obtained for Cs@PLGA, hollow-Cs and bare Cs-solution. All the measurements were taken in triplicate with ±5% error as shown in (figure3.1 (b)).

The BET surface area of PLGA template and Cs nanospheres after the removal of PLGA was 62.9m^2g^{-1} and 111.8m^2g^{-1} respectively (figure 3.2) indicating hollow morphology of the Cs nanospheres.

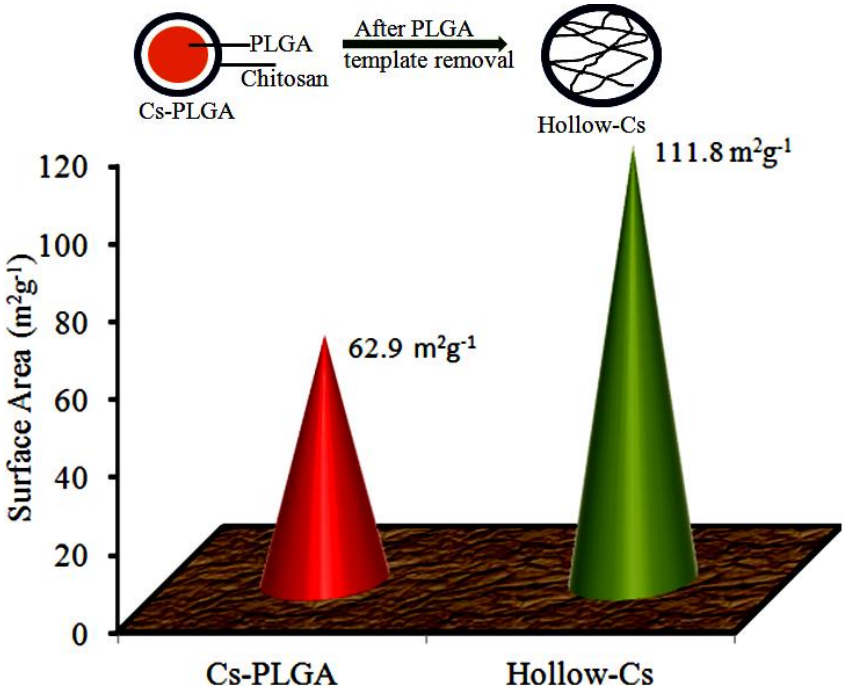

Figure 3.2: Surface area of core-shell Cs@PLGA nanospheres and hollow-Cs nanospheres after removal of PLGA template

TEM images of PLGA template, Cs@PLGA nanospheres, hollow-Cs nanospheres and ramipril loaded hollow–Cs nanospheres are shown in figure 3.3. A uniform dispersion of the Cs@PLGA and hollow-Cs nanospheres is observed. The core@shell structure can be seen in figure 3.3 (b). It was observed that the inner PLGA template core being solid is darker than the outer shell of chitosan layer (transparent gel). Nearly hollow morphology of the Cs nanospheres was also confirmed (figure 3.3 (c)) and ramipril loaded hollow-Cs were also obtained (figure 3.3 (d)).

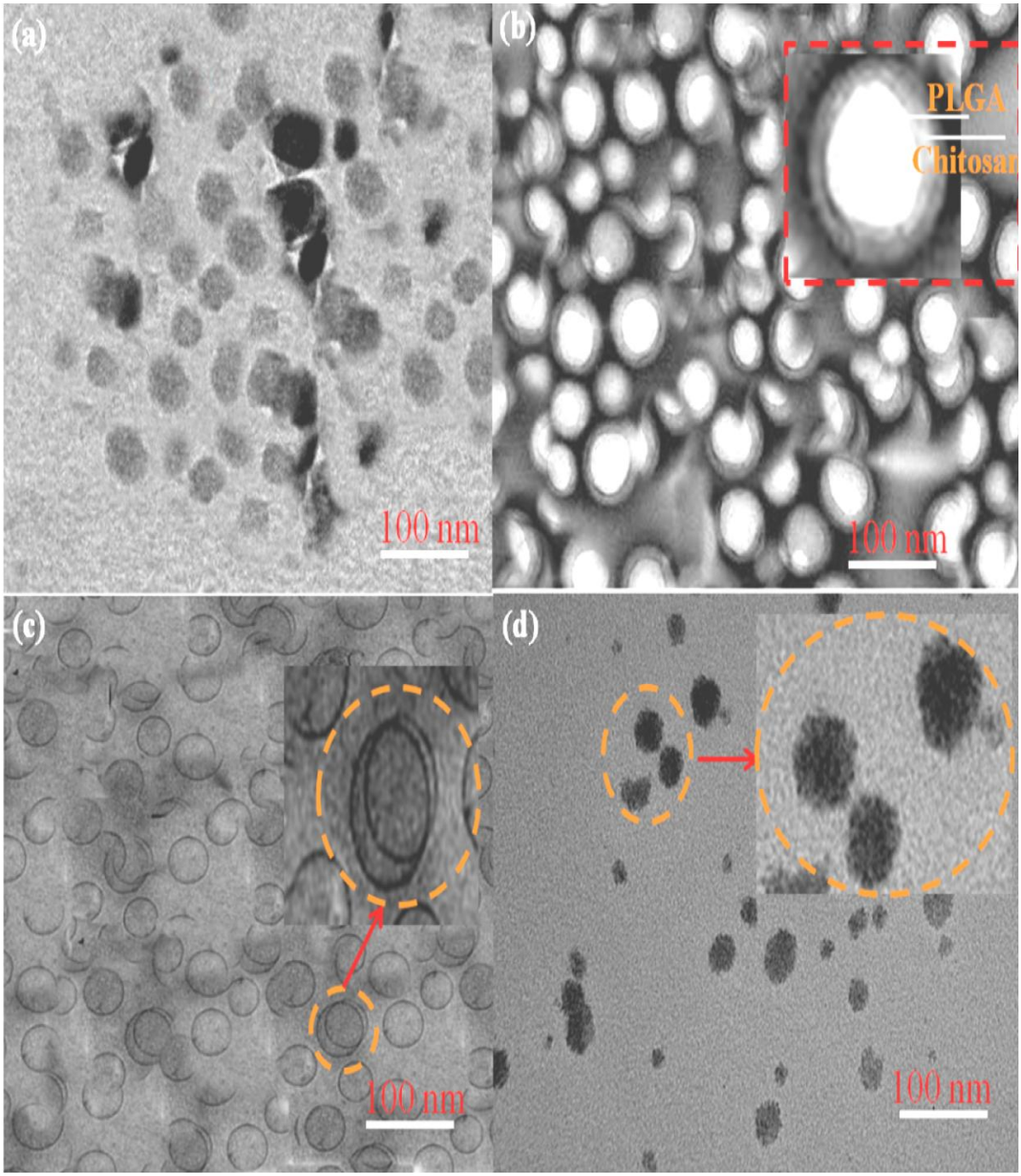

Figure 3.3: TEM images of (a) PLGA template (b) chitosan coated PLGA nanospheres (c) hollow chitosan nanospheres and (d) ramipril loaded hollow chitosan nanospheres

A Change in surface roughness of Cs@PLGA (246.752 nm) to (14.297 nm) for hollow- Cs was observed in the AFM study (figure 3.4 and 3.5) further confirming the hollow structure of the nanospheres.

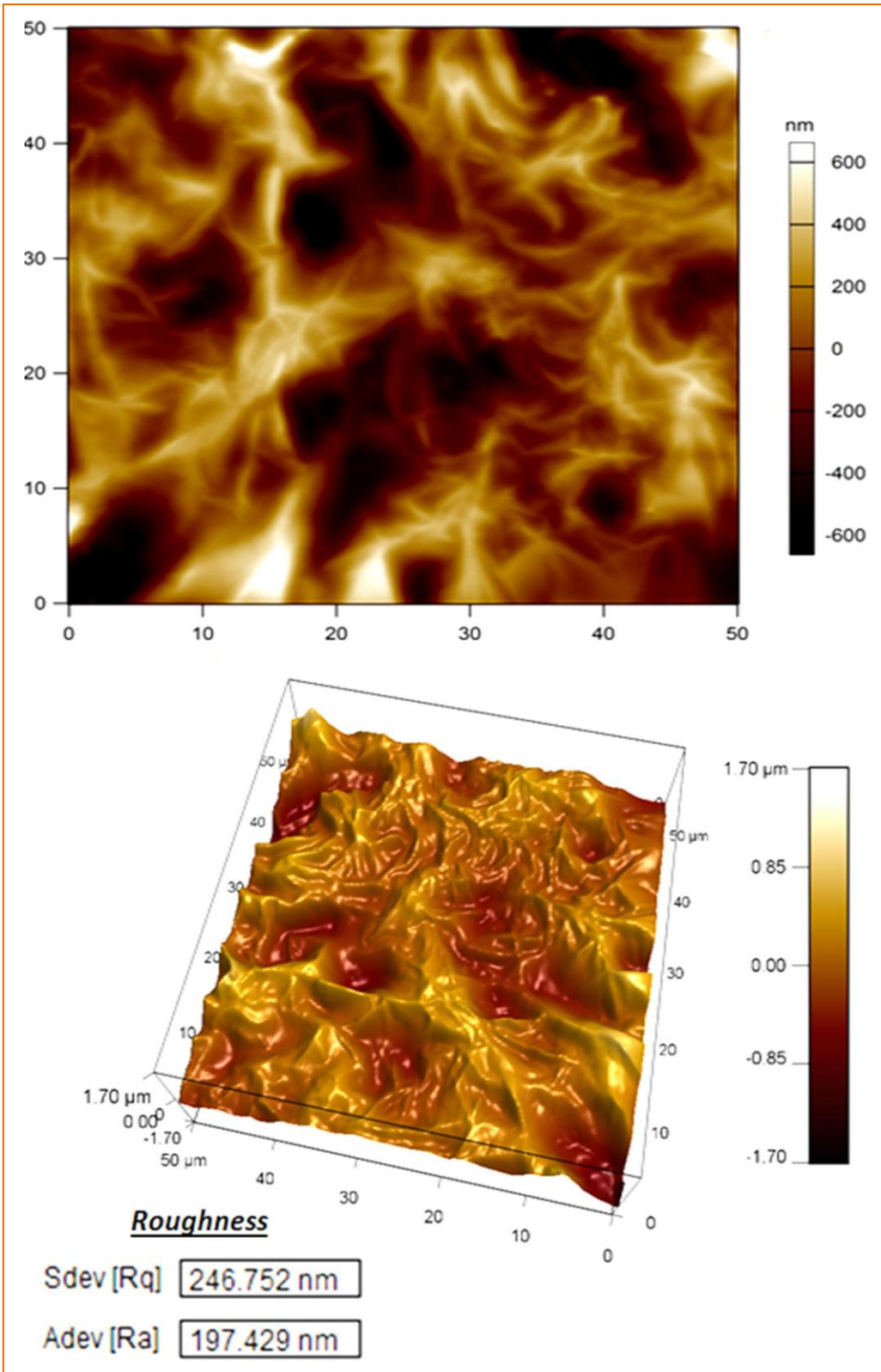

Figure 3.4: AFM images of Cs@PLGA in amplitude mode

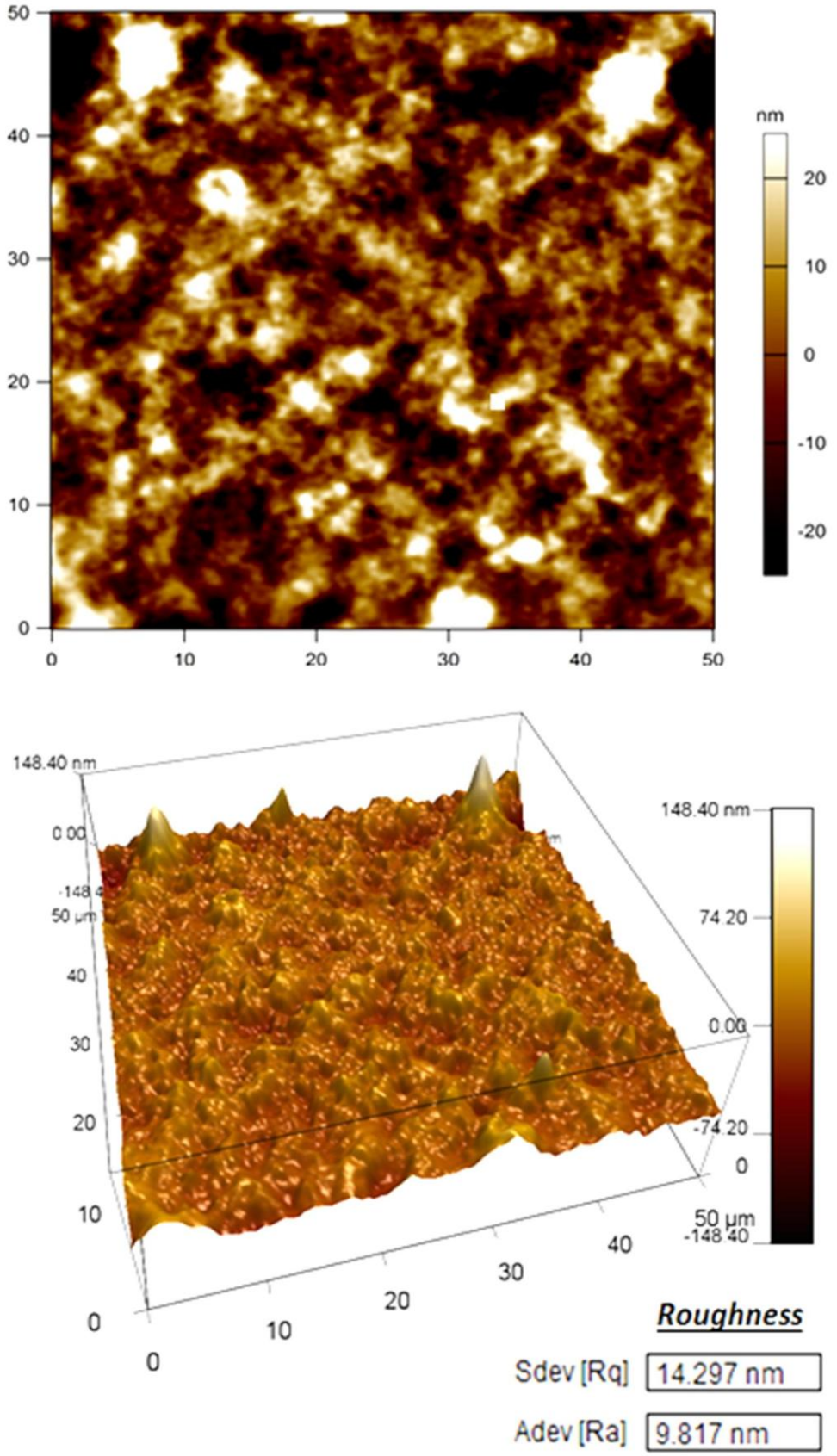

Figure 3.5: AFM images of chitosan after removal of template in amplitude mode

Thermo gravimetric analysis of Cs@PLGA and hollow-Cs is shown in figure 3.6. It was observed that compared to hollow-Cs, Cs@PLGA has low thermal degradation temperatures. Cs@PLGA showed initial weight loss due to moisture vaporization and the pyrolisis appeared around 250°C. Chain and branch bonding was thermally decomposed in the range of 300°-400°C. On the other hand in case of Cs, after initial evaporation of residual moisture, the thermal decomposition took place in two steps. Firstly at around 200-400°C depolymerisation and decomposition of glucosamine units of chitosan took place followed by oxidative decomposition of residues in temperature range of 400°-500°C. The thermal degradation patterns showed that the Cs nanospheres were stable in a temperature range (upto 200°C) where it can be used as delivery carrier.

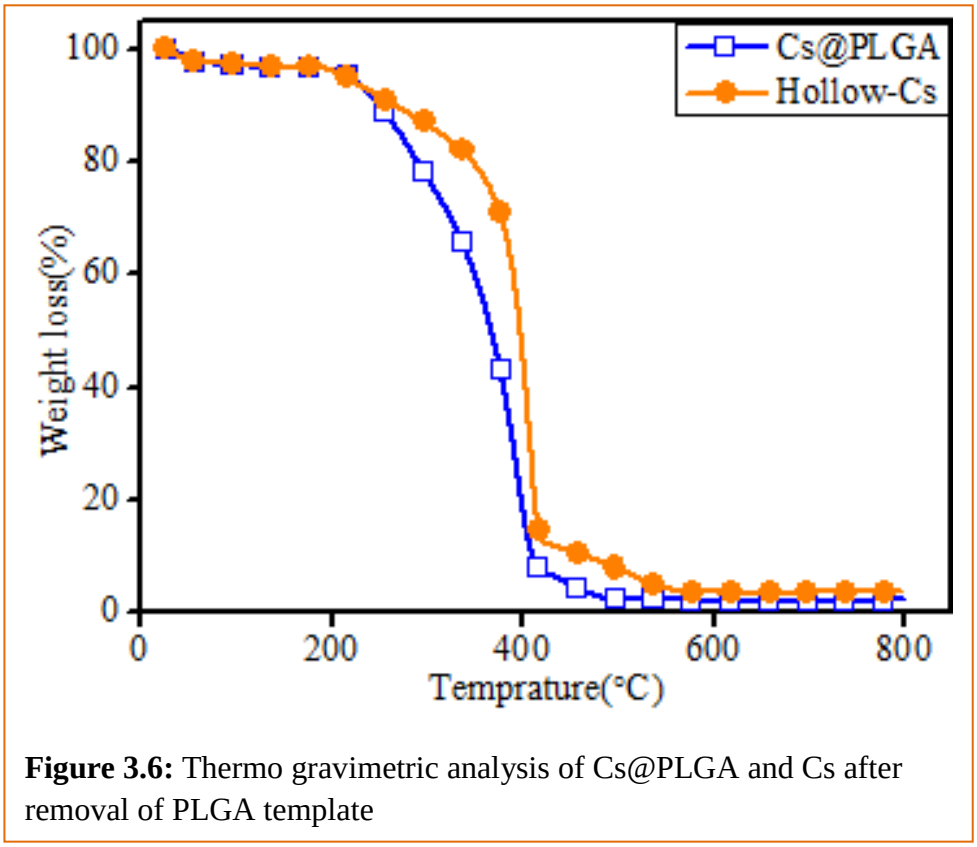

Figure 3.6: Thermo gravimetric analysis of Cs@PLGA and Cs after removal of PLGA template

4.3.2. Encapsulation of ramipril in hollow-Cs nanospheres

Diffusion of ramipril took place inside the hollow-Cs nanospheres since there is difference in the concentration of ramipril in the hollow nanospheres and outer surroundings [26]. Interaction between the amino group of chitosan and carboxylic group of ramipril (Figure 3.7**)** allows the entrapment of ramipril within the chitosan matrix.

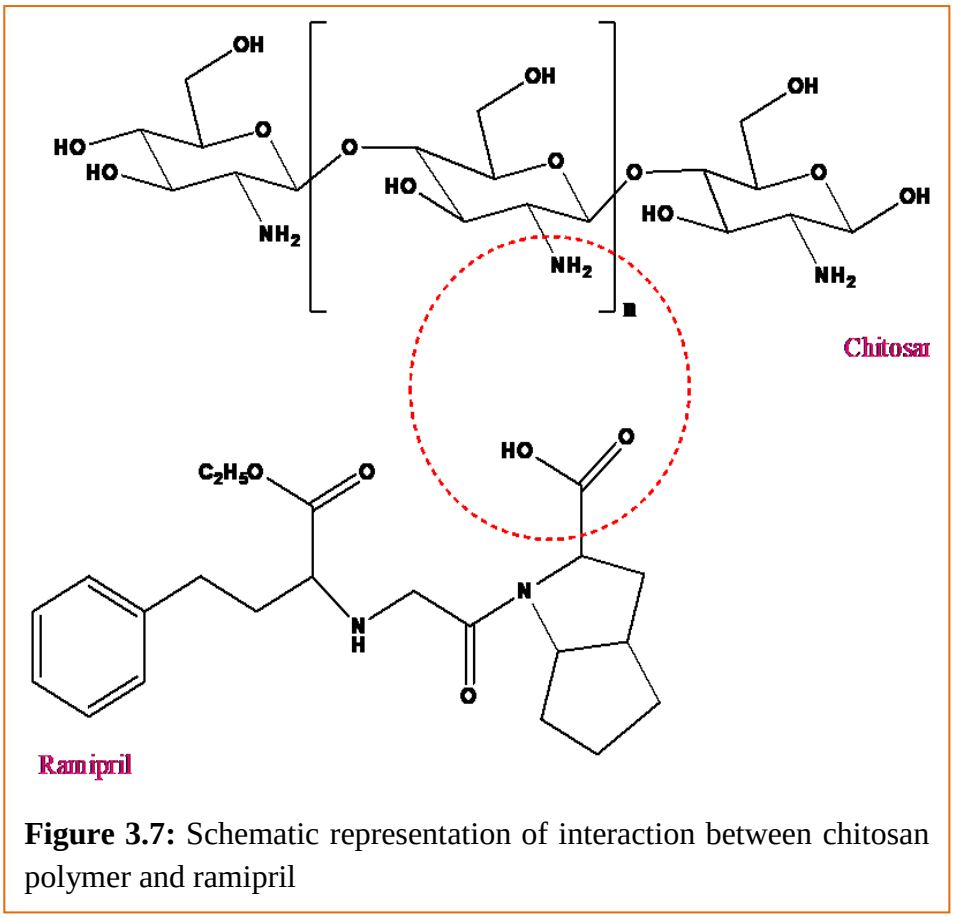

Figure 3.7: Schematic representation of interaction between chitosan polymer and ramipril

In order to obtain high drug loading in hollow nanospheres effect of different concentrations and time was investigated.

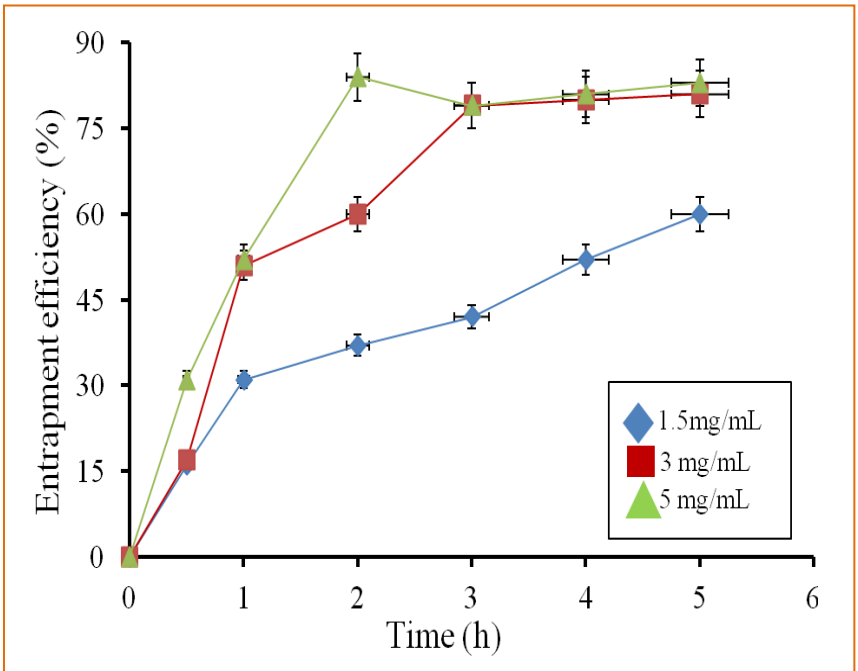

Figure 3.8: Influence of different concentrations of ramipril on entrapment efficiency

Figure 3.8 indicated that adsorption reached the peak and kept stable after 2h when ramipril concentration was 5 mg/ml. High entrapment efficiency of 90.8% and total drug content of 95.2% was obtained shown in figure 3.9.

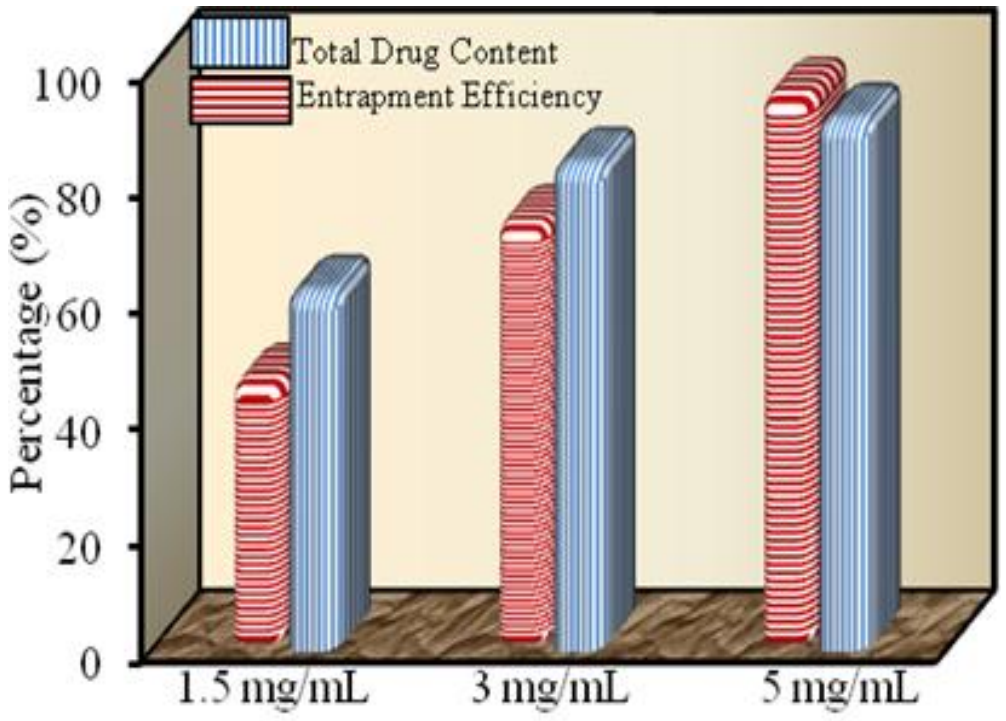

Figure 3.9: Total drug content and entrapment efficiency of drug in hollow-Cs nanospheres

4.3.3. In-vitro release of ramipril and kinetics study

A calibration curve for the standard ramipril solution was plotted and is shown in figure 3.10. The *in-vitro* release of ramipril in phosphate buffer solution (PBS) of pH-6.3 and acetate buffer solution (ABS) of pH- 3.3 was determined using HPLC (figure 3.11). The percent release of ramipril from hollow-Cs nanospheres incubated in Tris buffer, PBS and ABS is shown in figure 3.12. Around 45% of drug release in the first 5h is observed in ABS medium. This initial burst release is followed by levelling off. Nearly 86% of drug release is observed over 24h from NS in ABS, while 73% drug was released from NS in PBS and only around 48% of ramipril was released from tris buffer. pH of the medium played an important role in release of ramipril from Cs matrix. It is observed that release rate decreased with increase in pH of medium i.e. a more rapid release was observed at pH 3.3 than at pH 6.3and pH 8.0. This difference in release rate may be ascribed to the swelling behaviour of hollow-Cs nanospheres in different pH mediums.

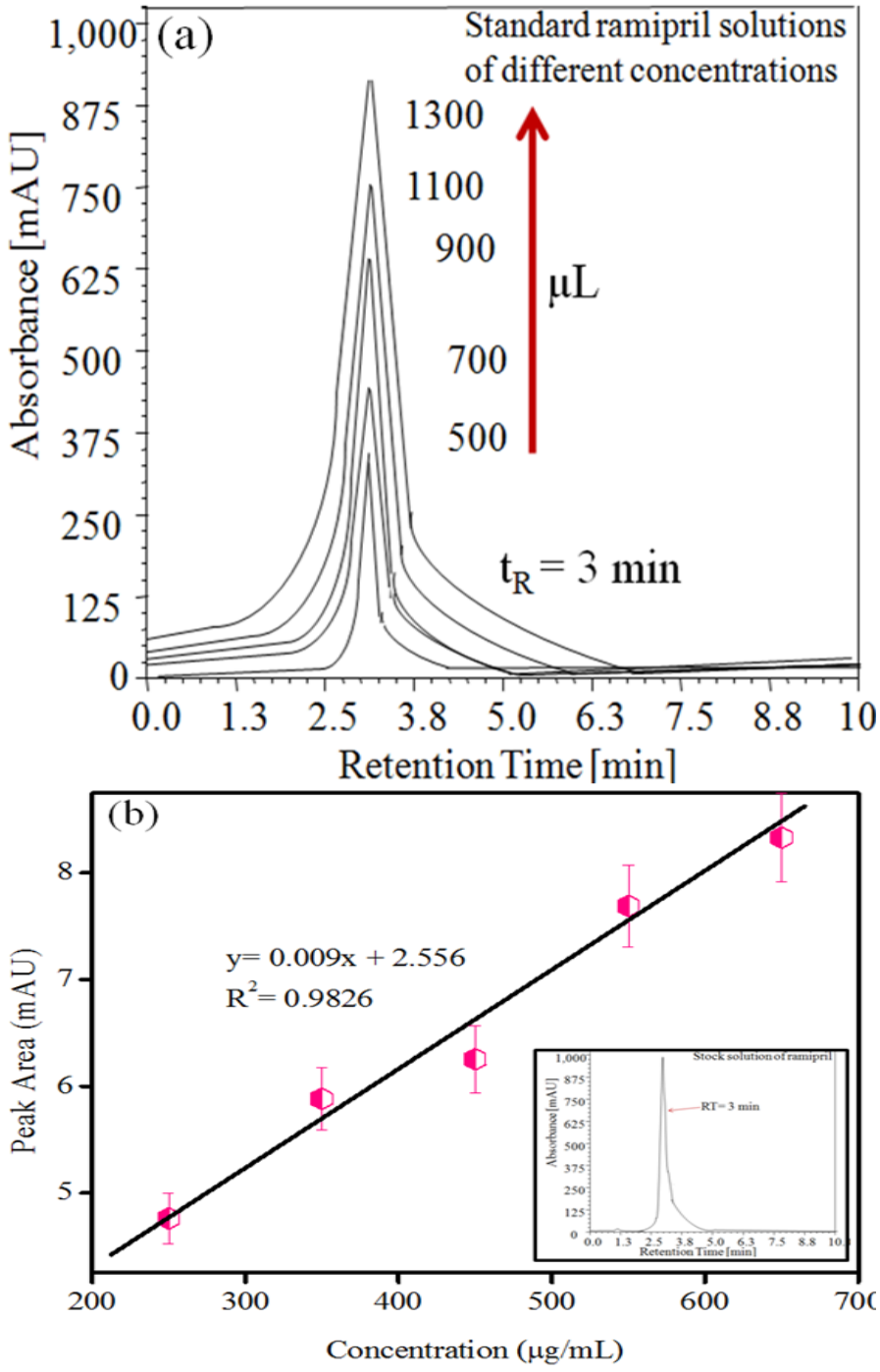

Figure 3.10: (a) HPLC chromatogram of standard ramipril solutions and (b) calibration curve for the standard solutions

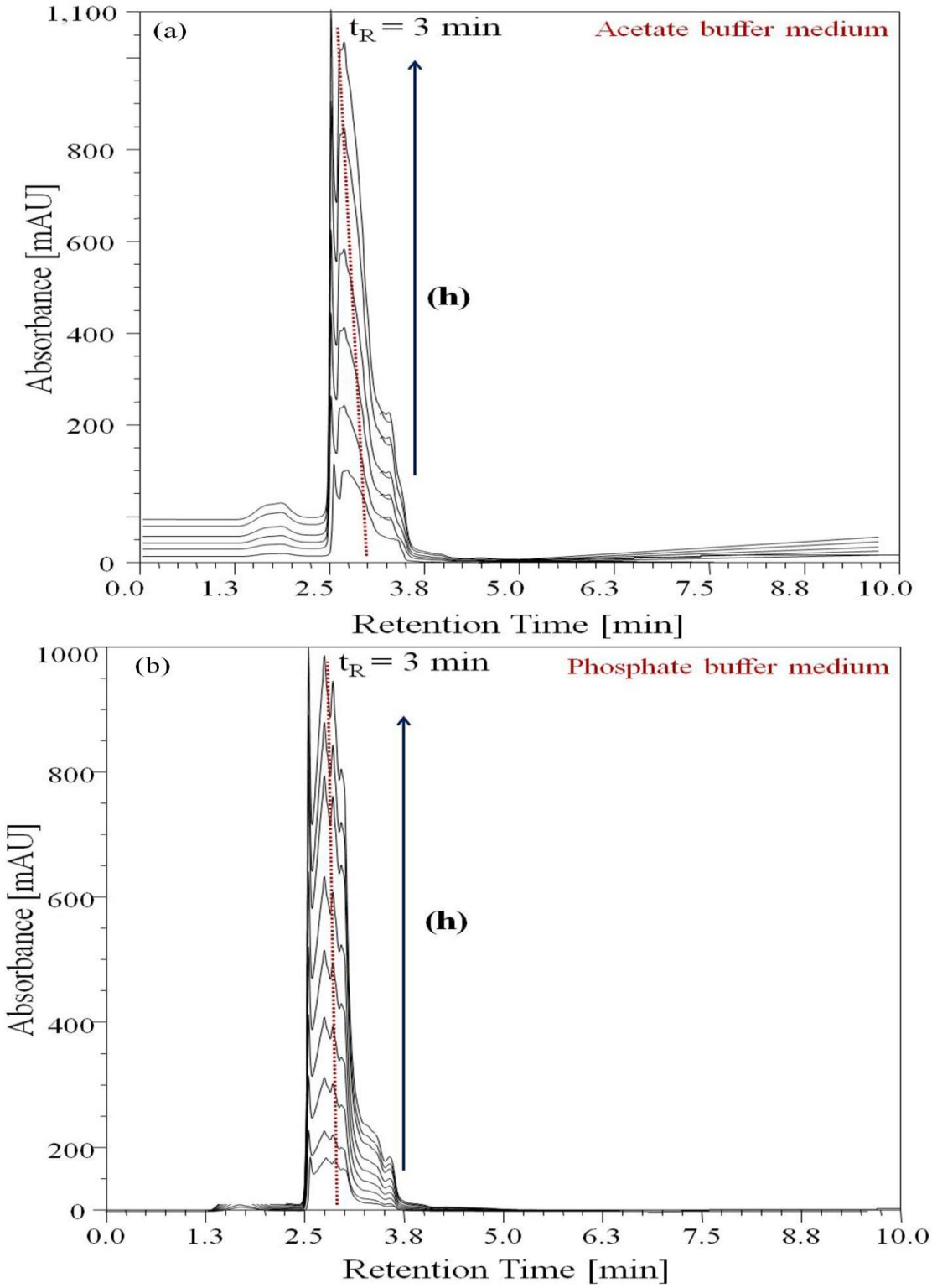

Figure 3.11: HPLC of ramipril release from chitosan matrix (t_R-3 min) in (a) acetate buffer and (b) phosphate buffer medium

The hollow-Cs nanospheres swell to a greater amount in acidic medium conditions due to breakage of amino groups, which in turn leads to breaking of strong hydrogen bonding within the chitosan chains, thereby making it easier for the drug to be diffused out of polymer matrix. However, at higher pH (8.0 & 6.3) it was observed that the swelling of hollow nanospheres is limited and hence ramipril could not diffuse out easily [25]. The experiments were repeated three times with ±5% error.

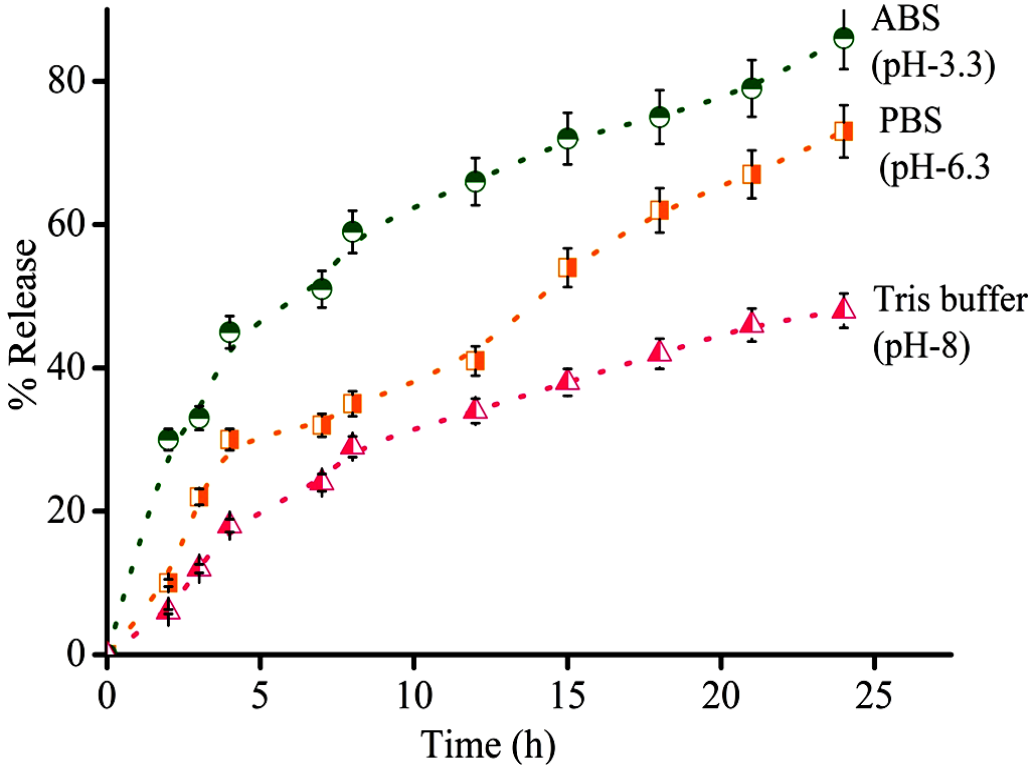

Figure 3.12: *In-vitro* release of ramipril from hollow-Cs incubated in phosphate buffer, acetate buffer solution and tris buffer at different time intervals

Mechanism of ramipril release from Cs matrix

The matrix of chitosan swells in a pH dependent manner when placed in an appropriate buffer solution thereby breaking the hydrogen bonding capacity of the chitosan. This pH sensitive behaviour is due to presence of amino groups on its chains. As the chitosan network contains pH-ionisable groups, a pH variation will modify the network electrical state and thus the swelling behaviour [27]. This pH-responsive behaviour could be ascribed to the

protonation of the primary amino group on the chitosan chain, resulting in the increase of electric density and repulsion force between crosslinked chitosan chains. This leads to breaking of interaction between the amino groups of chitosan and carboxylic acid of ramipril. The swelling creates a build up of an osmotic pressure due to which the ramipril starts diffusing out of the chitosan matrix. The sustained release of ramipril from chitosan is mainly due to the chitosan-ramipril interaction.

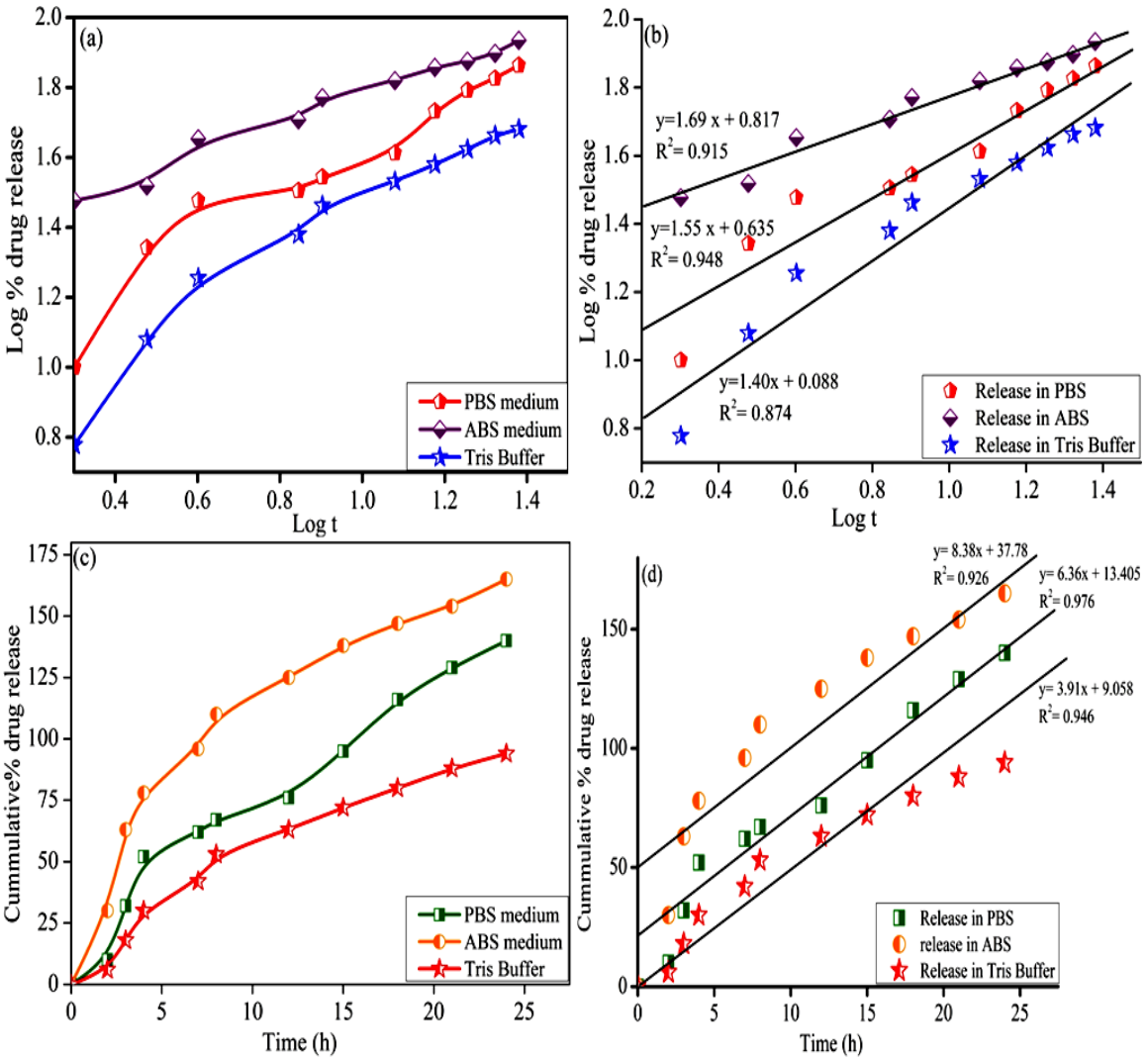

Figure 3.13: Kinetic models of drug release (a-b) Korsemeyer-Peppas plots and (c-d) Zero order plots in acetate buffer and phosphate buffer medium

Figure 3.13 shows the release exponent (n) values for different formulations obtained from fitting the drug release profile into the Korsemeyer-Peppas model. The 'n' value of 1.69 for ABS medium, 1.55for PBS medium and 1.40 for tris buffer medium (figure 3.13(b))

indicated that drug release follows a zero order (figure 3.13(c)) release mechanism and anomalous (non-fickian) diffusion mechanism, which signifies that release of ramipril from the matrix of hollow-Cs is diffusion as well as swelling controlled.

3.4 Conclusion

In summary, template method is used to fabricate biodegradable and biocompatible Cs nanospheres. PLGA was employed as template prepared by solvent evaporation method. An increase in size from 125-186 nm and shift in zeta potential indicated adsorption of chitosan layer over PLGA template. BET surface area analysis confirmed the formation of hollow Cs nanospheres which were further characterized by TEM and AFM. Higher entrapment efficiency (90.8%) was obtained when ramipril concentration was 5 mg/mL in polymer matrix. The release profile of ramipril was influenced by pH of the medium i.e. with increase in pH from 3.3 to 6.3 to 8.0 the release rate decreases. 86% drug was released in ABS (pH 3.3) while 73% and 48% of drug released from polymer matrix in PBS (pH 6.3) and tris buffer (pH 8.0) over 24 hours. The kinetic data obtained for the release profile of ramipril showed that release of ramipril was diffusion as well as swelling controlled.

3.5 References

[1] G. Polacco, M.G. Cascone, L. Lazzeri, S. Ferrara, P. Giusti, Polymer International, 51 (2002) 1464-1472.

[2] R. Muzzarelli, M. Mattioli-Belmonte, A. Pugnaloni, G. Biagini, Europe PMC, 87 (1999) 251-264.

[3] O. Stoilova, N. Koseva, T. Petrova, N. Manolova, I. Rashkov, M. Naydenov, Journal of Bioactive and Compatible Polymers, 16 (2001) 379-392.

[4] X. Wang, Y. Zhu, Q. Feng, F. Cui, J. Ma, Journal of Bioactive and Compatible Polymers 18 (2003) 135-146.

[5] M. Zhang, T. Tan, H. Yuan, C. Rui, Journal of Bioactive and Compatible Polymers, 18 (2003) 391-400.

[6] E.-R. Kenawy, F.I. Abdel-Hay, A.A. El-Magd, Y. Mahmoud, Journal of Bioactive and Compatible Polymers, 20 ((2005) 95-111.

[7] E.B. Denkbas, R.M. Ottenbrite, Journal of Bioactive and Compatible Polymers, 21 (2006) 351-368.

[8] Y. Ku, I.K. Shim, J.Y. Lee, Y.J. Park, S.H. Rhee, S.H. Nam, J.B. Park, C.P. Chung, S.J. Lee, Journal of Biomedical Materials Research Part A, 90 (2009) 766-772.

[9] Y. Wang, P. Li, L. Kong, AAPS Pharmscitech, 14 (2013) 585-592.
[10] J. Campos, M. Varas-Godoy, Z.S. Haidar, Nanomedicine, 12 (2017) 473-490.
[11] L. Qi, Z. Xu, X. Jiang, C. Hu, X. Zou, Carbohydrate Research, 339 (2004) 2693-2700.
[12] Y. Pan, Y.-j. Li, H.-y. Zhao, J.-m. Zheng, H. Xu, G. Wei, J.-s. Hao, International Journal of Pharmaceutics, 249 (2002) 139-147.
[13] H. Yi, L.-Q. Wu, W.E. Bentley, R. Ghodssi, G.W. Rubloff, J.N. Culver, G.F. Payne, Biomacromolecules, 6 (2005) 2881-2894.
[14] B. Wang, K. Chen, S. Jiang, F. Reincke, W. Tong, D. Wang, C. Gao, Biomacromolecules, 7 (2006) 1203-1209.
[15] D. Wei, W. Sun, W. Qian, Y. Ye, X. Ma, Carbohydrate Research, 344 (2009) 2375-2382.
[16] J. Bertling, J. Blömer, R. Kümmel, Chemical Engineering and Technology, 27 (2004) 829-837.
[17] J. Han, G. Song, R. Guo, Advanced Materials, 18 (2006) 3140-3144.
[18] W.-J. Liu, Z.-C. Zhang, W.-D. He, X.-W. Ge, H.-R. Liu, M.-Z. Wang, Z.-Q. Chang, Materials Letters, 61 (2007) 2818-2821.
[19] Y. Yang, Y. Chu, Y. Zhang, F. Yang, J. Liu, Journal of Solid State Chemistry, 179 (2006) 470-475.
[20] S. Stewart, G. Liu,), Chemistry of Materials, 11 (1999) 1048-1054.
[21] K. Breitenkamp, T. Emrick, Journal of the American Chemical Society, 125 (2003) 12070-12071.
[22] J.-W. Kim, Y.-G. Joe, K.-D. Suh, Colloid and Polymer Science, 277 (1999) 252-256.
[23] N. Singh, L.A. Lyon, Chemistry of Materials, 19 (2007) 719-726.
[24] T.H. Kim, K.H. Lee, Y.K. Kwon, Journal of Colloid and Interface Science, 304 (2006) 370-377.
[25] S.A. Agnihotri, N.N. Mallikarjuna, T.M. Aminabhavi, Journal of Controlled Release 100 (2004) 5-28.
[26] B. Sarmento, A. Ribeiro, F. Veiga, P. Sampaio, R. Neufeld, D. Ferreira, Pharmaceutical Research, 24 (2007) 2198-2206.
[27] J. Cha, W.B. Lee, C.R. Park, Y.W. Cho, C.H. Ahn, I.C. Kwon, Macromolecular Research, 14 (2006) 573–578.

CHAPTER 4

Cytotoxic Evaluation of Fe_3O_4 Modified PLGA-PEG for Improved Delivery of Methotrexate to Target Site in Cancer Therapy

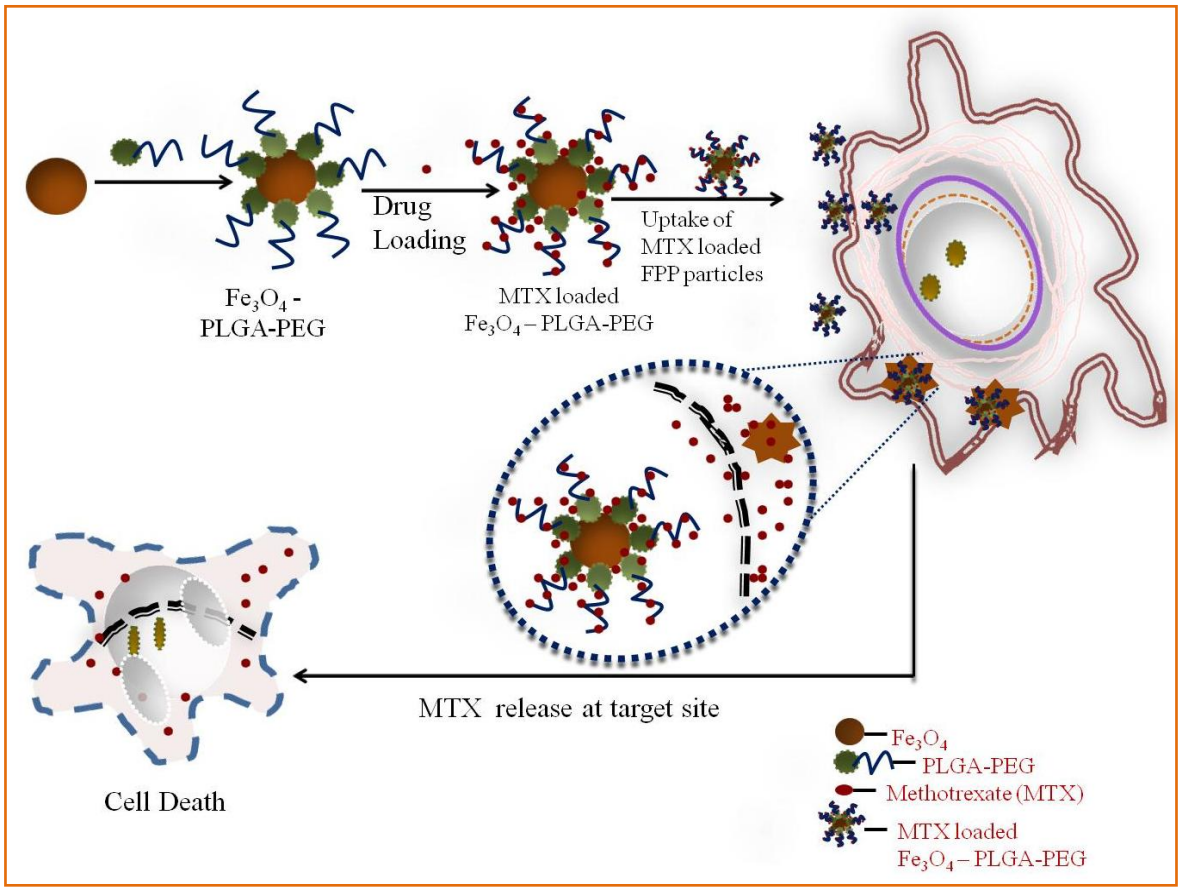

4.1 Introduction

Magnetic nanoparticles (MNPs) are gaining attention in the field of medicine [1],[2]. These MNPs posses attributes that allows them to be used as drug carrier [3, 4], in tumour therapy [5, 6] and MRI agents [7-9]. Other elements like manganese (Mn), copper (Cu), zinc (Zn) and nickel (Ni) can also be applied for preparation of ferrites having general formula M-Fe_2O_4 [10, 11]. However the most widely studied and applied magnetic nanoparticles are iron oxide NPs due to their well known biocompatibility compared to other heavy metal containing nanomaterials that are hard to be degraded and eliminated from the body [12].

PLGA is one of the most efficient biodegradable polymers to be used in the field of drug delivery. Surface modification of PLGA with poly ethylene glycol (PEG) renders it hydrophillicity and other physio-chemical properties. Block copolymers having hydrophilic segment have applications mainly due to their biodegradability, biocompatibility etc [13]. Various surface modified drug loaded PLGA nanoparticles have been synthesized and used for controlled/target drug delivery. Parveen et al. [14] reported the development of a surface coating by hydrophilic polymer PEG which was used to limit the phagocytic properties and to boost the endurance of the NPs. PLGA has been frequently used as a drug delivery carrier in treatment of cancer therapy. Qiong et al. [15] reported the release behaviour of docetaxel an antitumor drug from PLGA coated silica nanorattle. To further improve the targeting ability of PLGA-PEG towards cancer therapy these were modified with magnetic nanoparticles (Fe_3O_4). El-Boubbou et al. [16] reported the preparation of chemotherapeutic agent formed of stabilized metal oxide NPs, which was found to be more efficient than free DOX for the treatment of acute myeloid leukaemia. In lieu of the fact that environment of cancer cells have an acidic pH compared to healthy cells, Nejad et al. [17] reported the synthesis of novel electrospun magnetic nanofibers linked with dopamine based polymers for their use as hyperthermic chemotherapeutic agents. They observed that the catechol moieties over electrospun nanofibers bind with the borate containing anticancer drug BTZ and facilitated a pH dependent release of BTZ.

Methotrexate (MTX) {(2S)-2-[[4-[2,4-diaminopteridin-6-yl]methyl-methylamino]benzoyl]amino]pentanedioic acid} an antineoplastic antimetabolite (folate analog metabolic inhibitor) has broad range of medical applications in cancer treatment. It is a common drug for treatment of lung cancer as well as breast cancer. Apart from this MTX

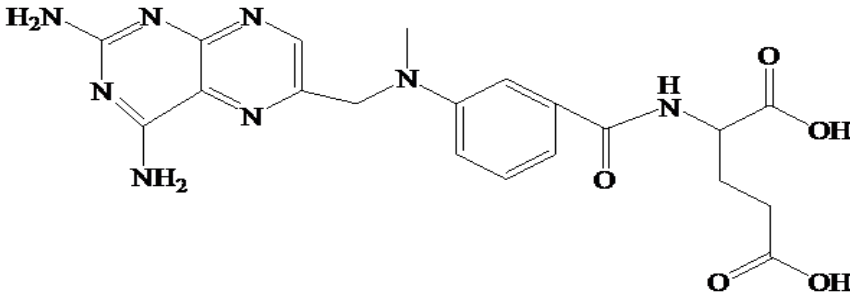

Figure 4.1: Structure of Methotrexate

is also widely used for treatment of rheumatoid arthritis. Although useful it has limited solubility in water besides having side effects [18, 19].

In the present study, Fe_3O_4 modified PLGA-PEG nanocomposite is prepared by double emulsion method to investigate its capability to deliver MTX. The drug release amount in cancer pH environment as well as the cytotoxic effect on the cell lines by *in-vitro* toxicity assays is further studied.

4.2 Experimental section

4.2.1 Materials

Ferric chloride hexahydrate ($FeCl_3.6H_2O$), Ferrous chloride tetrahydrate ($FeCl_2.4H_2O$), Poly-D, L-lactide-co-glycolide (50:50), Tween 80 and Methotrexate (MTX) were purchased from Sigma-Aldrich. PEG 6000 was purchased from Spectrochem India. All other reagents were obtained from Loba Chemie, India and used as received without further purification. De-ionized water was obtained using an ultra filtration system (Milli-Q, Millipore).

4.2.2 Preparation of magnetic (Fe_3O_4) nanoparticles

The magnetic (Fe_3O_4) NPs were prepared by chemical co-precipitation method, details of which are given in **Chapter 1, section 1.4.9.**

4.2.3 Preparation of Pegylated-PLGA

The details of this are given in **Chapter 1, section 1.4.6.**

4.2.4 Preparation of Methotrexate (MTX) loaded Fe_3O_4 –PLGA-PEG particles

MTX loaded particles were prepared by double emulsion method (o/w/o), details of which are given in **Chapter 1, section 1.4.10.**

4.2.5 Characterization

As synthesized core-shell NPs were characterized by various techniques, the details of the techniques are given in **Chapter 1**, **section 1.5**.

4.2.6 In-vitro release of MTX and kinetic studies

To study the release profile of the prepared MTX encapsulated Fe_3O_4-PLGA-PEG nanoparticles, preweighed nanoparticles (3 mg) were suspended in 20 mL of phosphate buffer solution (PBS) pH 7.3 and acetate buffer solution (ABS) pH 4.6. Samples were incubated at 37°C. At regular time intervals, 5 ml of sample was withdrawn and replaced with fresh PBS and ABS. The withdrawn sample was centrifuged at 10,000 rpm for 15 minutes and the amount of drug released was determined by HPLC using Phosphate buffer: ACN (20:80 v/v) and Acetate buffer: ACN (20:80 v/v) as mobile phase. 20 µL of sample was injected with a flow rate of 1.0 ml/min at 302 nm wavelength. Further, the data obtained from the *in-vitro* release study was fitted into different drug release kinetic models to determine the release exponent 'n' value for describing the mechanism of drug release and the resulting regression coefficient values were calculated.

4.2.7 In-vitro cytotoxicity assay

The cytotoxicity studies of bare MTX, PLGA-PEG and MTX loaded nanoparticles were done by MTT assay at Centre for Cellular and Molecular Biology (Hyderabad). SK-BR-3 (breast adinocarcinoma) cells and L929 non cancerous cells were used in this study. Both SK-BR-3 and L929 cell lines were cultured separately in Dulbecco's modified Eagle's medium (DMEM), enriched with 10% foetal bovine serum (FBS) and 1% antibiotic penicillin-streptomycin (Pen Strep). The cells were then kept in humidified incubator at 37°C with 5% CO_2. The assay was done for 1, 2, 3 and 4 days.

Further, cells with a density of $5x10^3$cells/well were seeded in 96 well plates and again incubated at 37°C with 5% CO_2 for 24h. After the attachment of cells they were washed with phosphate buffered saline (PBS), prior to treatment with medium containing 10% of bare nanoparticles, free MTX and MTX loaded nanoparticles. After the incubation of plates for 1, 2, 3 and 4 days, MTT assay was done and the absorbance values of the plates were read at

570 nm using a micro plate reader (ELX800; BioTek). The percentage cell viability was calculated using the equation [20]

$$\text{Cell viability (\%)} = \frac{\text{O. D of sample}}{\text{O. D of control}} \text{ x } 100$$

4.2.8 Fluorescent Imaging

The cells were cultured on cover slips-12 well plates with $40x10^3$cells/well and incubated with different nanoparticle formulations for 24h. After complete incubation, cells were washed with PBS thrice and fixed with 70% ethanol. The cells were stained with 10 µL of Gold Antifade Reagent containing DAPI (4',6-diamidino-2-phenylindole). Finally, the cover slip containing nanoparticle treated cells were placed over the glass slide.

4.3 Results and Discussion

4.3.1. Structural and morphological characterization

The average hydrodynamic size of the prepared Fe_3O_4 NPs, PLGA-PEG and FPP NC is determined by DLS shown in Table 4.1. It was observed that bare Fe_3O_4 NPs and PLGA-PEG have 90 nm and 125nm average size. However an increase in size was observed for FPP NC (140 nm) which indicates the formation of the nanocomposite. The low polydispersity values show that the particles were uniform in shape and evenly distributed in the solution.

Table 4.1: Average particle size and polydispersity of particles.

S.No	Sample	Average Particle Size(nm)	Polydispersity Index(PDI)
1.	Fe_3O_4 NP	90	0.42
2.	PLGA-PEG	125	0.49
3.	FPP	140	0.62

The FTIR spectra of Fe_3O_4, PLGA-PEG and FPP are shown in figure 4.2. A prominent stretching absorbance band at 578 cm^{-1} for Fe-O bond was observed in spectra of Fe_3O_4 [21, 22]. Band at 1748 cm^{-1} is observed for C=O stretching in the spectra of PLGA-PEG. Also a band at 1463 cm^{-1} for C-H deformation of O-CH_2 and 1112 cm^{-1} for stretching's due to asymmetric and symmetric C-C=O vibrations are observed respectively. Band in the fingerprint region is due to C-H aliphatic vibrations. Band for O-H stretching in the spectrum of PLGA-PEG is observed at 2921 cm^{-1} [23, 24]. The blue shifting of Fe-O band at 510 cm^{-1}

is accredited to the formation of Fe_3O_4-PLGA-PEG nanoparticle system [25]. The data showed the formation of magnetite modified PLGA-PEG nanocomposite.

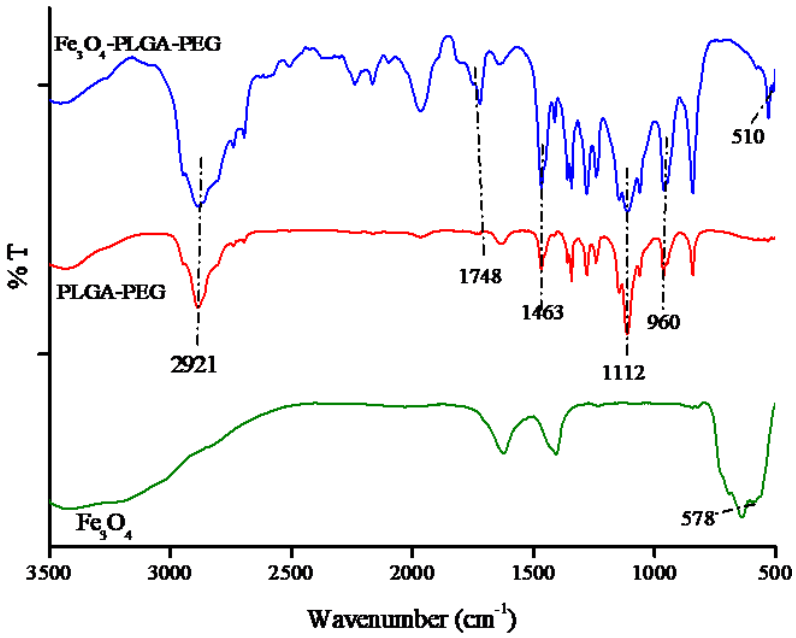

Figure 4.2: FTIR spectra of bare Fe_3O_4, PLGA-PEG and Fe_3O_4-PLGA-PEG nanocomposite

The XRD-diffraction pattern of the prepared Fe_3O_4 nanoparticles and the Fe_3O_4-PLGA-PEG nanocomposite are shown in figure 4.3. The characteristic peaks at 2Θ angles of 30.4, 35.6, 37.6, 43.4, 54.0, 57.4 and 63.1 which corresponds to (220), (311), (222), (400), (422), (511) and (440) diffraction planes are observed. These peaks are found to be consistent with JCPDS card no. 65-3107 [26, 27] indicating a spinel cubic structure of Fe_3O_4. Broad diffraction patterns are obtained which can be attributed to the smaller size of the nanoparticles. The average crystallite

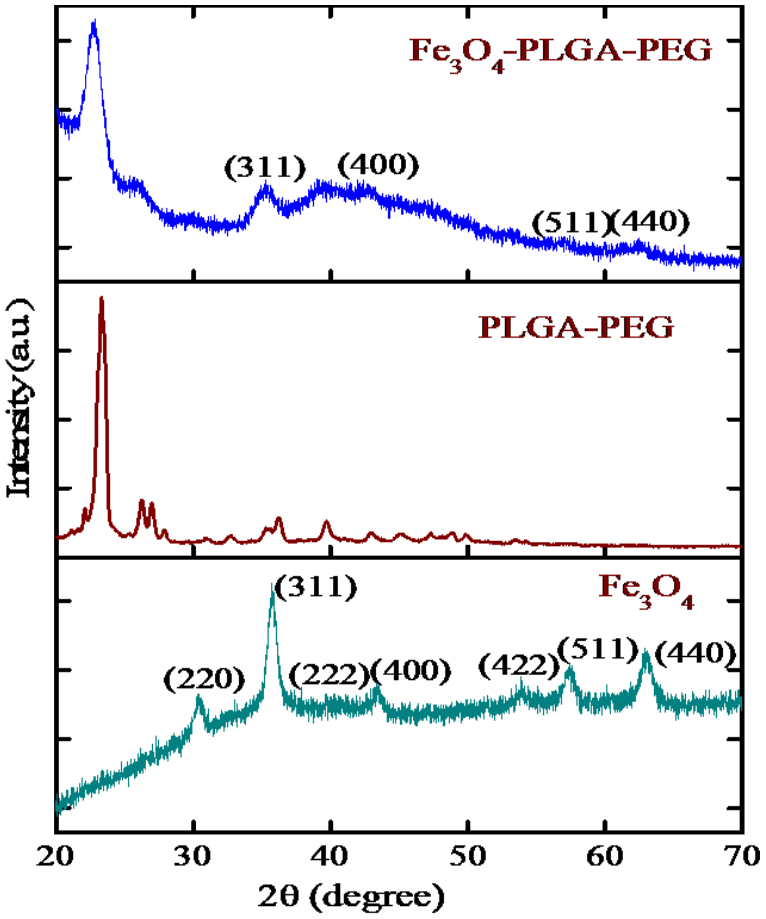

Figure 4.3: XRD diffractograms of bare Fe_3O_4, PLGA-PEG and Fe_3O_4-PLGA-PEG nanocomposite

size is obtained in the range of 10-20 nm as calculated using Debye-Scherrer equation. The FWHM (full width half maxima) for (220) plane is 0.30° showing high crystallinity of the sample. Slight changes in the 2Θ values for Fe_3O_4-PLGA-PEG nanocomposite are observed. This shift can be ascribed to the interaction between both the moieties.

Surface morphology of the prepared Fe_3O_4 nanoparticles and Fe_3O_4-PLGA-PEG nanocomposite is determined by TEM shown in figure 4.4.

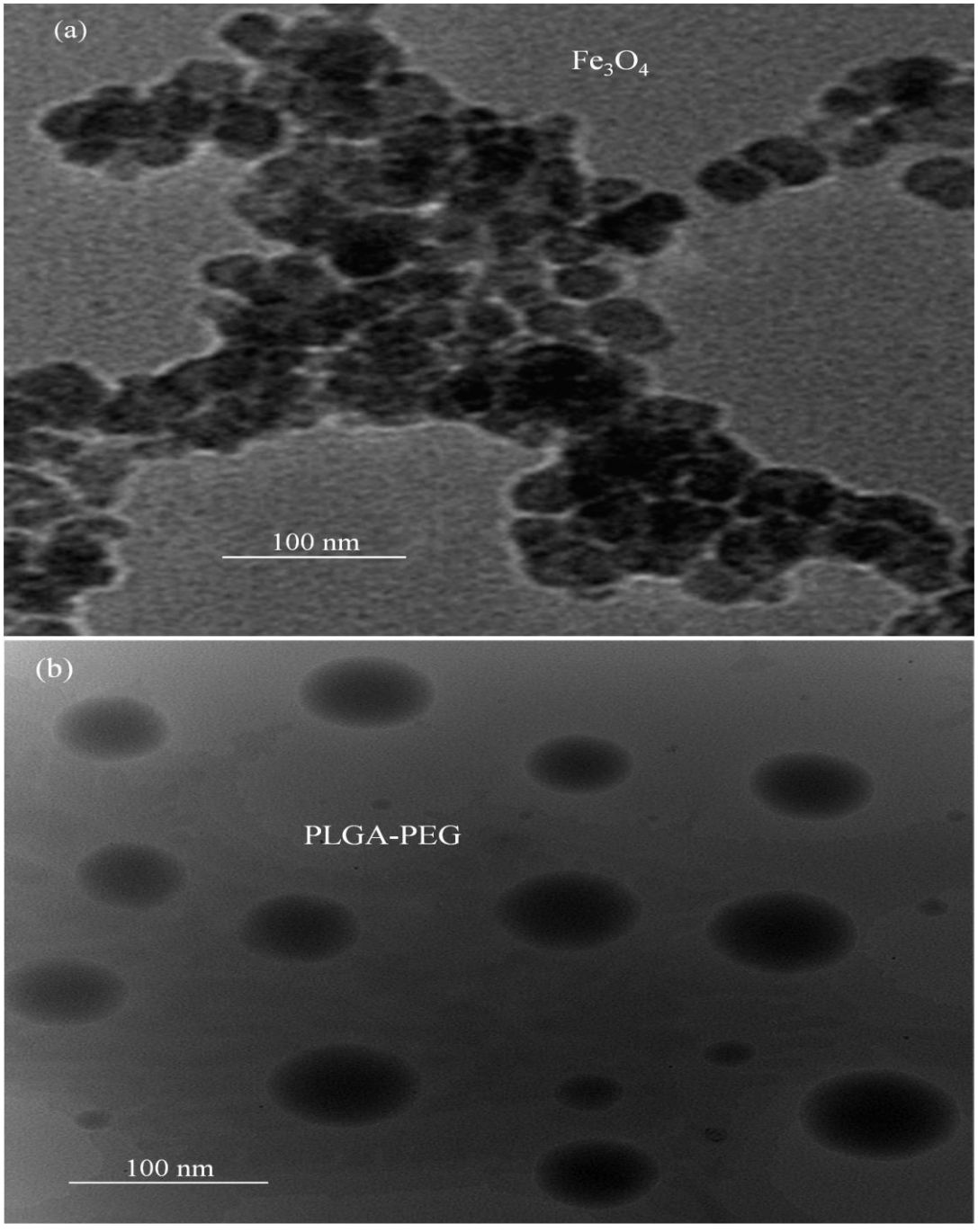

Figure 4.4: TEM images of (a) Fe_3O_4 nanoparticles, (b) PLGA-PEG

Spherical shape and nanocrystalline nature of the magnetite particles is clearly observed in figure 4.4 (a).

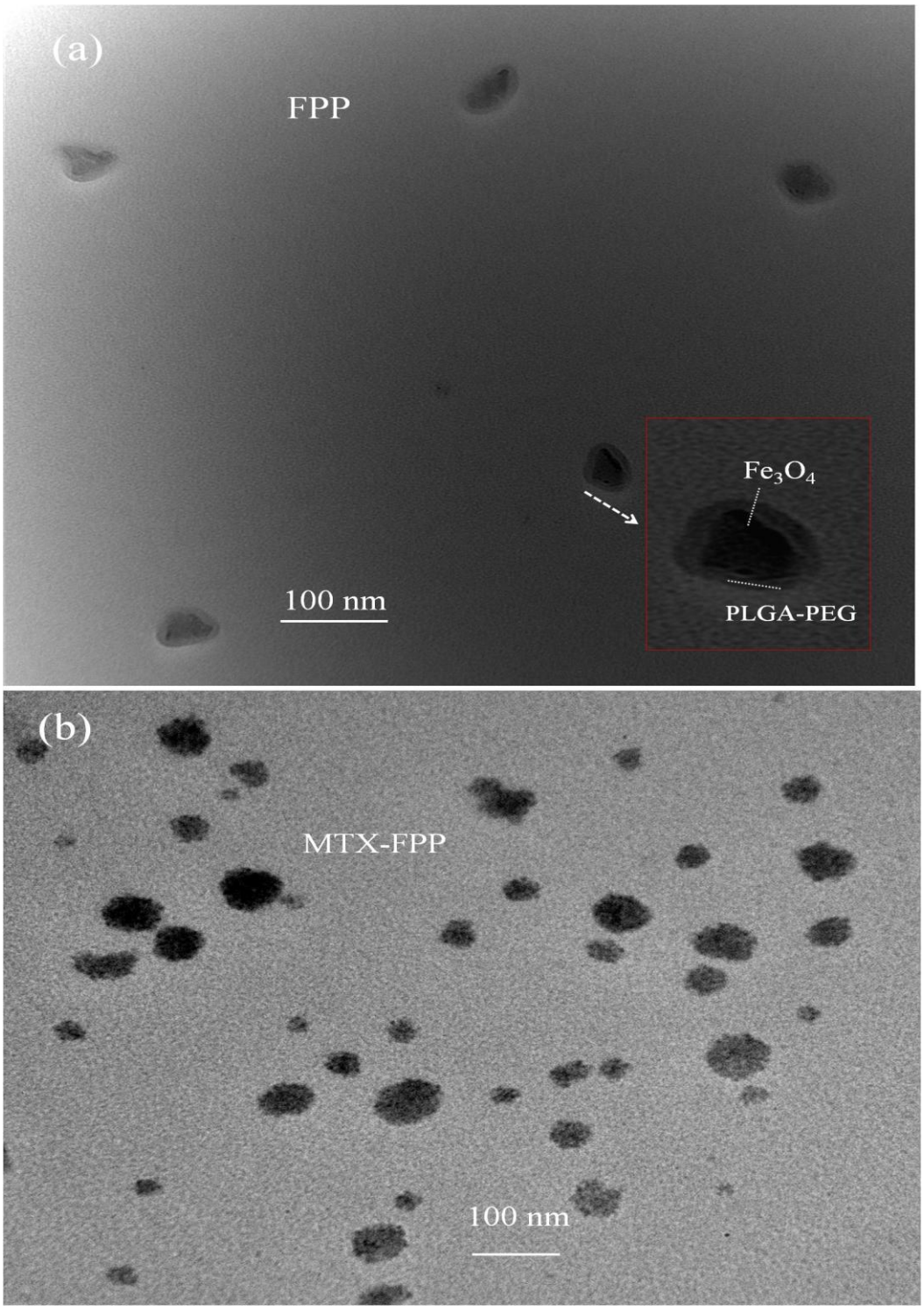

Figure 4.5: TEM images of (a) FPP nanocomposite (inset-magnified view of the nanocomposite) and (b) MTX loaded FPP

Size of particles ranged from 15-25 nm. The presence of agglomeration can be attributed to the presence of dipole-dipole interactions between the magnetic Fe_3O_4 nanoparticles. Uniform particle distribution and spherical morphology was clearly seen for the PLGA-PEG polymer (figure 4.4 (b)) and the particles ranged from 80-100 nm as observed from the image. Improved dispersion of the Fe_3O_4-PLGA-PEG was observed in figure 4.5 (a). This is may be due to the electrostatic repulsion force and possible steric hindrance between the magnetic nanoparticles and the polymer chains. Also an increase in size of the nanocomposite was observed in the range of 110-150 nm which clearly indicates the formation of Fe_3O_4-PLGA-PEG nanocomposite. MTX loaded FPP nanocomposite was observed in figure 4.5 (b).

The magnetism of the prepared Fe_3O_4 nanoparticles was simply done by dissolving 5mg of the nanoparticle in water in a glass vial and stirred well to make a suitable solution. A magnet was then rolled from outside walls of the vial and the magnetic separation was Fe_3O_4 nanoparticles from water was achieved as seen in figure 4.6.

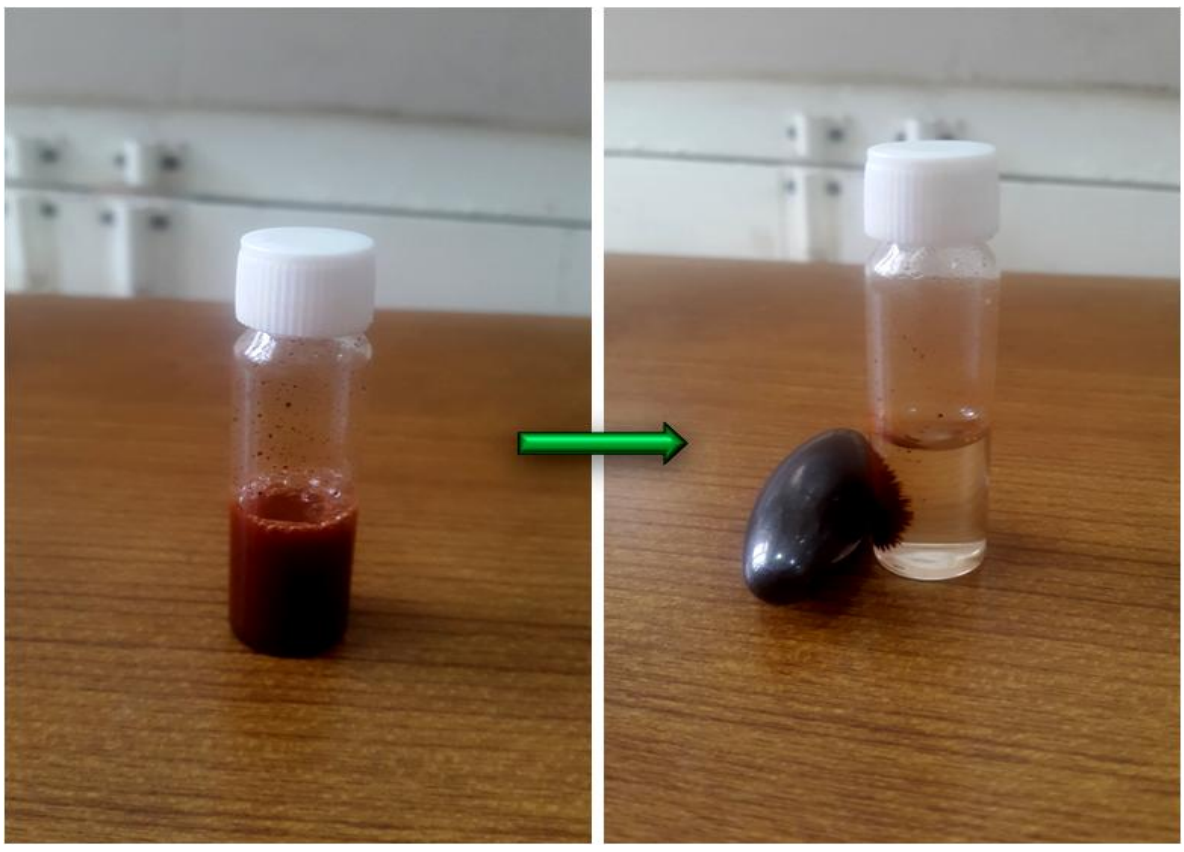

Figure 4.6: Magnetic separation of Fe_3O_4 nanoparticles in solution

Figure 4.7 and 4.8 shows the AFM images of bare Fe_3O_4 nanoparticles, PLGA-PEG and Fe_3O_4-PLGA-PEG nanocomposite in height mode.

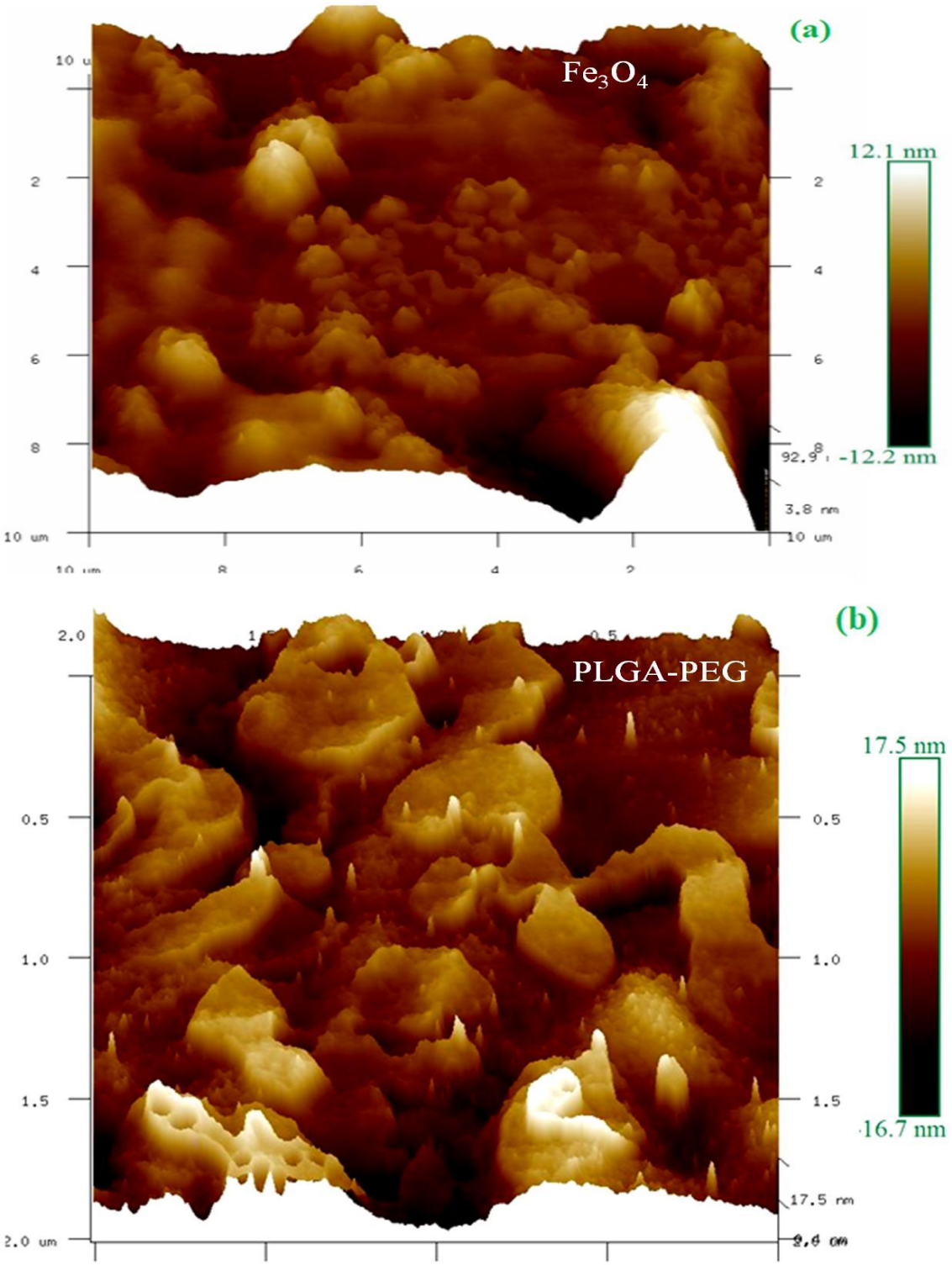

Figure 4.7: AFM images in height mode (scale-2µm) of (a) Fe_3O_4, (b) PLGA-PEG

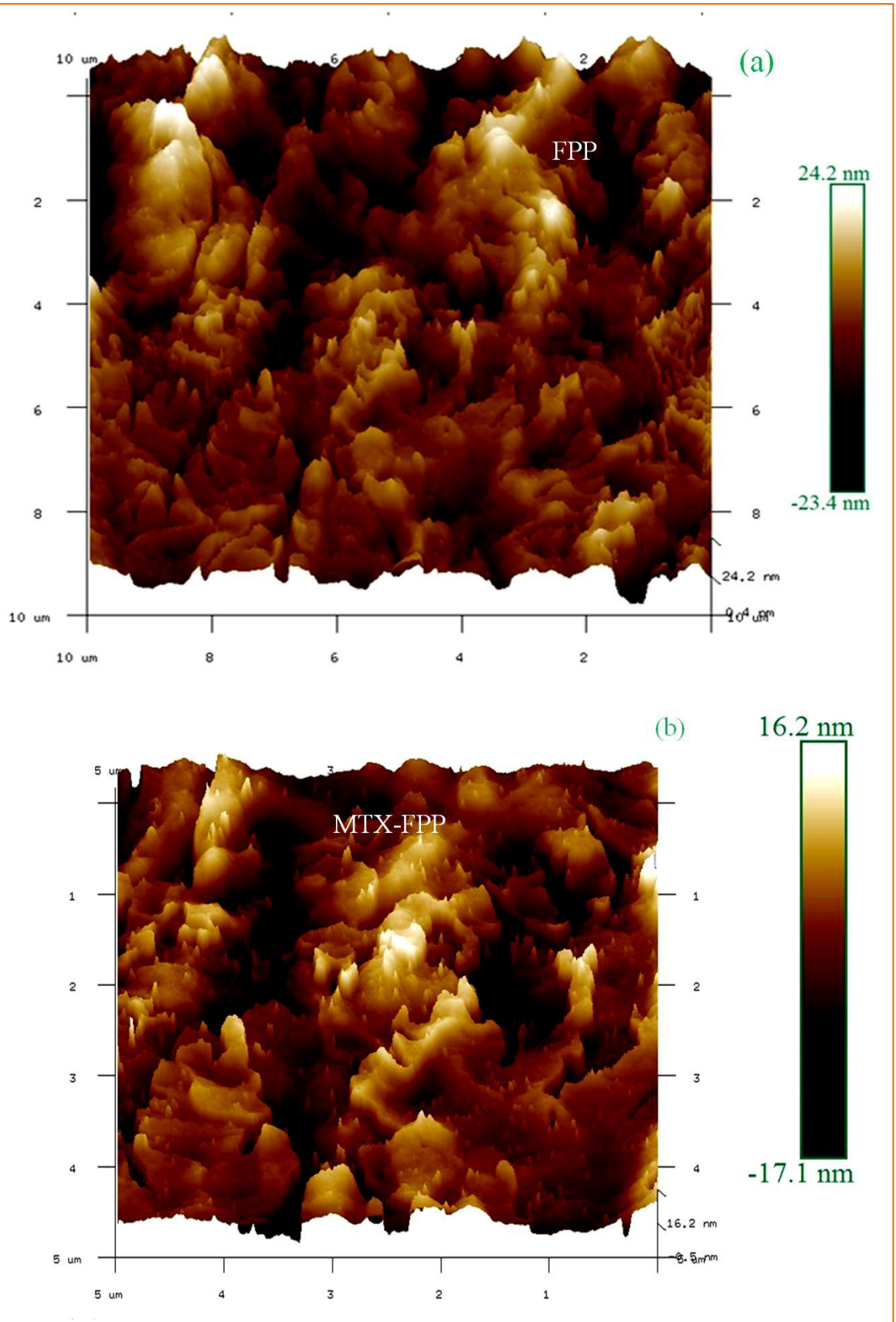

Figure 4.8: AFM images in height mode (scale-2μm) of (a) FPP nanocomposite and (b) MTX loaded FPP

Surface roughness (40.4nm) and average maximum height (20.6nm) for Fe_3O_4 is shown in figure 4.7 (a) while for PLGA-PEG the surface roughness (39.9nm) and average maximum height of 22.8nm is shown in figure 4.7 (b). An increase in surface roughness (61.0nm) along with average maximum height (31.6nm) after the interaction of the two moieties confirms the formation of Fe_3O_4-PLGA-PEG nanocomposite as shown in figure 4.8(a). Figure 4.8(b) shows the MTX loaded FPP nanocomposite.

TGA thermograms of pure Fe_3O_4, PLGA-PEG and Fe_3O_4-PLGA-PEG nanocomposite are shown in figure 4.9. The TGA curve of Fe_3O_4 shows about 5-6% of weight loss in the temperature ranging from 200-300°C. This weight loss can be attributed to loss of residual water in the sample [28]. In PLGA-PEG thermal decomposition initially is obtained due to loss of residual moisture followed by pyrolisis temperature appearing around 200°C. Further weight loss is obtained in the region of 300-600°C due to thermal decomposition of chain and branch bonding in polymer [29]. The TGA curve of Fe_3O_4-PLGA-PEG nanocomposite showed no weight loss upto 250°C. The weight loss mainly occurred in the temperature region of 300-500°C with negligible changes at temperature higher than this. This weight loss can be attributed to decomposition of organic polymer in this region [30]. The obtained results show that presence of Fe_3O_4 in the composite increases the overall thermal stability of the nanocomposite.

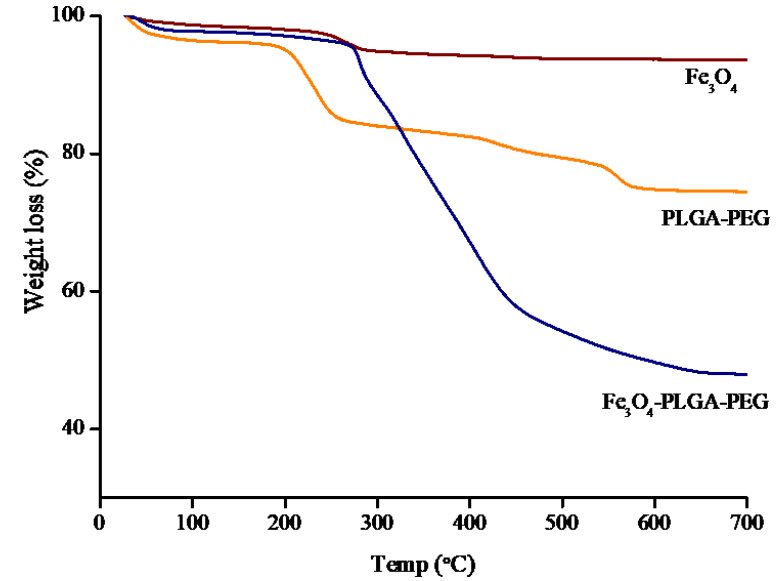

Figure 4.9: TGA thermograms of pure Fe_3O_4, PLGA-PEG and Fe_3O_4-PLGA-PEG nanocomposite

4.3.2. Drug loading and Entrapment Efficiency

According to drug bank, MTX is a hydrophobic drug with a very slight solubility of approximately 2.6mg/mL. PLGA-PEG copolymer has the ability to efficiently load these kinds of hydrophobic drugs. In order to obtain high drug loading, effect of different concentrations is studied. Table 4.2 demonstrates that highest drug loading (TDC) and

entrapment efficiency of 56.3% and 95.8% respectively when the MTX to polymer ratio was 1:1.

Table 4.2: Drug loading and Entrapment efficiency of MTX in different ratios of polymer and drug.

S.No.	Polymer : Drug	Drug loading (%)	Entrapment efficiency (%)
1.	1:0.25	45.2	81.3
2.	1:0.5	49.7	89.5
3.	1:1	56.3	95.8

4.3.3. In-vitro release of MTX and kinetic studies

The *in-vitro* release of MTX in phosphate buffer solution (PBS) of pH-7.3 and acetate buffer solution (ABS) of pH- 4.6 is determined using HPLC. A calibration curve for the standard ramipril solution was firstly plotted shown in figure 4.10. The percent release of MTX from Fe_3O_4-PLGA-PEG incubated in PBS and ABS is shown in figure 4.11. MTX showed three different phases of release pattern. Nearly 86% of MTX is released over 72h of incubation in ABS.

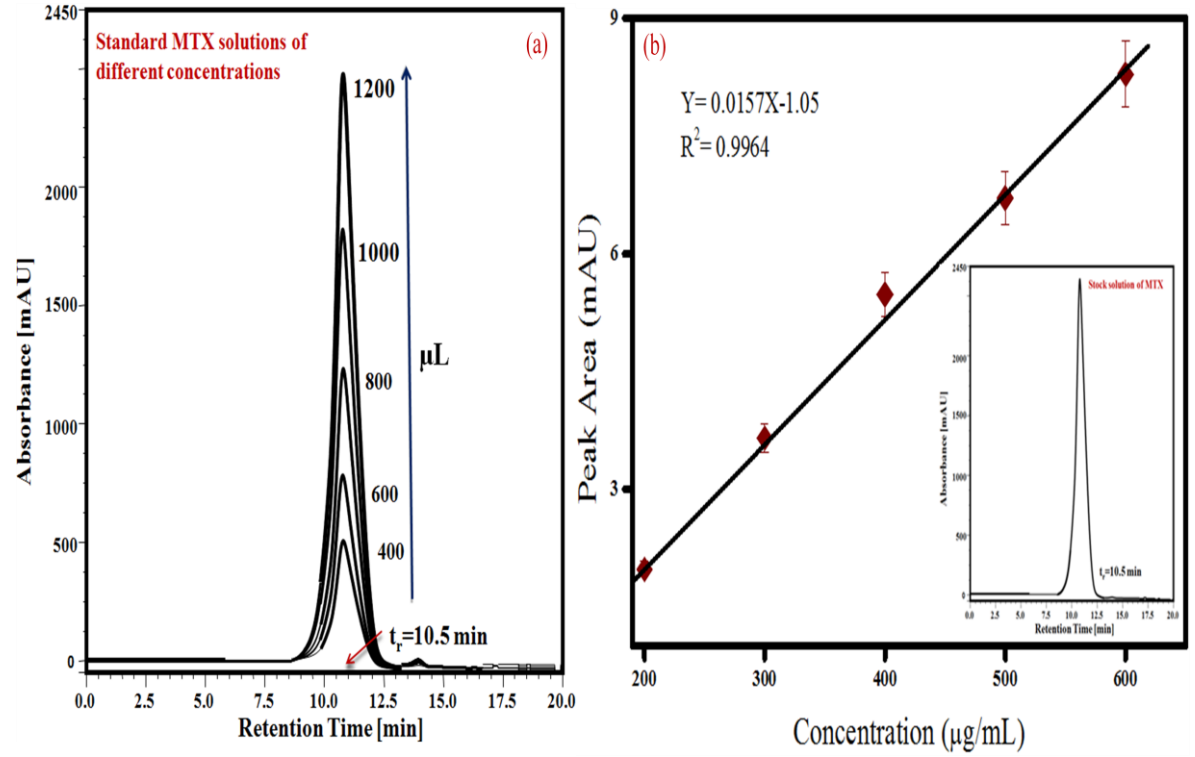

Figure 4.10: (a) HPLC chromatogram of standard MTX solutions and (b) calibration curve for the standard solutions (chromatogram of stock solution of MTX inset)

An initial burst release of MTX is observed for nearly 10h and then levelling off is seen upto 40h. This initial burst release of MTX is attributed to release of surface bounded MTX. An increase in release of MTX is seen for the next 30h. This gradual increase in release rate can be due to the breaking of bonds between surfaces of polymer which allows the drug to be released over a longer duration of time since the ester linkage hydrolysis of the polymer

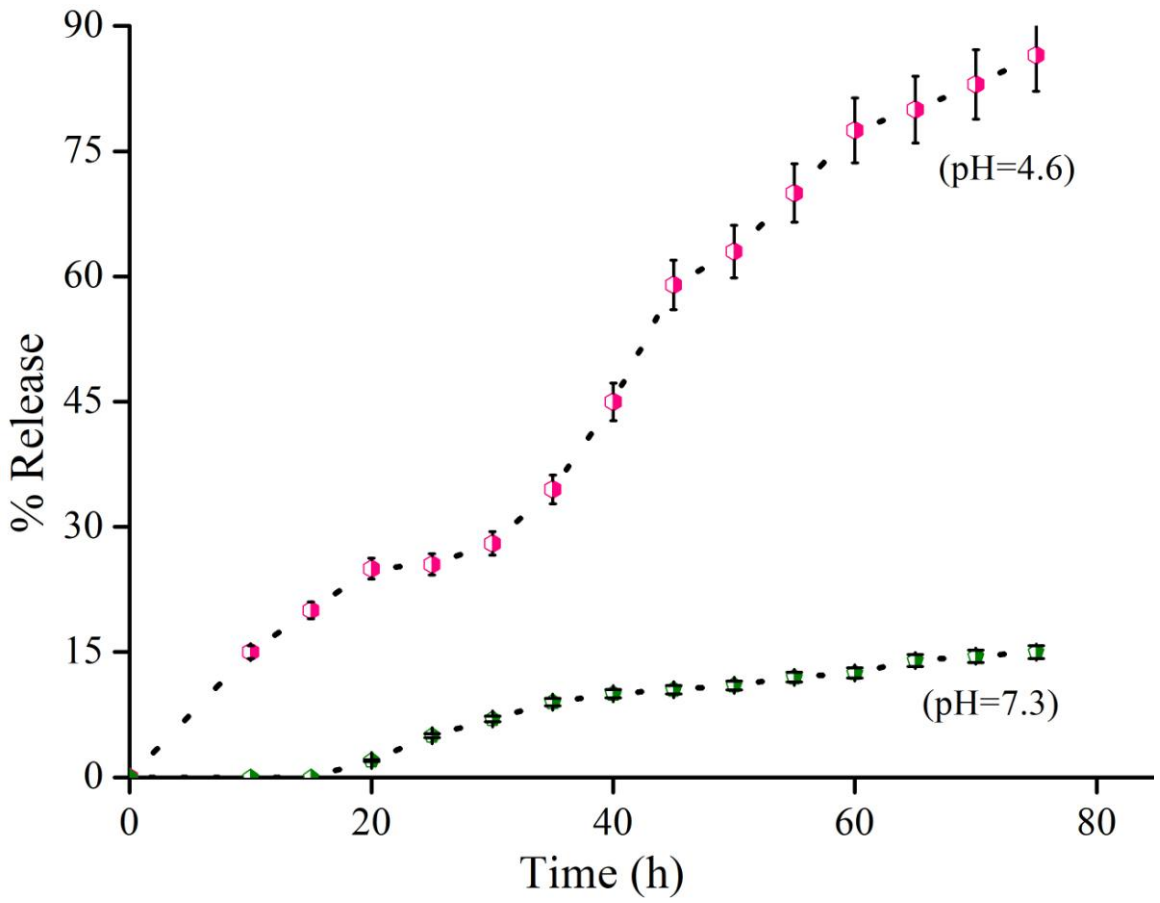

Figure 4.11: *In-vitro* release profile of MTX from Fe_3O_4-PLGA-PEG nanocomposite incubated in phosphate buffer and acetate buffer solution at different time intervals

causes increased swelling as the hydrolysis proceeds with time. Polymer swelling also increases in acidic pH environment because of the protonation of PEG groups attached to PLGA and the subsequent formation of positively charged chains in the polymer [31]. However, in case of release of MTX in PBS medium, no significant release is observed. Only 15% of MTX was nearly released after 72h. This shows that the release of MTX was highly influenced by pH of medium. These observations were in correlation with literature that since the magnetic nanoparticles has the ability to target the cancer cells, the MTX loaded magnetic nanoparticles show negligible release in physiological pH environment. However, they show

a significant release in acidic pH environment similar to that of cancer cells surrounding environment. The experiments were repeated three times with ±5% error.

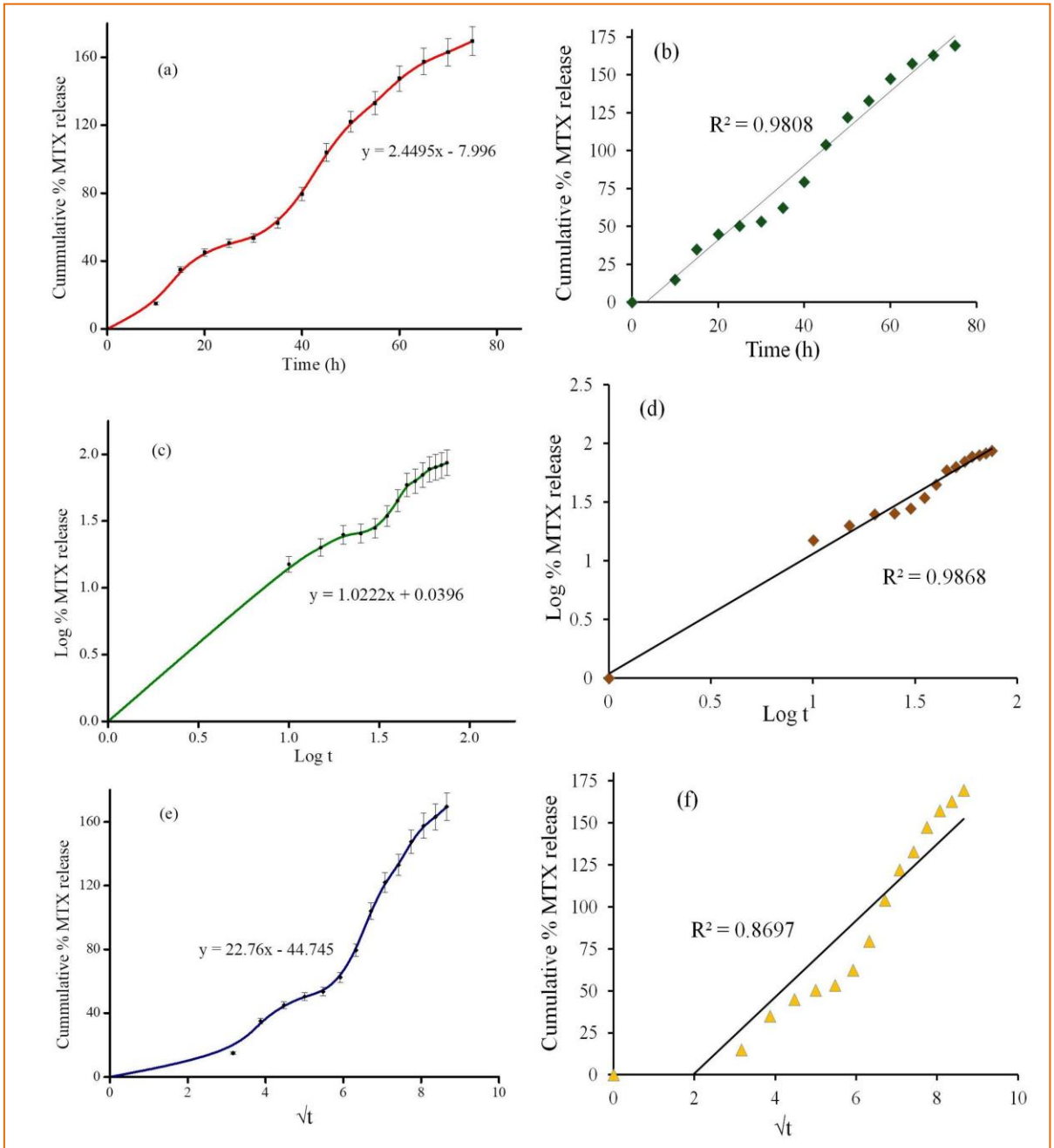

Figure 4.12: Kinetic models of MTX release (a-b) Zero order plot, (c-d) Korsmeyer-Peppas plot and (e-f) Higuchi plot at pH-4.6

The MTX release profile was fitted into various kinetic drug release models shown in figure 4.12. A non fickian supercase-II transport is observed as the release exponent n value of 1.0 (n>0.89) is obtained. It is indicated that the data fitted well in the Korsemeyer-Peppas model

of drug release (R^2=0.986) which signifies that MTX release from the matrix of polymer is swelling controlled and independent of time.

5.3.4. Cytotoxicity assay

The *in-vitro* release of free MTX and MTX from Fe_3O_4-PLGA-PEG nanocomposite in SK-BR-3 (breast adinocarcinoma) cell line is shown in figure 4.13. It is observed that after incubation of 4 days only 20% of MTX is released while almost 80% of MTX is released when it is loaded in Fe_3O_4-PLGA-PEG nanocomposite. This indicates that Fe_3O_4-PLGA-PEG acts as a good delivery agent for transporting MTX.

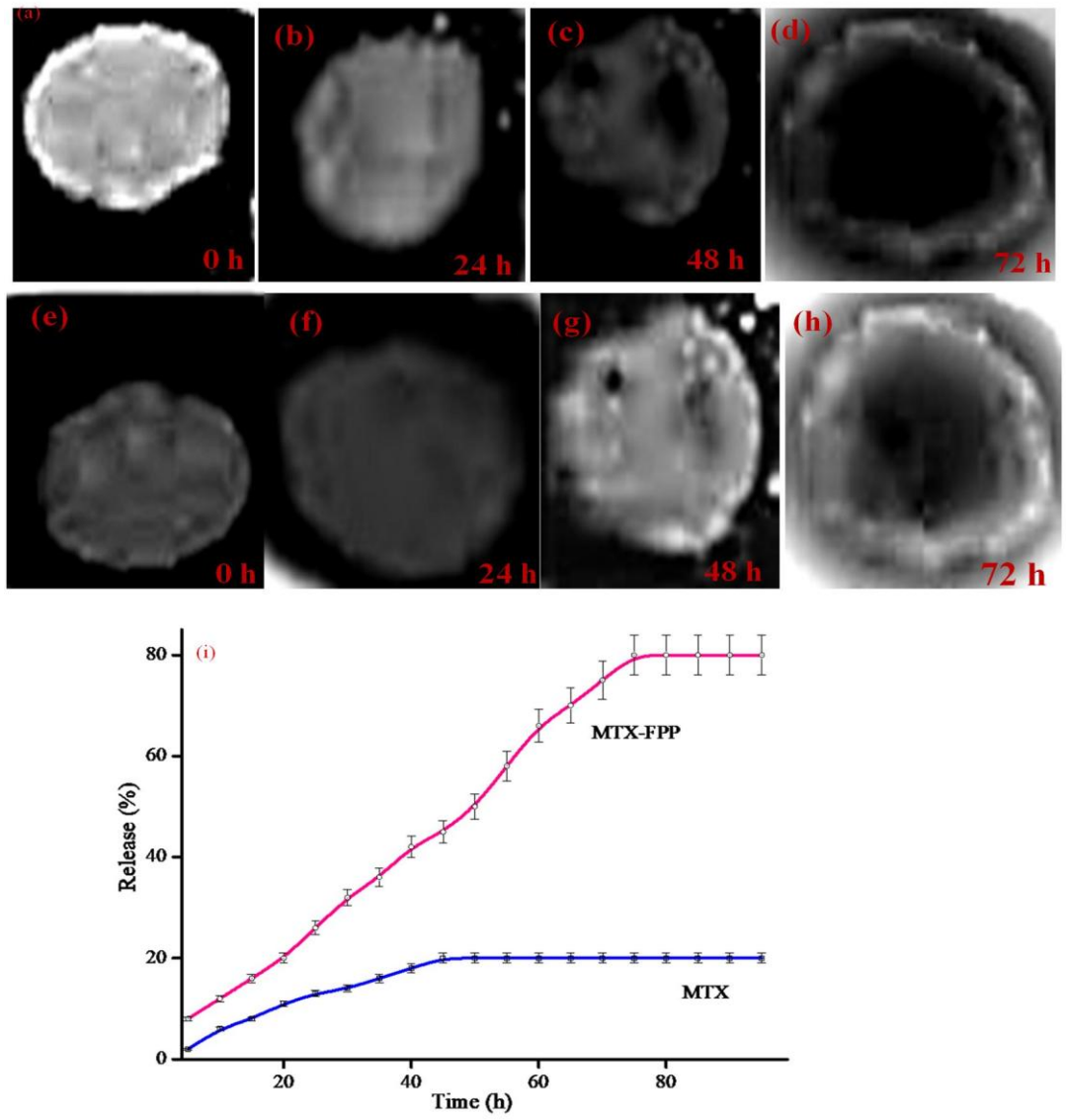

Figure 4.13: Live cell imaging of (a-d) MTX-FPP, (e-h) free MTX and (i) *in-vitro* release profile of MTX from FPP nanocomposite in SK-BR-3 (breast adinocarcinoma) cell line.

The cytotoxic cell viability assay of free MTX, bare nanoparticle and MTX loaded nanoparticle at different incubation period in SK-BR-3 (breast adinocarcinoma) cells is shown in figure 4.14. It was observed that bare nanoparticles do not show any prominent cytotoxic effects on the cells as there is nearly no cell death observed. For free MTX a

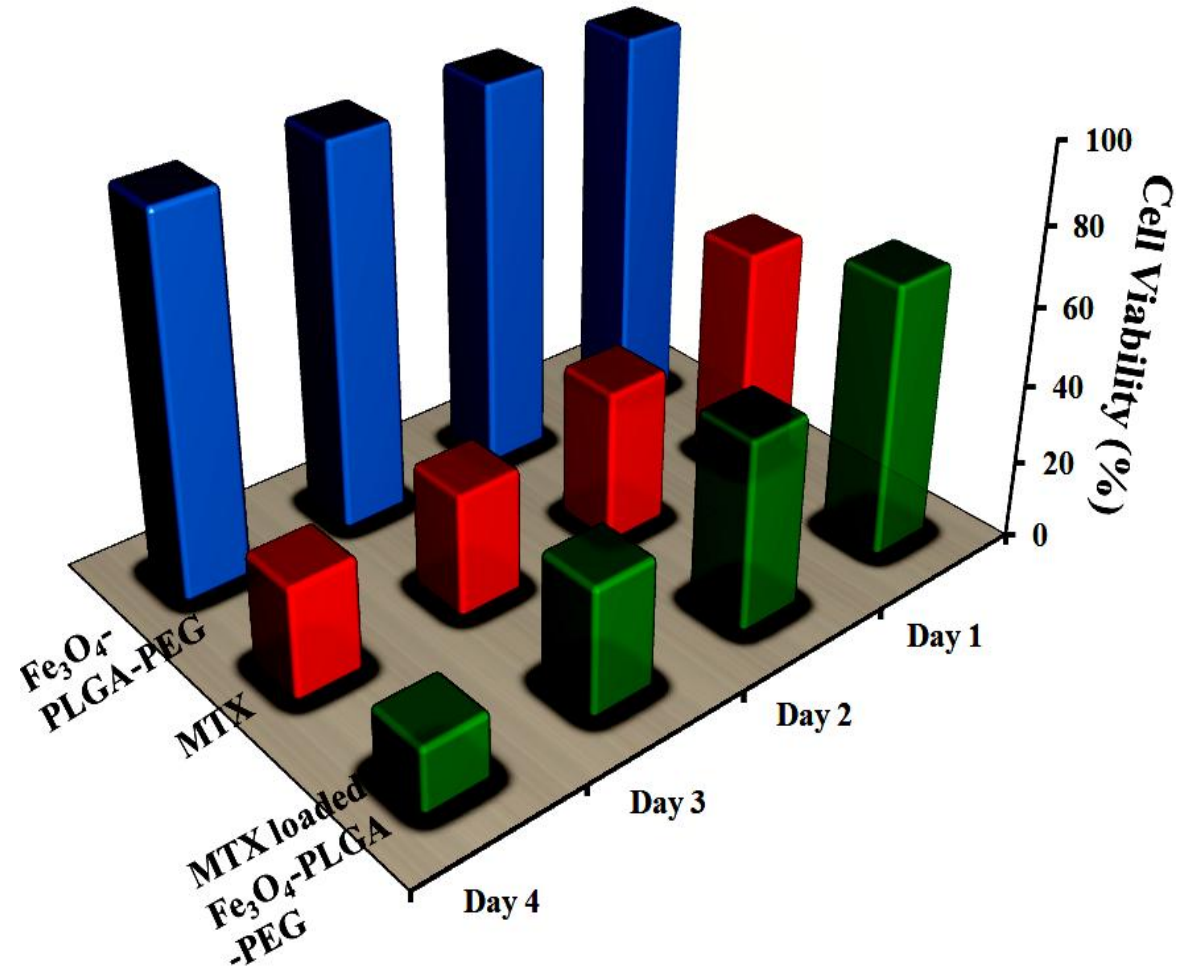

Figure 4.14: Cytotoxicity assay of free MTX, Fe_3O4-PLGA-PEG and MTX loaded Fe_3O4-PLGA-PEG at different incubation period in SK-BR-3 (breast adinocarcinoma) cells

decrease in viability is observed with increased incubation time. However, for MTX loaded nanoparticles in the same concentration range showed higher cytotoxic effects on SK-BR-3 cells with increased incubation time than free MTX. It is reported in the literature [32, 33] that nanoparticles internalize inside cells by endocytosis, while the free drugs can diffuse inside as minute molecules swiftly. Taking this hypothesis into account, it is postulated that at the end of fourth day the MTX is released from the nanoparticles inside the cells, without losing its cytotoxic effect on the cancer cells.

Similarly the cytotoxic cell viability assay of free MTX, bare nanoparticle and MTX loaded nanoparticle at different incubation period in L929 non cancerous cells shown in figure 4.15 is also done to ascertain the targeting ability of MTX on cancer cells. It was seen that bare

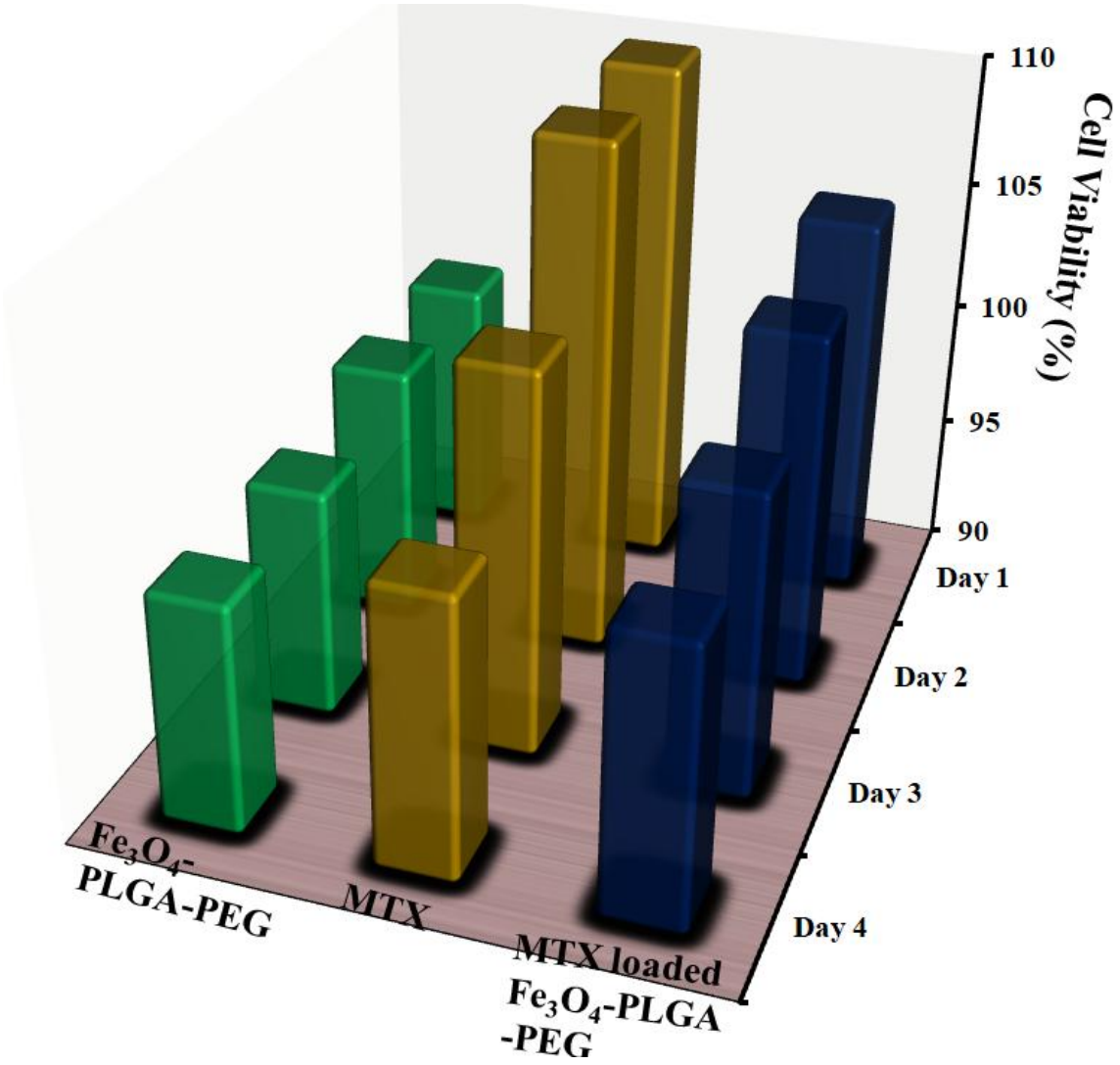

Figure 4.15: Cytotoxicity assay of free MTX, Fe_3O_4-PLGA-PEG and MTX loaded in Fe_3O_4-PLGA-PEG at different incubation period in L929 (non-cancerous) cells

nanoparticles do not show any effect on cell viability similar to SK-BR-3 cells. However, an inverse effect is observed in case of MTX and MTX loaded nanoparticles. An increase in cell growth is observed. This clearly indicates that MTX has no effect on healthy non cancerous cells and is well targeted towards the infected cells. All the experiments were repeated three times with ±5% error.

5.3.5. Fluorescent Imaging

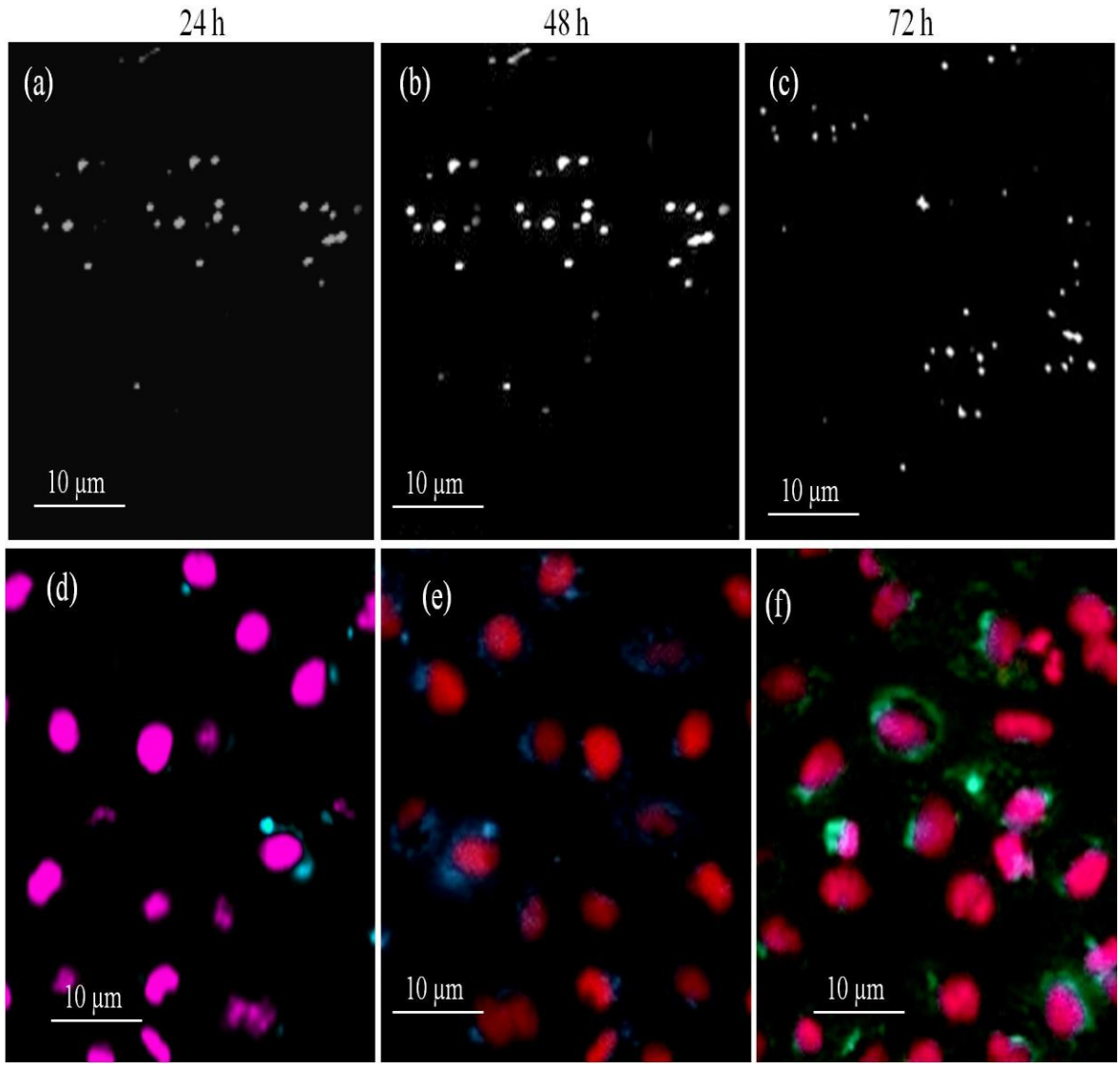

Figure 4.16: Fluorescence microscopy images of SK-BR-3 cells after incubation with (a-c) bare nanoparticle and (d-f) free MTX for 72 h

The fluorescent cell images show that MTX in free form localises in the nucleus to a greater extent than when encapsulated inside nanoparticles, indicating slower internalisation of NPs (figure 4.16 and 4.17). A variety of cell uptake mechanisms are reported in literature [34-36] for free drug and drug encapsulated nanoparticles. It was postulated that MTX releases from NPs due to acidic nature of lysosymal/endosomal compartments, allowing reaching the nucleus slowly. This deferred release of MTX is favourable for the overall effect on the cell.

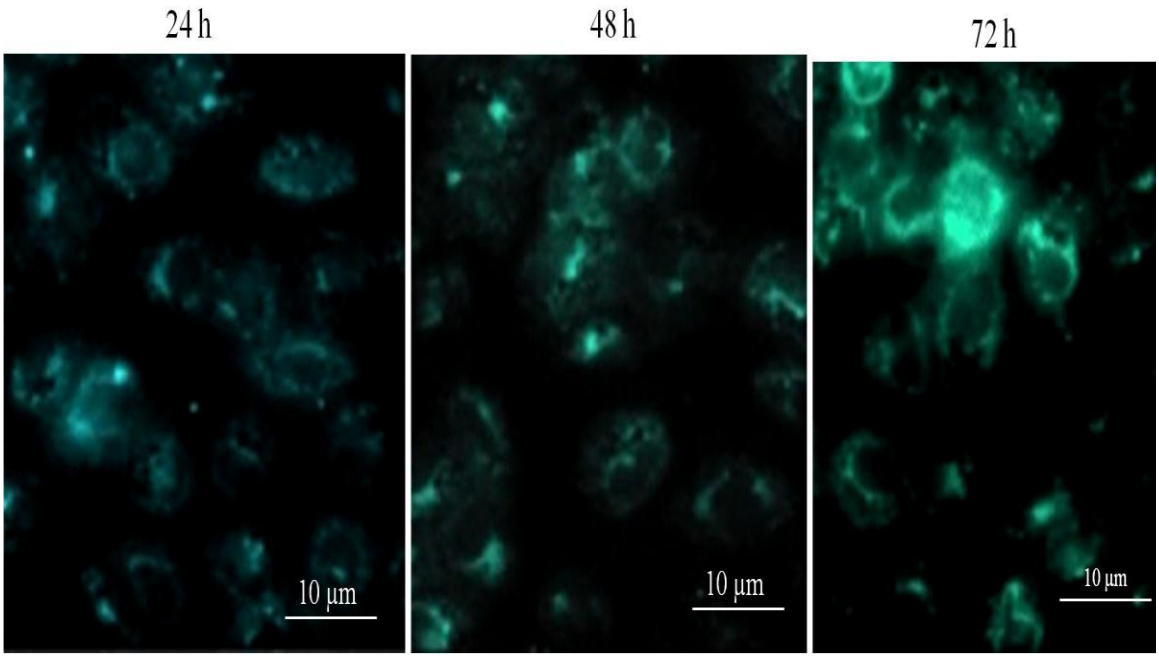

Figure 4.17: Fluorescence microscopy images of SK-BR-3 cells after incubation with MTX loaded nanoparticle for 72 h

4.4 Conclusion

In summary, surface modification of amphiphilic block polymer PLGA-PEG was done by magnetic Fe_3O_4 nanoparticles to improve the targeting ability of the PLGA-PEG for release of methotrexate. Firstly, the Fe_3O_4 nanoparticles are prepared by chemical co-precipitation method and then the Fe_3O_4 modified PLGA-PEG nanocomposite was prepared by double emulsion method. The synthesized nanoparticles were characterized using FTIR, XRD. Spinel cubic structure of Fe_3O_4 is obtained in the size range of 5-10 nm. A shift in 2ϴ values in Fe_3O_4- PLGA-PEG nanocomposite confirmed the interaction between the two moieties. Surface morphology of the Fe_3O_4-PLGA-PEG nanocomposite is obtained by TEM analysis. To obtain high drug loading, effect of different polymer to drug ratios are studied and high drug loading (56%) and entrapment efficiency (95%) is observed when drug to polymer ratio is 1:1. The *in-vitro* release profile of methotrexate indicated that there was a significant release of 86% of methotrexate over 72h which showed that the magnetic nanoparticles were able to release the drug in acidic environment. Further, the release data fitted well in the korsemeyer-peppas model of kinetic drug release (R^2=0.9868) which indicated that drug release was diffusion controlled. The *in-vitro* cytotoxicity assay of the free MTX and MTX loaded nanoparticles was done using SK-BR-3 (breast adinocarcinoma) cells and L929 non-

cancerous cells. It was observed that loaded MTX showed higher cytotoxic effect on the cancer cells rather than the free MTX and an inverse effect were observed in case of non-cancerous cells. Further, the fluorescent cell imaging was done to ascertain the release of MTX from nanoparticles. It is seen that MTX internalises into the nucleus slowly without losing its cytotoxic effect. These properties of Fe_3O_4 modified PLGA-PEG renders it effectiveness to be used as drug delivery carriers for cancer therapy.

4.5 References

[1] X. Wang, C.J. Summers, Z.L. Wang, Nano Letters, 4 (2004) 423-426.

[2] K.J. Widder, A.E. Senyei, D.G. Scarpelli, Proceedings of the Society for Experimental Biology and Medicine, 158 (1978) 141-146.

[3] M. Hałupka-Bryl, M. Bednarowicz, B. Dobosz, R. Krzyminiewski, T. Zalewski, B. Wereszczyńska, G. Nowaczyk, M. Jarek, Y. Nagasaki, Journal of Magnetism and Magnetic Materials, 384 (2015) 320-327.

[4] M. Branca, M. Marciello, D. Ciuculescu-Pradines, M. Respaud, M. del Puerto Morales, R. Serra, M.-J. Casanove, C. Amiens, Journal of Magnetism and Magnetic Materials, 377 (2015) 348-353.

[5] S. Jadhav, D. Nikam, V. Khot, S. Mali, C. Hong, S. Pawar, Materials Characterization, 102 (2015) 209-220.

[6] N. Thorat, R. Patil, V. Khot, A. Salunkhe, A. Prasad, K. Barick, R. Ningthoujam, S. Pawar, New Journal of Chemistry, 37 (2013) 2733-2742.

[7] H. Shokrollahi, A. Khorramdin, G. Isapour, Journal of Magnetism and Magnetic Materials, 369 (2014) 176-183.

[8] N. Sattarahmady, T. Zare, A. Mehdizadeh, N. Azarpira, M. Heidari, M. Lotfi, H. Heli, Colloids and Surfaces B: Biointerfaces, 129 (2015) 15-20.

[9] T. Zare, M. Lotfi, H. Heli, N. Azarpira, A. Mehdizadeh, N. Sattarahmady, M. Abdollah-Dizavandi, M. Heidari, Applied Physics A: Materials Science & Processing, 120 (2015).

[10] Z. Karimi, L. Karimi, H. Shokrollahi, Materials Science and Engineering: C, 33 (2013) 2465-2475.

[11] A. Tomitaka, T. Koshi, S. Hatsugai, T. Yamada, Y. Takemura, Journal of Magnetism and Magnetic Materials, 323 (2011) 1398-1403.

[12] M. Longmire, P.L. Choyke, H. Kobayashi, Nanomedicine, 3 (2008) 703-717.

[13] K.M. Huh, Y.W. Cho, K. Park, Drug Delivery Technology, 3 (2003) 42-44.

[14] M. Rajan, V. Raj, International Review of Chemical Engineering, 5 (2013) 145-155.

[15] L. Li, Y. Zhang, N. Hao, D. Chen, F. Tang, Chinese Science Bulletin, (2012) 1-9.
[16 K. El-Boubbou, D. Azar, A. Bekdash, R.J. Abi-Habib, Journal of Biomedical Nanotechnology, 13 (2017) 500-512.
[17] A. GhavamiNejad, A.R.K. Sasikala, A.R. Unnithan, R.G. Thomas, Y.Y. Jeong, M. Vatankhah-Varnoosfaderani, F.J. Stadler, C.H. Park, C.S. Kim, Advanced Functional Materials, 25 (2015) 2867-2875.
[18] G. Yousefi, S.M. Foroutan, A. Zarghi, A. Shafaati, Chemical and Pharmaceutical Bulletin, 58 (2010) 147-153.
[19] A. Taheri, F. Atyabi, F.S. Nouri, F. Ahadi, M.A. Derakhshan, M. Amini, M.H. Ghahremani, S.N. Ostad, P. Mansoori, R. Dinarvand, Journal of Nanomaterials, 2011 (2011) 1-7.
[20] S. Abbasi, G. Yousefi, O. Firuzi, S. Mohammadi-Samani, Journal of Applied Polymer Science, 133 (2016) 43233-43245 .
[21] A. Bordbar, A. Rastegari, R. Amiri, E. Ranjbakhsh, M. Abbasi, A. Khosropour, Biotechnology Research International, 2014 (2014) 1-6.
[22] N.M. Salem, A.M. Awwad, Nanoscience and Nanotechnology, 3 (2013) 35-39.
[23] C.D.A.C. Erbetta, R.J. Alves, J.M. Resende, R.F. de Souza Freitas, R.G. de Sousa, Journal of Biomaterials and Nanobiotechnology, 3 (2012) 208.
[24] T.P.T. Dao, T.H. Nguyen, T.H. Ho, T.A. Nguyen, M.C. Dang, Advances in Natural Sciences: Nanoscience and Nanotechnology, 5 (2014) 035013.
[25] D.V. Quy, N.M. Hieu, P.T. Tra, N.H. Nam, N.H. Hai, N. Thai Son, P.T. Nghia, N.T.V. Anh, T.T. Hong, N.H. Luong, Journal of Nanomaterials, 2013 (2013)1-6.
[26] K.Y. Rhee, D.-H. Jung, H. Kim, J. Marroquin, Carbon letters, 13 (2012) 126-129.
[27] A. Kumar, G. Sharma, M. Naushad, S. Thakur, Chemical Engineering Journal, 280 (2015) 175-187.
[28] S. Asgari, Z. Fakhari, S. Berijani, Journal of Nanostructures, 4 (2014) 55-63.
[29] M.F. Silva, A.A.W. Hechenleitner, J.M. Irache, A.J.A.d. Oliveira, E.A.G. Pineda, Materials Research, 18 (2015) 1400-1406.
[30] F.N. Almajhdi, H. Fouad, K.A. Khalil, H.M. Awad, S.H. Mohamed, T. Elsarnagawy, A.M. Albarrag, F.F. Al-Jassir, H.S. Abdo, Journal of Materials Science: Materials in Medicine, 25 (2014) 1045-1053.
[31] S.S. Abolmaali, A. Tamaddon, G. Yousefi, K. Javidnia, R. Dinarvand, International Journal of Nanomedicine, 9 (2014) 2833.

[32] Y.-l. Tan, C.-G. Liu, Journal of Materials Science: Materials in Medicine, 22 (2011) 1213-1220.
[33] F. Wang, D. Zhang, C. Duan, L. Jia, F. Feng, Y. Liu, Y. Wang, L. Hao, Q. Zhang, Carbohydrate Polymers, 84 (2011) 1192-1200.
[34] X.-B. Wang, H.-Y. Zhou, Biomedicine & Pharmacotherapy, 70 (2015) 123-128.
[35] C. Chittasupho, K. Lirdprapamongkol, P. Kewsuwan, N. Sarisuta, European Journal of Pharmaceutics and Biopharmaceutics, 88 (2014) 529-538.
[36] Q. Li, S. Lv, Z. Tang, M. Liu, D. Zhang, Y. Yang, X. Chen, International Journal of Pharmaceutics, 471 (2014) 412-420.

CONCLUSIONS

Chapter 1: Covers the general introduction to the biodegradable polymer nanoparticles (PNPs), their applications in various biological and pharmaceutics as drug delivery carriers for varied hydrophobic/hydrophilic drugs; importance of these PNPs over conventional medication. Effect of different shape, size and drug to polymer ratio for better release of drug from polymer matrix is also discussed. An overview of the various studies reported earlier for the preparation of different drug loaded nanocomposites having different characteristics is also discussed. A short description of methodology and characterization techniques for the determination of structural and morphological properties is also illustrated.

Chapter 2: Section A: Summarizes, the study showed that formulation approach can improve the therapeutic efficacy of ramipril. The nanoprecipitation method is suitable for preparation of ramipril loaded PLGA nanoparticles with fairly high encapsulation efficiency. Variations in PLGA and K P-188 concentrations lead to changes in entrapment efficiency and release profile of the drug. The synthesized nanoparticles were in a size range of 121-156 nm having uniform size. Highest percentage of entrapment efficiency was obtained in F_3 formulation. However, in F_2 formulation almost same amount of ramipril was released as entrapped. Formulation F_2 showed an initial burst release followed by sustained release up to 74% over 24 hours in PBS. This release pattern of ramipril from PLGA matrix was attributed to its non- fickian diffusion mechanism which indicates that the release is both diffusion and swelling controlled. The sustained release of ramipril from polymer matrix indicated that the use of similar formulations can be useful in reducing the frequency of administration of ramipril in the treatment of hypertension.

Section B: In summary, to improve the functionality of poly-lactic-co-glycolic acid and poly-lactic acid as therapeutic agents these were encapsulated within poly (N-isopropylacrylamide) shell. Poly (N-isopropylacrylamide) was chosen due to its ability to protect the core nanoparticles from aggregation and external stimuli. Also these (poly- lactic /poly-lactic-co-glycolic acid- poly N-isopropylacrylamide) core- shell nanoparticles are non-toxic in nature suggesting biocompatibility. These core-shell (poly- lactic /poly-lactic-co-glycolic acid- poly N-isopropylacrylamide) nanoparticles were then used to study the release profile of ramipril an antihypertensive drug. The synthesized nanocomposites were in a size range of 68 – 170nm. Higher percentage of entrapment efficiency (78%) was obtained for ramipril loaded

in poly-lactic-co-glycolic acid- poly N-isopropylacrylamide nanoparticles. Also, a sustained release upto 96% over 24 hours in PBS medium was obtained for poly-lactic-co-glycolic acid- poly N-isopropylacrylamide nanoparticles core-shell as a matrix. This release pattern is attributed to its non-fickian nature which suggested that release of ramipril is diffusion controlled. Overall, PLGA showed better characteristics than PLA as a drug carrier in case of ramipril adsorption over its matrix. These abilities of the core – shell nanoparticle system will prove to be important in future *in-vivo* studies focused on probing the capability of these nanoparticles to deliver the therapeutics.

Chapter 3: In the present study, template method is used to fabricate biodegradable and biocompatible hollow-Cs nanospheres. PLGA was employed as template prepared by solvent evaporation method. An increase in size from 125-186 nm and shift in zeta potential indicated adsorption of chitosan layer over PLGA template. BET surface area analysis confirmed the formation of hollow Cs nanospheres which were further characterized by TEM and AFM. Higher entrapment efficiency (90.8%) was obtained when ramipril concentration was 5 mg/mL in polymer matrix. The release profile of ramipril was influenced by pH of the medium i.e. with increase in pH from 3.3 to 6.3 to 8.0 the release rate decreases. 86% drug was released in ABS (pH 3.3) while 73% and 48% of drug released from polymer matrix in PBS (pH 6.3) and tris buffer (pH 8.0) over 24 hours. The kinetic data obtained for the release profile of ramipril showed that release of ramipril was diffusion as well as swelling controlled.

Chapter 4: In summary, methotrexate (anticancer drug) loaded Fe_3O_4-PLGA-PEG nanocomposite is prepared in order to improve the release of methotrexate to the target site. Drug loading (56%) and entrapment efficiency (95%) was effected by ratio of methotrexate to that of polymer. Significant release of 86% methotrexate in acidic tumor environment was seen over 72h *in-vitro.* Ability of the polymer nanocomposite to transport and release the drug to its target site is assed as compared to conventional mode of medication. Also a case II transport for release of methotrexate was observed. Further, methotrexate showed higher cytotoxic effect on SK-BR-3 (breast adinocarcinoma) cells when loaded in the composite as compared to when administered in free form. It is seen that methotrexate internalizes into the nucleus slowly without losing its cytotoxic effect when loaded in the nanocomposite. Significantly the drug did not show any cytotoxic effect on non cancerous L929 healthy cells. These properties of Fe_3O_4-PLGA-PEG nanocomposite to release drug in a controlled manner

to its target site renders them the ability to be used as delivery carriers for hydrophilic drugs having low bioavailability in cancer therapy.

List of Publications

1. Tanushree Basu, Bonamali Pal and Satnam Singh. **'**Synthesis and Characterization of Ramipril Embedded Nanospheres of Biodegradable Poly-D, L-Lactide-co-Glycolide and Their Kinetic Release Study.' *Advanced Science, Engineering and Medicine.* 8, **(2016)**, 444-449. **[IF-0.99]**

2. Tanushree Basu, Bonamali Pal and Satnam Singh. 'Fabrication and Characterization of Core- Shell Morphology of PLGA/PLA- pNIPAM Nanocomposite for Better Entrapment and Release Kinetics of Hypertensive Drugs.' *Particuology.* 40, **(2018)**, 169-176. **[IF-2.8]**

3. Tanushree Basu, Bonamali Pal and Satnam Singh. 'Hollow Chitosan Nanocomposite as Drug Carrier System for Controlled Delivery of Ramipril.' *Chemical Physics Letter.* 706, **(2018)**, 465-471. **[IF-1.86]**

4. Tanushree Basu, Satnam Singh and Bonamali Pal. 'Fe_3O_4 @ PLGA-PEG Nanocomposite for Improved Delivery of Methotrexate in Cancer Treatment.' *Chemistry Select.* 3, **(2018)**, 8522-8528. **[IF-1.5]**

Other Publications

1. Tanushree Basu, Khyati Rana, Niranjan Das and Bonamali Pal. 'Selective detection of Mg^{2+} ions via enhanced fluorescence emission using Au–DNA nanocomposites.' *Beilstein Journal of Nanotechnology* 8 (2017) 762–771. **[IF- 2.8]**

Paper Presented in Conferences

1. Tanushree Basu, Satnam Singh and Bonamali Pal, **"**Preparation of antihypertensive drug loaded particles fabricated using biodegradable poly-D, L-lactide-co-glycolide polymer," presented in National conference on New frontiers in chemical sciences 01 (NFCS-2014), held in , Khalsa college , Patiala on 15th November, 2014.

2. Tanushree Basu, Satnam Singh and Bonamali Pal, "Preparation and study of entrapment efficiency and release profile of antihypertensive drug through poly-D,L-lactide-co-glycolide polymer," presented in National conference on Synergistic Aspects of Chemical and Other Sciences (SACOS-2015), held in, Punjabi University, Patiala on 19th -20th February, 2015.

3. Tanushree Basu, Satnam Singh and Bonamali Pal, "Effect of different pH mediums on release of ramipril from matrix of core shell hollow chitosan nanospheres," presented in National conference on Synergistic Aspects of Chemical and Other Sciences (SACOS-2016), held in, Punjabi University, Patiala on 4th -5th February, 2016.

4. Tanushree Basu, Satnam Singh and Bonamali Pal, ''Preparation of core-shell chitosan nanospheres using PLGA template and to study release kinetics of Ramipril from polymer matrix," presented in International Conference on Nanoscience and Technology (ICONSAT-2016) held at IISER Pune, on 29th to 2nd March, 2016.

5. **Tanushree Basu** and Bonamali Pal, ''Synthesis of Gold-DNA nanocomposites for highly sensitive magnesium ion detection," presented in Powder, Granule and Bulk Solids: Innovations and Applications (PGBSIA-2016) held at Ramada, Jaipur, on 1st to 3rd dec, 2016.

Article

Advanced Science, Engineering and Medicine
Vol. 8, 1–6, 2016
www.aspbs.com/asem

Copyright © 2016 American Scientific Publishers
All rights reserved
Printed in the United States of America

Synthesis and Characterization of Ramipril Embedded Nanospheres of Biodegradable Poly-*D*,*L*-Lactide-co-Glycolide and Their Kinetic Release Study

Tanushree Basu[1], Bonamali Pal[2], and Satnam Singh[2,*]

[1]*Thapar University, Patiala 147004, Punjab, India*
[2]*School of Chemistry and Biochemistry, Thapar University, Patiala 147004, Punjab, India*

Development of biodegradable polymers for controlled drug delivery has gained immense importance as these can be broken down into biologically acceptable monomeric units that can be eliminated by natural metabolic pathways from the body. In order to improve the therapeutic efficacy of ramipril, an antihypertensive drug, a study has been carried out to ascertain the duration of its action. Ramipril loaded biodegradable nanoparticles of poly-*D*,*L*-lactide-co-glycolide (PLGA) were prepared by nanoprecipitation using tribloere stabilizer kolliphore P-188 (K P-188). Four different formulations F_1 to F_4 were prepared by altering the weight of K P-188:PLGA as 1:1.25, 1:2.50, 1:0.62 and 1:0.80. These were characterised by zeta potential, SEM and TEM studies. The F_3 formulation showed highest drug content and entrapment efficiency of 94% and 84%, respectively. *In-vitro* release study of these formulations at pH 7.3 in phosphate buffer indicated F_2 formulation to be efficient with an initial burst release followed by 74% sustained release of ramipril over 24 hours. The korsemeyer–peppas model for determining the kinetic drug release showed that ramipril release form PLGA matrix followed zero order rate kinetics and an anomalous (non-fickian) diffusion mechanism.

Keywords: Biodegradable Polymer, PLGA, Antihypertensive Drug, Ramipril, Drug Content, Entrapment Efficiency, Drug Release.

1. INTRODUCTION

It is estimated that about 40% of new chemical entities or many existing drugs, although efficient are poorly water soluble or lipophilic in nature yet lead to poor oral bioavailability, high intra and inter-subject variability and lack of dose proportionality.[1] A new and novel field of biodegradable polymer nanoparticles (PNPs) is an emerging field. Over the past few decades, there has been considerable interest in developing biodegradable nanoparticles (NPs) varying from 10–1000 nm[2] as effective drug delivery devices.

Liposomes have been used as potential drug carriers instead of conventional dosage forms because of their unique advantages like their ability to protect drugs from degradation, target the drug to the site of action and reduce the toxicity or side effects.[3] However, developmental work on liposome has been limited due to inherent problems such as low encapsulation efficiency, rapid leakage of water-soluble drug in the presence of blood components and poor storage stability. However, polymeric NPs offer some specific advantages over liposomes. For instance, NPs help to increase the stability of drugs/proteins and possess useful controlled release properties. Polymers are very convenient materials for the manufacture of numerous and varied molecular designs that can be integrated into unique nanoparticle structures with many potential medical applications.[4] Among those, polymeric nanoparticulate systems from biodegradable and biocompatible polymer are interesting alternative for controlled drug delivery and drug targeting.[5–7] Poly(*D*,*L*-lactide-co-glycolide) (PLGA) has gained attention for the preparation of wide variety of delivery systems containing several drugs[8,9] due to their biodegradable, biocompatible properties[10,11] and low toxicity[12] and has been approved for human use by FDA.[13] The copolymers of PLGA degrade in body via hydrolytic cleavage

*Author to whom correspondence should be addressed.

Particuology 40 (2018) 169–176

Contents lists available at ScienceDirect

Particuology

journal homepage: www.elsevier.com/locate/partic

Fabrication of core–shell PLGA/PLA–pNIPAM nanocomposites for improved entrapment and release kinetics of antihypertensive drugs

Tanushree Basu, Bonamali Pal, Satnam Singh*

School of Chemistry and Biochemistry, Thapar Institute of Engineering and Technology, Patiala 147004, Punjab, India

ARTICLE INFO

Article history:
Received 14 April 2017
Received in revised form 6 October 2017
Accepted 13 October 2017
Available online 3 February 2018

Keywords:
Poly(lactic-co-glycolic) acid
Polylactic acid
Poly(*N*-isopropylacrylamide)
Antihypertensive drug
Entrapment efficiency
Drug release

ABSTRACT

Polylactic acid (PLA) and poly(lactic-co-glycolic) acid (PLGA) are two commonly applied biodegradable polymers for the preparation of nanocomposites used in drug-delivery systems. However, these polymers lack desirable attributes such as resistance to aggregation during long-term storage due to lyophilisation. To improve their efficacy, in this work, PLA and PLGA were encapsulated within a shell of poly(*N*-isopropylacrylamide) (pNIPAM) using a single emulsion technique followed by an aqueous free radical precipitation polymerisation process, yielding core–shell PLA/PLGA–pNIPAM nanocomposites. The nanocomposites were characterised using zeta potential, dynamic light scattering, and transmission electron microscopy analyses and were further applied as a delivery system for ramipril, an antihypertensive drug. The drug-loaded PLGA–pNIPAM core–shell nanoparticles exhibited a higher drug content (91%) and entrapment efficiency (78%) than their PLA counterparts. An in vitro release study of the formulations at pH 7.3 in phosphate-buffered saline indicated that PLGA was more efficient than PLA with a sustained release of 86% of ramipril from the polymer matrix within 24 h. Furthermore, to determine the release kinetics, the data were fitted to Korsmeyer–Peppas and Higuchi models; the release of ramipril from the polymer matrix followed zero-order rate kinetics and an anomalous (non-Fickian) diffusion mechanism.

© 2018 Chinese Society of Particuology and Institute of Process Engineering, Chinese Academy of Sciences. Published by Elsevier B.V. All rights reserved.

Introduction

Biodegradable colloidal particles have received significant interest as a possible means of delivering drugs by several routes of administration (Lemoine et al., 1996). Polymeric nanoparticles (NPs) help to increase the stability of drugs/proteins and possess useful controlled release properties. Special interest has been focused on the use of particles prepared from polyesters such as poly(lactic-co-glycolic) acid (PLGA) and polylactic acid (PLA) because of their biocompatibility and biodegradability via natural pathways in the body (Basu, Pal, & Singh, 2016; Jain, 2000; Panyam, Zhou, Prabha, Sahoo, & Labhasetwar, 2002). PLGA copolymers degrade in the body via hydrolytic cleavage of ester linkage to lactic and glycolic acid. These two monomers are metabolised in the body through the Krebs cycle before finally being eliminated in the form of CO_2 and H_2O. Although PLGA and PLA NPs have been used commercially by many investigators because of their advantageous properties, certain issues remain that limit their use for drug delivery (Anderson & Shive, 1997; Hans & Lowman, 2002; Panyam & Labhasetwar, 2003; Wischke & Schwendeman, 2008). The long-term storage of aqueous suspensions of PLGA and PLA NP systems is difficult because of the hydrolytic degradation of the polymer and subsequent release of the encapsulated therapeutics. To overcome this issue, researchers have used lyophilisation to prepare therapeutics containing PLGA and PLA NPs for long-term storage. However, this simple solution introduces an additional difficulty i.e., lyophilisation causes the NPs to aggregate into clumps that upon rehydration, readily fall out of the solution (Chacon, Molpeceres, Berges, Guzman, & Aberturas, 1999; Holzer et al., 2009).

In an attempt to overcome the limitations linked to PLGA and PLA NPs and to increase their functionality, in this work, these NPs were encapsulated within a shell of poly(N-isopropylacrylamide) (pNIPAM) because of its versatility and beneficial inherent properties. The pNIPAM shell can be synthesised as a homopolymer or as a copolymer with incorporation of various chemical moieties with defined concentrations that can be further modified with active targeting functional groups. In addition, it is one of the most stimuli-responsive polymers (Zhang & Zhuo, 2000). pNIPAM shows great potential for applications in biomedical fields (De Groot et al., 2001; Duracher, Elaïssari, Mallet, & Pichot, 2000; Suzuki, Yumura, Tanaka, & Akashi, 2001) and for the immobilisa-

* Corresponding author.
E-mail address: ssingh@thapar.edu (S. Singh).

https://doi.org/10.1016/j.partic.2017.10.002
1674-2001/© 2018 Chinese Society of Particuology and Institute of Process Engineering, Chinese Academy of Sciences. Published by Elsevier B.V. All rights reserved.

Chemical Physics Letters 706 (2018) 465–471

Contents lists available at ScienceDirect

Chemical Physics Letters

journal homepage: www.elsevier.com/locate/cplett

Research paper

Hollow chitosan nanocomposite as drug carrier system for controlled delivery of ramipril

Tanushree Basu, Bonamali Pal, Satnam Singh *

School of Chemistry and Biochemistry, Thapar Institute of Engineering & Technology, Patiala, Punjab, India

ARTICLE INFO

Article history:
Received 16 April 2018
In final form 26 June 2018
Available online 28 June 2018

Keywords:
PLGA
Chitosan
Core@shell
Hollow nanospheres
Ramipril
Entrapment efficiency
Drug release

ABSTRACT

Hollow biodegradable polymer nanoparticles as drug carrier possess effective low density and higher surface area. Chitosan hollow nanospheres were prepared using poly-D,L-lactide-co-glycolide as template by single emulsion method. The DLS studies showed increase in size from 125 nm to 186 nm for the formation of core@shell structure. The BET surface area increased from 62 $m^2 g^{-1}$ for chitosan@poly-D,L-lactide-co-glycolide to 111 $m^2 g^{-1}$ for hollow chitosan nanospheres. TEM analyses indicated core@shell, chitosan@poly-D,L-lactide-co-glycolide and the hollow morphology of the chitosan nanospheres. Ramipril in acetone (1.5 mg/mL, 3 mg/mL and 5 mg/mL) was physically adsorbed onto hollow chitosan nanospheres and the amount of adsorbed ramipril was determined by HPLC. Higher entrapment efficiency (91%) with 96% of the drug content was observed for the sample with 5 mg/mL of the drug. The *in-vitro* release of ramipril of 86% and 73% was achieved in acetate (pH-3.3) and phosphate (pH-6.3) buffers respectively while only 48% of ramipril in Tris buffer (pH-8.0) medium. Korsemeyer-Peppas model of drug release indicated the release of ramipril being swelling controlled.

© 2018 Elsevier B.V. All rights reserved.

1. Introduction

Biodegradable polymers have gained immense importance in the field of controlled drug delivery due to their various properties like small size and simplistic fabrication techniques. The main advantage of these biodegradable drug loaded polymers is their enhanced therapeutic effect of drug, subsequent lower dose requirement and reduction in toxic side effects [1]. Poly-D,L-lactide-co-glycolide (PLGA) and chitosan (Cs) are two widely used biodegradable polymers. PLGA is biocompatible, non-toxic biopolymer [2] that degrades into lactic and glycolic acid in the body that are utilized into the natural metabolic pathway kreb's cycle also called as the TCA cycle inside the body and finally eliminates out as H_2O & CO_2. Similarly, Cs, a biopolymer of chitin is an exceptional flocculent, adhering to negatively charged surfaces is non-toxic, biocompatible, biodegradable and also have fungicidal activities [3–7], besides having a unique chemical structure as a linear polyelectrolyte with a high charge density and reactive hydroxyl and amino groups [8]. Chitosan and its derivatives are widely used as drug delivery vehicles [9] like; chitosan modified with PLGA nanoparticles for improved drug delivery was reported by Wang and co-workers [10]. Also, Campos and co-workers [11] reported the use of chitosan as solid lipid nanoparticle (SLN) for effective delivery of paclitaxel. Chitosan microspheres have also been used in gastric drug delivery [12]. To increase insulin's intestinal absorption and enhance its pharmacological bioavailability insulin loaded chitosan nanospheres have been used [13]. Chitosan also exhibits various fascinating biological activities which include induced disease resistance in plants, antimicrobial activity, etc. [14,15]. All these properties of chitosan makes it useful in many different fields that includes food and chemical engineering, pharmaceuticals, nutrition, etc. [16].

In recent years, hollow nanospheres have attracted great potential as drug delivery carriers due to high surface area and low effective density [17]. Several methods for preparation of hollow nanospheres are available [18] like emulsion polymerization [19,20], self-assembly of block copolymers [21–23], template polymerization [24,25], etc. Although, there are many methods to prepare hollow nanospheres still the template method is the most frequently used method, as it can control the core size and hollow structure can easily be obtained after removal of the template by evaporation or thermolysis. Drug loading in the polymer nanoparticles takes place by two ways firstly, addition of drug during the preparation of particles itself and secondly, after the formation of the particles. In case of hollow nanospheres, the second method is applied i.e. the drug is loaded afterwards and hence, the aqueous/organic interface produced by water-in-oil micro emulsion

* Corresponding author.
E-mail address: ssingh@thapar.edu (S. Singh).

https://doi.org/10.1016/j.cplett.2018.06.053
0009-2614/© 2018 Elsevier B.V. All rights reserved.

ChemPubSoc Europe

DOI: 10.1002/slct.201801769

Chemistry SELECT Full Papers

Materials Science inc. Nanomaterials & Polymers

Fe_3O_4 @ PLGA-PEG Nanocomposite for Improved Delivery of Methotrexate in Cancer Treatment

Tanushree Basu, Satnam Singh, and Bonamali Pal*[a]

Magnetic Fe_3O_4 nanoparticles are gaining significance in drug delivery applications owing to their targeting capability. Surface modification of amphiphilic block polymers by Fe_3O_4 nanoparticles increases their properties. In this study, Fe_3O_4 @ PLGA-PEG nanocomposite is prepared by double emulsion (w/o/w) method. A shift in the 2Θ values for the composite in XRD attributes to interaction between Fe_3O_4 and PLGA-PEG. Also, a shift in the Fe-O band in the FTIR spectrum of Fe_3O_4@PLGA-PEG from 578 cm^{-1} to 510 cm^{-1} confirms the formation of nanocomposite. Surface morphology of the prepared nanocomposite is analyzed by TEM and AFM. Decrease in agglomeration due to electrostatic repulsion between the polymer chains and magnetic particles is observed while an increased surface area (61.0nm) confirms the formation of the nanocomposite. To determine the effectiveness of the prepared magnetically modified nanoparticles, methotrexate (anticancer drug) is encapsulated into the nanocomposite. High entrapment efficiency of 95% is observed when polymer:drug is 1:1. The *in-vitro* release profile shows that pH of release medium plays a significant role. At physiological pH of 7.3 there is only 15% methotrexate release while nearly 86% of methotrexate release is observed at acidic pH of 4.6 over 72h. Korsemeyer-Peppas model of drug release (R^2-0.9868) represents swelling controlled release of methotrexate. Further, the cytotoxic cell viability assay on SK-BR-3 (breast adinocarcinoma) cells showed that methotrexate loaded onto the nanocomposite showed higher cell viability as compared to free methotrexate after 96h of incubation. The fluorescent cell imaging also showed that methotrexate released slowly from the nanoparticles and diffused into the nucleus without losing its cytotoxic effect on the cancer cells. Based on these properties of the magnetically modified PLGA-PEG nanoparticles they can be used as targeting drug delivery agents in treatment of cancer therapy.

Introduction

Recent advancements in nanotechnology have developed new research strategies in the field of drug delivery. The use of biodegradable polymeric nanoparticles for targeted as well as controlled drug delivery is fast emerging and replacing the conventional mode of medication in the last decade . Magnetic nanoparticles (MNPs) are gaining attention in the field of medicine . These MNPs posses certain attributes that allows them to be used as drug carrier's,[3] in tumour therapy[4] and MRI agents.[5] Although iron (Fe) is mostly used but other elements like manganese (Mn), copper (Cu), zinc (Zn) and nickel (Ni) can also be applied for preparation of ferrites having general formula M-Fe_2O_4.[6]

Poly (lactic-co-glycolic) acid (PLGA) is one of the most efficient biodegradable polymers to be used in the field of drug delivery. Surface modification of PLGA with poly ethylene glycol (PEG) renders it hydrophillicity and other physiochemical properties. Block copolymers having hydrophilic segment have applications mainly due to their biodegradability, biocompatibility etc.[7] Various surface modified drug loaded PLGA nanoparticles have been synthesized and used for controlled/target drug delivery. Parveen et al. reported the development of a surface coating by hydrophilic polymer PEG which was used to limit the phagocytic properties and to boost the endurance of the NPs.[8] PLGA has been frequently used as a drug delivery carrier in treatment of cancer therapy in recent times. Fang Qiong et.al reported the release behaviour of docetaxel an antitumor drug from PLGA coated silica nanorattle.[9] To further improve the targeting ability of PLGA-PEG towards cancer therapy they are modified with MNPs (Fe_3O_4). The as prepared MNPs have the capability to target the tumour tissues. El-Boubbou et.al reported the preparation of chemotherapeutic agent formed of stabilized metal oxide NPs[10] which was found to be more efficient than free DOX for the treatment of acute myeloid leukaemia (AML). Also,FG. Souza Jr et.al,[11] associated cotrimoxizole (antibiotic) to multi block polymer aiming to reach a controlled drug release system. In addition to PLGA there are several other polymer particles which are used in pH dependent release of drug from its matrix. Z. Deng et.al investigated the use of silica coated hollow chitosan nanospheres for the release of model protein BSA from its matrix. They reported about 83% of BSA release from Cs-SiO_2 hollow NPs in PBS at pH 4.0 compared to when released (17.4%) at pH 7.4. This variation in release behaviour of BSA is attributed to swelling behaviour of Cs-SiO_2 hollow NPs in acidic medium.[12] Also, Basu et.al reported the pH dependent release of ramipril from hollow chitosan matrix.[13]

[a] *T. Basu, Dr. S. Singh, Dr. B. Pal*
School of Chemistry and Biochemistry, Thapar Institute of Engineering & Technology, Patiala-147004, India
Tel.: +91-175-239-3443
Fax: +91-175-236-4498
E-mail: bpal@thapar.edu

Supporting information for this article is available on the WWW under https://doi.org/10.1002/slct.201801769

© 2018 Wiley-VCH Verlag GmbH & Co. KGaA, Weinheim

Thesis

ORIGINALITY REPORT

6%	3%	4%	1%
SIMILARITY INDEX	INTERNET SOURCES	PUBLICATIONS	STUDENT PAPERS

PRIMARY SOURCES

1	Nibedita Banik, Anowar Hussain, Anand Ramteke, Hemanta K. Sharma, Tarun K. Maji. "Preparation and evaluation of the effect of particle size on the properties of chitosan-montmorillonite nanoparticles loaded with isoniazid", RSC Advances, 2012 Publication	2%
2	Mostafa Rahimnejad, Ghasem Najafpour, Gholamreza Bakeri. "Investigation and modeling effective parameters influencing the size of BSA protein nanoparticles as colloidal carrier", Colloids and Surfaces A: Physicochemical and Engineering Aspects, 2012 Publication	1%
3	www.mdpi.com Internet Source	1%
4	www.linknovate.com Internet Source	1%
5	Do Kyung Kim. "Nanomaterials for Controlled	

Release of Anticancer Agents", Nanotechnologies for the Life Sciences Online, 09/15/2007

Publication

1%

Exclude quotes	On	Exclude matches	< 8 words
Exclude bibliography	On		